ORNL/TM-1999/299

OAK RIDGE
NATIONAL
LABORATORY

Neutronics Benchmarks of Mixed-Oxide Fuels using the SCALE/CENTRM Sequence

D. F. Hollenbach
P. B. Fox

MANAGED AND OPERATED BY
LOCKHEED MARTIN ENERGY RESEARCH CORPORATION
FOR THE UNITED STATES
DEPARTMENT OF ENERGY

ORNL/TM-1999/168

Computational Physics and Engineering Division

Neutronics Benchmarks of Mixed-Oxide Fuels using the SCALE/CENTRM Sequence

D. F. Hollenbach
P. B. Fox

Date Published: February 2000

Prepared by the
OAK RIDGE NATIONAL LABORATORY
Oak Ridge, Tennessee 37831-6370
managed by
LOCKHEED MARTIN ENERGY RESEARCH CORP.
for the
U.S. DEPARTMENT OF ENERGY
under contract DE-AC05-96OR22464

CONTENTS

Page

LIST OF FIGURES

LIST OF FIGURES (continued)

LIST OF FIGURES (continued)

LIST OF TABLES

LIST OF TABLES (continued)

LIST OF TABLES (continued)

LIST OF TABLES (continued)

LIST OF TABLES (continued)

LIST OF TABLES (continued)

LIST OF TABLES (continued)

ACKNOWLEDGMENTS

This work is supported jointly by the DOE Nuclear Criticality Safety Program and the DOE Fissile Material Disposition Program.

The author would like to thank the following individuals for their contributions: M. L. Williams, Louisiana State University, who wrote CENTRM and was available whenever problems were encountered with the code; L. M. Petrie for his assistance in implementing CENTRM into the SCALE sequence; W. C. Jordan and R. Q. Wright for testing and often breaking the code; M. E. Dunn and N. M. Greene for help creating the point cross-section library used by CENTRM; and J. B. Anderson for preparing this report.

ABSTRACT

The purpose of this study is to determine and document the reactor physics parameters (multiplication factors, spatially dependent flux ratios, and spacially dependent reaction rates) for several distinct sets of problems using two distinct resonance cross-section processing techniques. In SCALE, by default, resonances are processed using NITAWL, which utilizes the Nordheim Integral Treatment. The results produced using this sequence are considered to be the base results. A second set of results are produced by replacing NITAWL with CENTRM/PMC. CENTRM produces point-wise fluxes for a given geometry configuration and set of isotopes. Using these fluxes, PMC produces problem-dependent self-shielding cross sections. Both sequences use ENDF/B-V cross-section data.

1. INTRODUCTION

This report examines four sets of problems that are used to evaluate the differences between the NITAWL resonance processor and the CENTRM/PMC resonance processor. All the problems are predominantly thermal, with the energy of the average lethargy causing fission (EALCF) being below 1 eV. They are all water-moderated fuel rod lattices of various dimensions and fuel materials. The objective of this report is to compare the differences between the NITAWL and CENTRM/PMC resolved-resonance processors for the class of problems presented in this report. The existence of severe resonance overlap when mixing uranium and plutonium could cause a significant problem with the NITAWL results. CENTRM/PMC does not contain this potential problem, which is a limitation of the Nordheim Integral Treatment.

All problem were processed using SCALE5.0, which allows one to choose which resolved resonance processor will be used to self-shield the nuclides, NITAWL or CENTRM/PMC. SCALE5.0 is a developmental version of the SCALE code system. The current version of SCALE, SCALE4.4, does not contain CENTRM but is essentially the same in all other aspects to SCALE5.0. SCALE5.0 has the ability to use either NITAWL or CENTRM/PMC as the resolved-resonance processor. All problems were run first using CENTRM/PMC and then using NITAWL. The results were then analyzed and compared. [1, 2]

1.1 THE SCALE 5.0 SEQUENCES

SCALE 5.0 contains two distinct sequences used for processing cross-section data. The original sequence consisting of the codes CSAS, BONAMI, and NITAWL process all resolved resonance data in NITAWL. The new computational sequence added to SCALE5.0 uses the following sequence to process the cross sections: CSAS, BONAMI, NITAWL, CENTRM, PMC, WORKER. CENTRM/PMC process the resolved resonances cross sections in the unit cell. All other resolved resonance cross sections are processed using NITAWL. To calculate the desired physics parameters, the three experimental benchmark sets then use KENO-V.a and the set of computational benchmarks uses XSDRNPM. Many of the physics parameters are compared with direct experimental data and others are compared only with the same parameters calculated using difference codes and cross sections.

1.2 NITAWL

NITAWL performs problem-dependent resonance self-shielding using the Nordheim Integral Treatment, which involves solving for the energy dependence of the neutron flux in a material region containing a resonance absorber and a maximum of two moderating materials. The resonance self-shielding is made with reference to infinite dilution cross-section values. The material region is either infinite or a one-dimensional (1-D) slab, cylinder, or sphere surrounded by moderator. In the moderator, the neutron flux is assumed to be spatially flat and slowly varying with energy. The presence of more than one fuel region in the moderator, such as a lattice, is accounted for using a Dancoff factor.

There are many problems where the Nordheim Integral Treatment may not be appropriate because of the following assumptions:

1. Each resonance nuclide can be treated without consideration of other resonance nuclides present in the system.
2. The neutron flux is spatially uniform in the absorber and moderator regions.
3. Neutron transport into and out of the absorber region can be treated with first-flight escape probabilities.
4. The presence of other absorber lumps in the system can be accounted for with a Dancoff factor which corresponds to the first-flight transmission probability across the moderator. A Dancoff factor of zero corresponds to a single lump in the moderator. A Dancoff factor of 1 corresponds to an infinite medium of the absorber material with no moderator outside the absorber lump.

1.3 CENTRM/PMC

The new resolved-resonance processor is composed of two codes that are executed sequentially. The first code, CENTRM, is a discrete-ordinance code that produces a point-wise continuous-energy flux spectrum for a given infinite or 1-D problem. Subsequently, PMC uses this point flux spectrum to collapse point cross sections to a problem-dependent multigroup cross-section set. To generate the flux profile and produce new group cross sections, the two codes use a pointwise continuous cross-section library that contain all the nuclides present in the selected multigroup cross-section library. All the cases in this report were analyzed using the 238-group ENDF/B-V multigroup cross-section library.

CENTRM has several options that determine the range over which the flux spectrum will be generated and the parameters used for generating the flux spectrum. Although pointwise continuous in energy, the flux spectrum is generated on a specified 1-D spacial mesh. For all cases in this report, the spatial mesh is over an infinite cylinder that is automatically generated by the code. The flux spectrum is generated from 20 MeV to 1.0E-5 eV over the spatial mesh using a default quadrature of 8. CENTRM uses the specified quadrature to generate Legendre coefficients for the scattering component of the pointwise flux.

CENTRM is capable of using a fixed or fission input source to generate the flux profile. For simplicity and because the benchmarks are fission problems, a spacially flat fission source is assumed as an initial guess. Two other parameters that can affect the flux are the point convergence criterion and the tolerance used for thinning the pointwise cross sections. These parameters are both set to default values of 0.0001 for the convergence criterion and 0.0025 for the thinning tolerance.

In order for CENTRM to generate the flux profile it first combines the pointwise continuous-energy cross sections of all nuclides in each zone. Each zone contains only one material but is divided into many intervals, with each interval being a mesh point where the entire energy spectrum of the flux is calculated. There is no code limit on the number of materials and 1-D zones. However, for large problems involving many materials and zones, computer memory and CPU speed may be a limiting factor.

By default, the flux profile is generated using an S_N calculation over the entire spectrum. The option exists to perform several other types of calculations independently over the fast, thermal, and

pointwise ranges. Over all energy ranges, scattering for the pointwise continuous cross sections is assumed to be elastic and isotropic in the center of mass system. Consequently, no scattering data are contained in the point library, only 1-D cross sections.

PMC replaces the cross sections for specified nuclides and energy groups in the problem-dependent multigroup library. PMC reads the pointwise flux file, the pointwise continuous cross sections, and the problem-dependent multigroup library; generates new multigroup data from the point data; and finally rewrites the multigroup library with the new multigroup data. PMC can produce multigroup cross sections over three ranges for all nuclides: the entire point library range, the resolved resonance range, or the pointwise flux range. For the problems, in this report PMC produces multigroup cross sections over the resolved resonance range of each nuclide in the unit cell data.

PMC has three methods for computing the scattering component of the new multigroup cross sections. The P_N components of the original multigroup scattering cross sections can be renormalized to the new 1-D scattering cross sections. The P_N components of the original multigroup scattering cross sections can be renormalized using the scalar flux. Finally, new P_N components for the scattering cross section can be computed using the pointwise flux moments. For the problems in this report, the first option of renormalizing the P_N components using the new 1-D cross sections is used.

A set of pointwise continuous cross sections are available for use by CENTRM and PMC. The point cross sections used in the report were generated using the AMPX code system from the ENDF/B-V nuclear data library. The library contains all the nuclides present in both the 238-group and 44-group ENDF/B-V multigroup libraries. The library contains the total, elastic scattering, and radiative capture cross sections for each nuclide. If a nuclide is fissionable, the fission cross section is also present. Also, if a nuclide contains inelastic data at higher energies, inelastic data are also included in the library. The pointwise continuous library is divided up into files, with each file containing all the cross-section data for one nuclide. The ENDF/B-V pointwise library was generated to be used with the ENDF/B-V multigroup libraries. Using it with any other type of library, such as one generated using ENDF/B-VI data, could produce incorrect results.

2. MIX-COMP-THERM-2 (PNL-30 to PNL-35)

2.1 DESCRIPTION

This section describes a set of six critical experiments, each consisting of a square-pitched array of mixed plutonium-uranium fuel rods submerged in water surrounded by a water reflector. The water contains boron concentrations from 0.9 to 767.2 ppm. This set of experiments is contained in the *International Handbook of Evaluated Criticality Safety Benchmark Experiments*.[3]

This set of experiments was performed between December 1975 and March 1976 at the Plutonium Recycle Critical Facility at Pacific Northwest Laboratory. The benchmark experiments are light-water-moderated critical assemblies consisting of a core array supported by upper and lower lattice plates. The lattice plates are 2.54 cm thick and located at the top and bottom of the fuel region . The reactor is brought to critical by raising the water level in the tank, thus avoiding the use of control rods. The fuel rods sit on a support plate above the bottom of the tank. The tank is wide enough to assume an infinite moderator on the sides and bottom (~30 cm of water).

All fuel rods have the same physical dimensions. A schematic diagram of the fuel rods and bottom reflector is given in Fig. 2.1. Each fuel rod has an active fuel length of 86.6775 cm, 0.5 cm of UO_2 at the bottom of the fuel, a 0.6985-cm cladding plug on the bottom and a 0.8255-cm cladding plug on the top. The fuel has a radius of 0.64135 cm. The cladding has an outside radius of 0.71755 cm. A 0.3175-cm water gap is located between the top of the aluminum support plate and the bottom of the lower lattice plate. The aluminum support plate is 2.8575 cm thick. There is a 0.889-cm water gap between the bottom of the lead plate and the top of the upper lattice plate. The lead plate is 0.9525 cm thick. The top reflector varies depending on the water level for the particular problem.

The primary differences between the six benchmarks are lattice pitch, number of rods in the lattice, water level, and boron concentrations. All other benchmark characteristics are constant. There are three different lattice pitches, with each pitch used in two problems: 1.778 cm, 2.20914 cm, and 2.51447 cm. The fuel is arranged in a square-pitched lattice. The characteristics of each of the four lattices are given in Table 2.1. Table 2.2 contains the atom densities for all the materials in the problem except B-10 and B-11. The atom densities in Table 2.2 are constant for all benchmarks. Table 2.3 contain the atom densities of B-10 and B-11 for each benchmark. All material temperatures are assumed to be 23°C (295 K).

As shown in Table 2.1, the six benchmark problems change by moderator boron concentration, number of fuel rods, lattice pitch and upper-reflector thickness. To simplify the accumulation of power densities, advantage was taken in the symmetry of the problem whenever possible. The entire problem was explicitly modeled, but instead of having a separate unit for each pin, 1/8th symmetry was used for every problem except PNL-32. Due to an irregular placement of outer rods, this problem needed to be modeled using a unit for each pin. The lattice is then filled from the 1/8th section by inserting additional pins in a mirror image. Figures 2.2 through 2.6 show the lattice map for each problem. Figure 2.4 shows a full-lattice mapping; the other figures contain only 1/8th lattices. The remaining lattice can be extrapolated from these 1/8th sections.

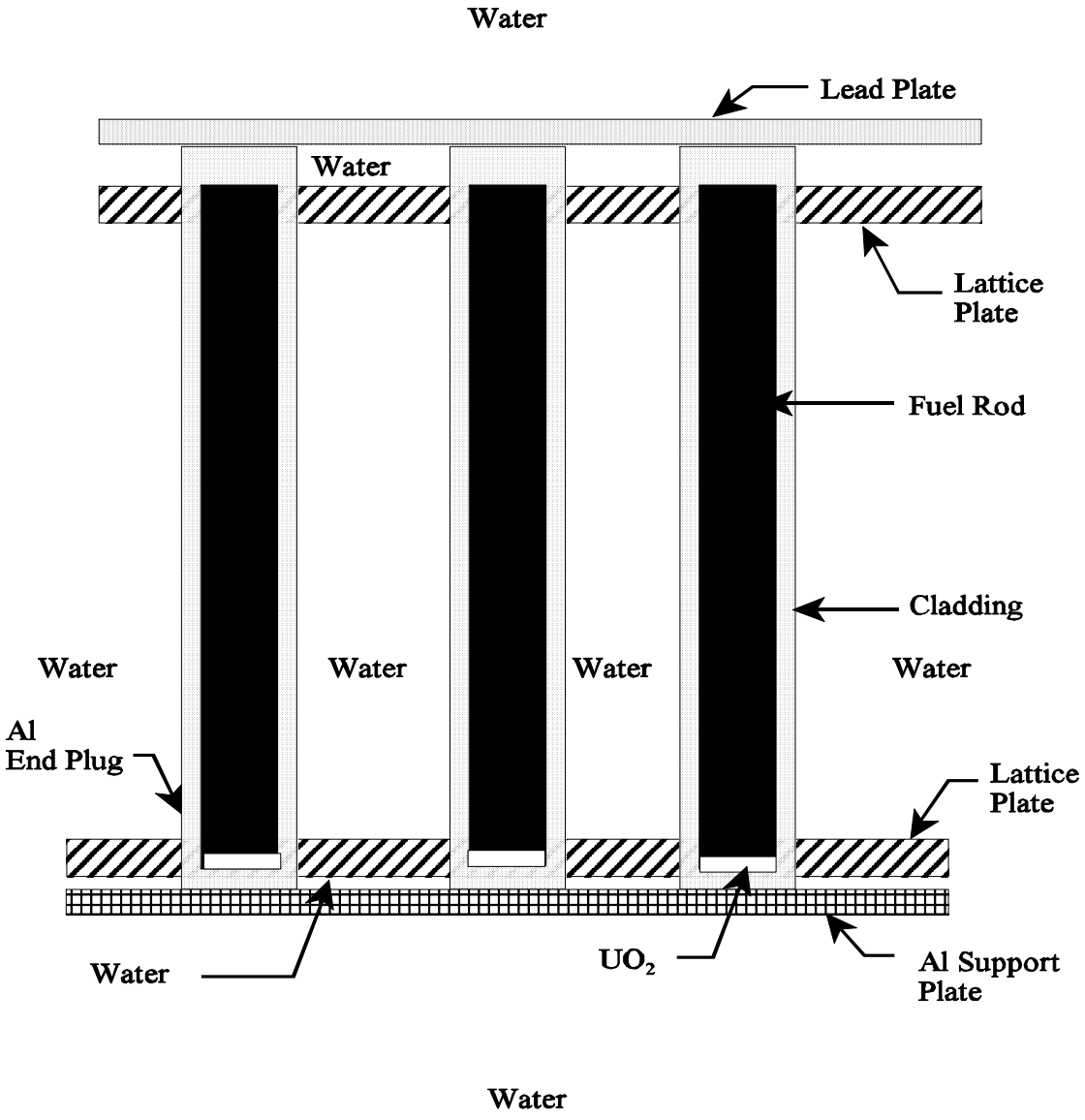

Fig. 2.1. Schematic of the PNL fuel rods with reflector.

Table 2.1. Lattice description for benchmarks

Benchmark No.	Boron con. (ppm)	Critical No. rods	Lattice pitch (cm)	Water level above lead (cm)
30	1.7	469	1.778	13.462
31	687.9	761	1.778	13.462
32	0.9	195	2.20914	3.937
33	1090.4	761	2.20914	13.462
34	1.6	160	2.51447	0.508
35	767.2	689	2.51447	13.462

Table 2.2. Constant benchmark atom densities

Material	Isotope	Atom density (atoms/barn-cm)	Material	Isotope	Atom density (atoms/barn-cm)
Fuel	U-234	1.2458×10^{-6}	Lattice plate	Si	1.3742×10^{-2}
UO_2-PuO_2	U-235	1.4886×10^{-4}	Support plate	Fe	4.5919×10^{-2}
(9.54 g/cc)	U-236	2.0936×10^{-9}		Cu	1.1532×10^{-4}
	U-238	2.0936×10^{-2}		Mn	9.6395×10^{-4}
	Pu-238	3.8836×10^{-8}		Mg	1.2388×10^{-4}
	Pu-239	3.9462×10^{-4}		Cr	1.7409×10^{-3}
	Pu-240	3.3206×10^{-5}		Zn	1.6617×10^{-2}
	Pu-241	1.6081×10^{-6}		Ti	4.6052×10^{-4}
	Pu-242	1.1882×10^{-7}		Al	1.5025×10^{-3}
	Am-241	1.4954×10^{-6}			
	O-16	4.3779×10^{-2}			
Natural UO_2	U-234	1.2406×10^{-6}	Cladding	Sn	4.8328×10^{-4}
(9.286 g/cc)	U-235	1.4824×10^{-4}		Fe	9.5642×10^{-5}
	U-236	2.0848×10^{-9}		Cr	7.6093×10^{-5}
	U-238	2.0525×10^{-2}		Ni	3.0336×10^{-5}
	O-16	4.1943×10^{-2}		Zr	4.2621×10^{-2}
			Lead	Pb	3.2174×10^{-2}

Table 2.3. Moderator atom densities

Benchmark No.	Atom densities (atoms/barn-cm)			
	H	O	B-10	B-11
PNL-30	6.6706×10^{-2}	3.3353×10^{-2}	1.8706×10^{-8}	7.5770×10^{-8}
PNL-31	6.6605×10^{-2}	3.3400×10^{-2}	7.5838×10^{-6}	3.0718×10^{-5}
PNL-32	6.6706×10^{-2}	3.3353×10^{-2}	9.9034×10^{-9}	4.0114×10^{-8}
PNL-33	6.6672×10^{-2}	3.3427×10^{-2}	1.2034×10^{-5}	4.8746×10^{-5}
PNL-34	6.6706×10^{-2}	3.3353×10^{-2}	1.7606×10^{-8}	7.1313×10^{-8}
PNL-35	6.6682×10^{-2}	3.3405×10^{-2}	8.4597×10^{-5}	3.4266×10^{-5}

2.2 ANALYSIS

All six computational benchmarks in this section were processed twice using SCALE 5.0. The set labeled NITAWL uses the NITAWL resonance processor to self-shield the resolved resonance region for all nuclides in the fuel and clad. An identical set, labeled CENTRM, replaces NITAWL with the CENTRM/PMC code sequence for the nuclides in the unit cell. The NITAWL and CENTRM results are then compared.

Table 2.4 contains the k_{eff} and energy of the average lethargy causing fission (EALCF). The k_{eff} values for all the benchmark cases are close to 1.0: the worst NITAWL benchmark is 0.90% high, and the worst CENTRM case is 0.68% high. A small negative bias does appear between NITAWL and CENTRM, with the CENTRM cases about 0.25% lower on average than the NITAWL cases.

The EALCF is also shown in this table. The EALCF values listed are from the CENTRM cases. EALCF is the energy of the average lethargy causing fission and is calculated by summing the lethargies of the neutrons that undego fission, dividing the value by the number of fissions, and converting this value to energy. For all cases, the difference between this value for CENTRM and NITAWL was less than 0.1%. Both CENTRM and NITAWL produce excellent and consistent results for the k_{eff} and fission energy for this set of problems.

Additional parameters calculated for each problem include: pin-power distributions; absortption, σ_f, and fission reaction rates and fluxes in the pin fuel, clad, and moderator; and four group cross sections and fluxes for a corner outside pin and the innermost pin. Each of these sets of data are calculated using both CENTRM and NITAWL. All the data for each case are contained in Figs. 2.7a through 2.12b and Tables 2.5 through 2.64.

The pin-power distributions for this problem assumed 1/8th core symmetry with a surrounding reflector for all benchmark cases except PNL-32. Because of a lack of symmetry in two outer pins the entire assembly needed to be modeled. The pin-power data consist of a value and a standard deviation for each pin. The values for the pin powers are actually in units of fissions per cm^3-s-source particle $\times 10^{-5}$. The value in parentheses is the percent standard deviation of the pin-power value.

In most cases the CENTRM and NITAWL results for each benchmark case fall within 2 standard deviations. The peak-to-low power changes with change in pitch and boron concentration.

The peak-to-low power ratio changed from a low of 1.86 for the smallest pitch with no boron added to a high of 4.19 at the largest pitch with added boron. The addition of boron significantly shifts the flux profile to the center of the assembly by depressing the thermal flux in the moderator.

The reaction rates, total fluxes, and flux ratios for the CENTRM and NITAWL cases of each benchmark case are also in good agreement, seldom varying by more than 1%. These values are included for a corner pin and the center pin for each case. All the reaction rates and fluxes increase as the pins approach the center of the assembly if the outer two layers of the arrays are excluded. The lowest power pin occurs in either the outer layer or the next inner layer of the array. The flux ratios over the fuel, clad, and moderator are relatively constant for a given pitch and boron concentration. However, as the pitch increases, the proportion of the total pin flux in the moderator increases.

Finally, four-group fluxes and cross sections were calculated for selected nuclides in the fuel region of the same corner and center pins. The macroscopic cross sections listed include the radiative capture, fission, and nu*fission cross sections for U-235, U-238, and Pu-239. The four groups are collapsed from the 238-group multigroup cross-section set using the flux profile calculated in KENO-V.a as follows: group 1 is from 20 Mev to 9.5 keV, group 2 is from 9.5 keV to 3.0 eV, group 3 is from 3 eV to 0.4 eV, and group 4 is from 0.4 eV to 10^{-5} eV. The 0.4 eV was chosen as a boundary because it is the cadmium cutoff energy. Groups 2 and 3 contain the resolved resonance regions for most of the nuclides used in these cases. Most of the cross-section data for the CENTRM and NITAWL cases of a given benchmark case agree within 1%.

2.3 CONCLUSIONS

For this set of benchmark cases, using either NITAWL and CENTRM as the resonance region processor produces acceptable results of the k_{eff} values. All other values produced using CENTRM and NITAWL are also consistent with each. For all cases, the k_{eff}*'s* produced using CENTRM are slightly lower, ~0.25%, than those produced using NITAWL to do the resonance self-shielding. As a result, the average k_{eff} of all the CENTRM cases is closer to 1.0 than the average k_{eff} of all the NITAWL cases for this set of benchmarks. The pin-power distributions, fluxes, reactions rates, and macroscopic cross sections all agree to approximately 1% between CENTRM and NITAWL.

The presence of boron in the moderator depresses the fraction of the flux in the moderator, thus creating a larger difference between the highest- and lowest-power pins. No significant differences were identified between the results produced by NITAWL and CENTRM for these benchmark cases.

Table 2.4. Comparison of k_{eff} and EALCF from CENTRM and NITAWL

CASE MIX-COMP-THERM-2	NITAWL k_{eff} (±F)	CENTRM k_{eff} (±F)	% DIFF	EALCF (eV)
PNL-30	1.000 (0.0005)[a]	0.9966 (0.0004)	-0.34	0.575
PNL-31	1.0026 (0.0004)	0.9987 (0.0003)	-0.39	0.768
PNL-32	1.0021 (0.0004)	1.0000 (0.0004)	-0.21	0.193
PNL-33	1.0090 (0.0003)	1.0064 (0.0004)	-0.26	0.282
PNL-34	1.0046 (0.0004)	1.0020 (0.0005)	-0.26	0.138
PNL-35	1.0079 (0.0004)	1.0068 (0.0004)	-0.11	0.182

[a] Values in parentheses is the percent standard deviation.

											69
										67	68
									64	65	66
								60	61	62	63
							55	56	57	58	59
						49	50	51	52	53	54
					42	43	44	45	46	47	48
				34	35	36	37	38	39	40	41
			25	26	27	28	29	30	31	32	33
		M	16	17	18	19	20	21	22	23	24
	M	M	M	8	9	10	11	12	13	14	15
M	M	M	M	M	1	2	3	4	5	6	7

Fig. 2.2. Pin layout of benchmark case PNL-30.

											109
										107	108
									104	105	106
								100	101	102	103
							95	96	97	98	99
						89	90	91	92	93	94
					82	83	84	85	86	87	88
				74	75	76	77	78	79	80	81
			65	66	67	68	69	70	71	72	73
		55	56	57	58	59	60	61	62	63	64
	44	45	46	47	48	49	50	51	52	53	54
32	33	34	35	36	37	38	39	40	41	42	43
M	21	22	23	24	25	26	27	28	29	30	31
M	M	M	12	13	14	15	16	17	18	19	20
M	M	M	M	M	5	6	7	8	9	10	11
M	M	M	M	M	M	M	M	1	2	3	4

Fig. 2.3. Pin layout of benchmark cases PNL-31 and PNL-33.

M	M	M	M	M	M	M	193	194	195	M	M	M	M	M	M	M
M	M	M	M	M	M	187	188	189	190	191	192	M	M	M	M	M
M	M	M	M	178	179	180	181	182	183	184	185	186	M	M	M	M
M	M	M	167	168	169	170	171	172	173	174	175	176	177	M	M	M
M	M	154	155	156	157	158	159	160	161	162	163	164	165	166	M	M
M	139	140	141	142	143	144	145	146	147	148	149	150	151	152	153	M
M	124	125	126	127	128	129	130	131	132	133	134	135	136	137	138	M
107	108	109	110	111	112	113	114	115	116	117	118	119	120	121	122	123
90	91	92	93	94	95	96	97	98	99	100	101	102	103	104	105	106
73	74	75	76	77	78	79	80	81	82	83	84	85	86	87	88	89
M	58	59	60	61	62	63	64	65	66	67	68	69	70	71	72	M
M	43	44	45	46	47	48	49	50	51	52	53	54	55	56	57	M
M	M	30	31	32	33	34	35	36	37	38	39	40	41	42	M	M
M	M	M	19	20	21	22	23	24	25	26	27	28	29	M	M	M
M	M	M	M	10	11	12	13	14	15	16	17	18	M	M	M	M
M	M	M	M	M	4	5	6	7	8	9	M	M	M	M	M	M
M	M	M	M	M	M	M	1	2	3	M	M	M	M	M	M	M

Fig. 2.4. Pin layout of benchmark case PNL-32.

								27
							25	26
						22	23	24
					18	19	20	21
				13	14	15	16	17
			M	8	9	10	11	12
		M	M	M	4	5	6	7
	M	M	M	M	M	M	2	3
M	M	M	M	M	M	M	M	1

Fig. 2.5. Pin layout of benchmark case PNL-34.

										99
									97	98
								94	95	96
							90	91	92	93
						85	86	87	88	89
					79	80	81	82	83	84
				72	73	74	75	76	77	78
			64	65	66	67	68	69	70	71
		55	56	57	58	59	60	61	62	63
	45	46	47	48	49	50	51	52	53	54
34	35	36	37	38	39	40	41	42	43	44
M	24	25	26	27	28	29	30	31	32	33
M	M	15	16	17	18	19	20	21	22	23
M	M	M	7	8	9	10	11	12	13	14
M	M	M	M	M	1	2	3	4	5	6

Fig. 2.6. Pin layout of benchmark case PNL-35.

											2.475 (0.91)
										2.458 (0.46)	2.460 (0.46)
									2.413 (0.48)	2.427 (0.31)	2.423 (0.44)
								2.235 (0.48)	2.337 (0.35)	2.354 (0.35)	2.386 (0.43)
							2.095 (0.46)	2.183 (0.35)	2.220 (0.32)	2.275 (0.33)	2.293 (0.46)
						1.883 (0.57)	1.982 (0.35)	2.074 (0.32)	2.127 (0.36)	2.150 (0.35)	2.168 (0.49)
					1.636 (0.58)	1.761 (0.41)	1.860 (0.35)	1.947 (0.35)	1.999 (0.36)	2.033 (0.35)	2.042 (0.49)
				1.423 (0.62)	1.534 (0.40)	1.616 (0.35)	1.707 (0.41)	1.792 (0.38)	1.833 (0.35)	1.874 (0.35)	1.877 (0.50)
			1.530 (0.56)	1.381 (0.46)	1.416 (0.43)	1.483 (0.40)	1.557 (0.42)	1.624 (0.38)	1.670 (0.33)	1.710 (0.38)	1.714 (0.55)
		0	2.213 (0.35)	1.510 (0.44)	1.358 (0.41)	1.367 (0.43)	1.423 (0.42)	1.493 (0.39)	1.530 0.43)	1.566 (0.39)	1.566 (0.55)
	0	0	0	2.160 (0.37)	1.519 (0.43)	1.391 (0.43)	1.437 (0.44)	1.480 (0.39)	1.539 (0.40)	1.566 (0.39)	1.573 (0.54)
0	0	0	0	0	2.311 (0.40)	2.001 (0.43)	2.035 (0.39)	2.124 (0.40)	2.197 (0.36)	2.225 (0.39)	2.254 (0.57)

Fig. 2.7a. Pin-power distribution for CENTRM benchmark PNL-30. Value in parentheses is the percent standard deviation.

											2.509 (0.86)
										2.465 (0.42)	2.484 (0.42)
									2.402 (0.39)	2.440 (0..)32	2.451 (0.43)
								2.268 (0.48)	2.325 (0.33)	2.350 (0.32)	2.378 (0.46)
							2.115 (0.45)	2.180 (0.36)	2.246 (0.34)	2.285 (0.35)	2.287 (0.44)
						1.891 (0.50)	1.999 (0.35)	2.088 (0.32)	2.138 (0.32)	2.166 (0.36)	2.181 (0.49)
					1.642 (0.55)	1.773 (0.40)	1.865 (0.38)	1.941 (0.32)	1.998 (0.36)	2.033 (0.32)	2.037 (0.47)
				1.424 (0.59)	1.525 (0.40)	1.622 (0.39)	1.734 (0.37)	1.802 (0.35)	1.862 (0.36)	1.885 (0.32)	1.904 (0.53)
			1.511 (0.56)	1.397 (0.41)	1.409 (0.41)	1.491 (0.37)	1.568 (0.41)	1.640 (0.42)	1.686 (0.31)	1.712 (0.39)	1.711 (0.55)
		0	2.211 (0.36)	1.510 (0.38)	1.350 (0.41)	1.372 (0.40)	1.440 (0.39)	1.498 (0.37)	1.544 (0.42)	1.571 (0.39)	1.589 (0.52)
	0	0	0	2.156 (0.35)	1.499 (0.41)	1.405 (0.45)	1.436 (0.39)	1.489 (0.38)	1.550 (0.40)	1.571 (0.39)	1.567 (0.57)
0	0	0	0	0	2.299 (0.39)	2.002 (0.42)	2.039 (0.35)	2.122 (0.36)	2.201 (0.34)	2.231 (0.35)	2.259 (0.50)

Fig. 2.7b. Pin-power distribution for NITAWL benchmark PNL-30. Value in parentheses is the percent standard deviation.

Table 2.5. PNL-30 CENTRM reaction rates and fluxes

Pin	Region	$\langle\sigma_a\phi\rangle$ (cm^{-3} - s^{-1})	$\langle\nu\sigma_f\phi\rangle$ (cm^{-3} - s^{-1})	$\langle\sigma_f\phi\rangle$ (cm^{-3} - s^{-1})	$\langle\phi\rangle$ (cm - s^{-1})	$\langle\phi\rangle/\langle\phi\rangle_t$
	Fuel	1.417E-05	2.311E-05	8.244E-06	1.385E-2	0.412
1	Clad	2.864E-07	0.0	0.0	2.672E-3	0.079
	Mod.	5.922E-07	0.0	0.0	1.710E-2	0.509
	Fuel	1.809E-05	2.453E-05	8.727E-06	3.412E-2	0.410
69	Clad	4.701E-07	0.0	0.0	6.638E-3	0.080
	Mod.	5.476E-07	0.0	0.0	4.237E-2	0.510

Table 2.6. PNL-30 NITAWL reaction rates and fluxes

Pin	Region	$\langle\sigma_a\phi\rangle$ (cm^{-3} - s^{-1})	$\langle\nu\sigma_f\phi\rangle$ (cm^{-3} - s^{-1})	$\langle\sigma_f\phi\rangle$ (cm^{-3} - s^{-1})	$\langle\phi\rangle$ (cm - s^{-1})	$\langle\phi\rangle/\langle\phi\rangle_t$
	Fuel	1.407E-05	2.297E-05	8.192E-06	1.384E-2	0.412
1	Clad	2.802E-07	0.0	0.0	2.660E-3	0.079
	Mod.	5.895E-07	0.0	0.0	1.707E-2	0.509
	Fuel	1.835E-05	2.515E-05	8.948E-06	3.395E-2	0.410
69	Clad	4.678E-07	0.0	0.0	6.629E-3	0.080
	Mod.	5.644E-07	0.0	0.0	4.232E-2	0.510

Table 2.7. PNL-30, Pin-1 four-group fluxes

Group	CENTRM Φ (cm^{-2} - s^{-1})	NITAWL Φ (cm^{-2} - s^{-1})
1	7.308E-05	7.296E-05
2	2.292E-05	2.291E-05
3	5.145E-06	5.269E-06
4	2.251E-05	2.239E-05

Table 2.8. PNL-30, Pin-1 four-group U-235 cross sections

Group	CENTRM cross sections (cm^{-1})			NITAWL cross sections (cm^{-1})		
	Σ_a	$\langle\Sigma_f\rangle$	Σ_f	Σ_a	$\langle\Sigma_f\rangle$	Σ_f
1	2.31102E-04	5.17496E-04	2.00508E-04	2.30990E-04	5.17470E-04	2.00433E-04
2	5.24167E-03	8.10227E-03	3.32510E-03	5.22152E-03	8.04138E-03	3.30010E-03
3	8.11652E-03	1.64870E-02	6.76610E-03	8.06149E-03	1.64181E-02	6.73784E-03
4	7.34638E-02	1.52885E-01	6.27423E-02	7.34430E-02	1.52842E-01	6.27253E-02

Table 2.9. PNL-30, Pin-1 four-group U-238 cross sections

Group	CENTRM cross sections (cm^{-1})			NITAWL cross sections (cm^{-1})		
	Σ_a	$\langle\Sigma_f\rangle$	Σ_f	Σ_a	$\langle\Sigma_f\rangle$	Σ_f
1	6.78395E-03	1.18456E-02	4.21512E-03	6.78829E-03	1.18801E-02	4.22404E-03
2	4.50410E-02	5.66348E-06	2.34636E-06	4.43898E-02	5.54963E-06	2.29918E-06
3	1.10308E-02	3.81572E-08	1.58093E-08	1.10387E-02	3.82177E-08	1.58343E-08
4	4.21801E-02	1.98117E-07	8.20835E-08	4.21730E-02	1.98085E-07	8.20706E-08

Table 2.10. PNL-30, Pin-1 four-group Pu-239 cross sections

Group	CENTRM cross sections (cm^{-1})			NITAWL cross sections (cm^{-1})		
	Σ_a	$\langle\Sigma_f\rangle$	Σ_f	Σ_a	$\langle\Sigma_f\rangle$	Σ_f
1	7.31247E-04	2.10623E-03	6.81955E-04	7.31013E-04	2.10628E-03	6.81768E-04
2	1.46556E-02	2.42259E-02	8.41230E-03	1.42800E-02	2.35796E-02	8.18791E-03
3	4.46091E-02	8.80453E-02	3.05734E-02	4.45318E-02	8.79178E-02	3.05291E-02
4	3.81701E-01	7.65540E-01	2.64839E-01	3.80931E-01	7.64203E-01	2.64376E-01

Table 2.11. PNL-30, Pin-69 four-group fluxes

Group	CENTRM Φ (cm^{-2} - s^{-1})	NITAWL Φ (cm^{-2} - s^{-1})
1	1.978E-04	1.958E-04
2	7.342E-05	7.309E-05
3	1.445E-05	1.458E-05
4	1.901E-05	1.966E-05

Table 2.12. PNL-30, Pin-69 four-group U-235 cross sections

Group	CENTRM cross sections (cm^{-1})			NITAWL cross sections (cm^{-1})		
	Σ_a	$\langle\Sigma_f\rangle$	Σ_f	Σ_a	$\langle\Sigma_f\rangle$	Σ_f
1	2.40583E-04	5.25394E-04	2.05274E-04	2.40289E-04	5.25082E-04	2.05125E-04
2	5.09194E-03	7.87946E-03	3.23366E-03	4.90525E-03	7.60379E-03	3.12052E-03
3	8.03087E-03	1.62800E-02	6.68118E-03	8.07572E-03	1.64173E-02	6.73752E-03
4	6.44140E-02	1.33756E-01	5.48922E-02	6.49323E-02	1.34838E-01	5.53362E-02

Table 2.13. PNL-30, Pin-69 four-group U-238 cross sections

Group	CENTRM cross sections (cm^{-1})			NITAWL cross sections (cm^{-1})		
	Σ_a	$\langle\Sigma_f\rangle$	Σ_f	Σ_a	$\langle\Sigma_f\rangle$	Σ_f
1	6.48013E-03	1.00639E-02	3.58425E-03	6.50153E-03	1.01355E-02	3.61266E-03
2	4.33496E-02	5.86890E-06	2.43146E-06	4.25035E-02	5.67595E-06	2.35151E-06
3	1.10028E-02	3.78364E-08	1.56763E-08	1.10397E-02	3.81740E-08	1.58162E-08
4	3.74989E-02	1.75656E-07	7.27780E-08	3.77530E-02	1.76873E-07	7.32818E-08

Table 2.14. PNL-30, Pin-69 four-group Pu-239 cross sections

Group	CENTRM cross sections (cm^{-1})			NITAWL cross sections (cm^{-1})		
	Σ_a	$\langle\Sigma_f\rangle$	Σ_f	Σ_a	$\langle\Sigma_f\rangle$	Σ_f
1	7.34312E-04	2.06900E-03	6.75303E-04	7.34377E-04	2.07025E-03	6.75577E-04
2	1.41486E-02	2.33093E-02	8.09402E-03	1.38472E-02	2.29011E-02	7.95226E-03
3	4.37500E-02	8.64152E-02	3.00072E-02	4.41986E-02	8.73169E-02	3.03204E-02
4	4.24647E-01	8.20289E-01	2.83994E-01	4.24708E-01	8.21267E-01	2.84326E-01

											1.824 (0.90)
										1.821 (0.58)	1.818 (0.53)
									1.780 (0.50)	1.785 (0.32)	1.817 (0.48)
								1.693 (0.56)	1.725 (038.)	1.759 (0.36)	1.764 (0.47)
							1.611 (055.)	1.650 (0.34)	1.683 (0.35)	1.706 (0.36)	1.687 (0.50)
						1.492 (0.52)	1.535 (0.38)	1.601 (0.35)	1.624 (0.40)	1.633 (0.38)	1.634 (052.)
					1.338 (0.58)	1.419 (0.41)	1.476 (0.41)	1.509 (0.35)	1.550 (0.37)	1.562 (0.41)	1.570 (0.57)
				1.202 (064.)	1.271 (0.42)	1.332 (0.39)	1.385 (0.40)	1.437 (0.36)	1.460 (0.44)	1.488 (0.40)	1.500 (0.51)
			1.018 (0.65)	1.098 (0.46)	1.175 (0.42)	1.245 (0.48)	1.304 (0.38)	1.346 (0.40)	1.359 (0.40)	1.393 (0.40)	1.393 (0.59)
		0.861 (0.74)	0.930 (0.45)	1.016 (0.48)	1.078 (0.45)	1.139 (0.45)	1.195 (0.46)	1.228 (0.40)	1.261 (0.41)	1.282 (0.45)	1.288 (0.58)
	0.719 (0.74)	0.777 (0.57)	0.849 (0.55)	0.919 (0.46)	0.978 (0.53)	1.026 (0.43)	1.088 (0.43)	1.121 (0.49)	1.157 (0.44)	1.164 (0.45)	1.181 (0.66)
0.924 (0.72)	0.737 (0.59)	0.737 (0.54)	0.771 (0.57)	0.822 (0.52)	0.872 (0.47)	0.918 (0.48)	0.965 (0.46)	1.011 (0.51)	1.043 (0.47)	1.054 (0.45)	1.056 (0.64)
0	0.985 (0.52)	0.860 (0.51)	0.772 (0.55)	0.756 (0.56)	0.787 (0.57)	0.818 (0.53)	0.862 (0.51)	0.888 (0.48)	0.916 (0.53)	0.932 (0.42)	0.944 (0.67)
0	0	0	1.046 (0.49)	0.900 (0.48)	0.789 (0.52)	0.782 (0.57)	0.792 (0.56)	0.788 (0.56)	0.803 (0.49)	0.820 (0.51)	0.821 (0.70)
0	0	0	0	0	1.065 (0.45)	0.946 (0.50)	0.890 (0.55)	0.781 (0.59)	0.745 (0.55)	0.751 (0.60)	0.764 (0.79)
0	0	0	0	0	0	0	0	1.051 (0.45)	0.917 (0.54)	0.911 (0.50)	0.903 (0.77)

Fig. 2.8a. Pin-power distribution for CENTRM benchmark PNL-31. Value in parentheses is percent standard deviation.

											1.829 (1.01)
										1.827 (0.51)	1.832 (0.53)
									1.775 (0.50)	1.798 (0.35)	1.794 (0.52)
								1.722 (0.57)	1.742 (0.35)	1.776 (0.37)	1.785 (0.51)
							1.612 (0.53)	1.666 (0.36)	1.698 (0.38)	1.716 (0.35)	1.724 (0.50)
						1.502 (0.53)	1.549 (0.38)	1.593 (0.40)	1.640 (0.35)	1.644 (0.37)	1.646 (0.56)
					1.353 (0.57)	1.418 (0.43)	1.474 (0.37)	1.525 (0.38)	1.566 (0.38)	1.580 (0.38)	1.572 (0.51)
				1.192 (0.61)	1.274 (0.44)	1.343 (0.39)	1.402 (0.41)	1.435 (0.38)	1.478 (0.41)	1.493 (0.37)	1.486 (0.58)
			1.017 (0.66)	1.107 (0.47)	1.177 (0.43)	1.252 (0.40)	1.299 (0.39)	1.359 (0.42)	1.381 (0.44)	1.384 (0.40)	1.399 (0.55)
		0.860 (0.75)	0.929 (0.51)	1.010 (0.46)	1.079 (0.46)	1.145 (0.45)	1.202 (0.41)	1.245 (0.43)	1.272 (0.39)	1.295 (0.43)	1.297 (0.59)
	0.722 (0.79)	0.771 (0.55)	0.841 (0.55)	0.915 (0.51)	0.977 (0.43)	1.041 (0.47)	1.106 (0.47)	1.131 (0.43)	1.162 (0.43)	1.179 (0.48)	1.181 (0.60)
0.937 (0.68)	0.736 (0.61)	0.728 (0.54)	0.766 (0.58)	0.825 (0.55)	0.880 (0.47)	0.917 (0.49)	0.982 (0.47)	1.013 (0.45)	1.031 (0.46)	1.049 (0.45)	1.064 (0.66)
0	0.991 (0.51)	0.853 (0.52)	0.774 (0.57)	0.771 (0.53)	0.795 (0.53)	0.827 (0.53)	0.866 (0.48)	0.891 (0.52)	0.918 (0.52)	0.925 (0.44)	0.936 (0.67)
0	0	0	1.039 (0.54)	0.888 (0.51)	0.787 (0.50)	0.778 (0.47)	0.787 (0.60)	0.798 (0.55)	0.803 (0.52)	0.811 (0.51)	0.817 (0.72)
0	0	0	0	0	1.064 (0.49)	0.952 (0.45)	0.896 (0.51)	0.782 (0.53)	0.751 (0.55)	0.757 (0.55)	0.744 (0.80)
0	0	0	0	0	0	0	0	1.052 (0.48)	0.917 (0.52)	0.905 (0.49)	0.914 (0.71)

Fig. 2.8b. Pin power distribution for NITAWL benchmark PNL-31. Value in parentheses is percent standard deviation.

Table 2.15. PNL-31 CENTRM reaction rates and fluxes

Pin	Region	$\langle\sigma_a\phi\rangle$ (cm^{-3} - s^{-1})	$\langle\nu\sigma_f\phi\rangle$ (cm^{-3} - s^{-1})	$\langle\sigma_f\phi\rangle$ (cm^{-3} - s^{-1})	$\langle\phi\rangle$ (cm - s^{-1})	$\langle\phi\rangle/\langle\phi\rangle_t$
	Fuel	6.732E-06	1.0493E-05	3.738E-06	7.748E-3	0.412
1	Clad	1.407E-07	0.0	0.0	1.494E-3	0.079
	Mod.	5.801E-07	0.0	0.0	9.563E-3	0.509
	Fuel	1.352E-05	1.821E-05	6.477E-06	2.577E-2	0.410
109	Clad	3.513E-07	0.0	0.0	5.039E-3	0.081
	Mod.	8.806E-07	0.0	0.0	3.197E-2	0.509

Table 2.16. PNL-31 NITAWL reaction rates and fluxes

Pin	Region	$\langle\sigma_a\phi\rangle$ (cm^{-3} - s^{-1})	$\langle\nu\sigma_f\phi\rangle$ (cm^{-3} - s^{-1})	$\langle\sigma_f\phi\rangle$ (cm^{-3} - s^{-1})	$\langle\phi\rangle$ (cm - s^{-1})	$\langle\phi\rangle/\langle\phi\rangle_t$
	Fuel	6.745E-06	1.049E-05	3.740E-06	7.754E-3	0.412
1	Clad	1.404E-07	0.0	0.0	1.500E-3	0.079
	Mod.	5.820E-07	0.0	0.0	9.588E-3	0.509
	Fuel	1.362E-05	1.838E-05	6.538E-06	2.583E-2	0.411
109	Clad	3.478E-07	0.0	0.0	5.033E-3	0.080
	Mod.	8.960E-07	0.0	0.0	3.200E-2	0.509

Table 2.17. PNL-31, Pin-1 four-group fluxes

Group	CENTRM Φ (cm^{-2} - s^{-1})	NITAWL Φ (cm^{-2} - s^{-1})
1	4.151E-05	4.145E-05
2	1.455E-05	1.468E-05
3	3.350E-06	3.351E-06
4	9.754E-06	9.744E-06

Table 2.18. PNL-31, Pin-1 four-group U-235 cross sections

Group	CENTRM cross sections (cm^{-1})			NITAWL cross sections (cm^{-1})		
	σ_a	$\langle\sigma_f$	σ_f	σ_a	$\langle\sigma_f$	σ_f
1	2.34277E-04	5.20559E-04	2.02137E-04	2.34433E-04	5.20890E-04	2.02275E-04
2	5.31166E-03	8.16900E-03	3.35248E-03	5.27939E-03	8.08910E-03	3.31969E-03
3	8.11675E-03	1.65287E-02	6.78319E-03	8.06329E-03	1.64082E-02	6.73381E-03
4	7.08071E-02	1.47273E-01	6.04396E-02	7.10855E-02	1.47857E-01	6.06792E-02

Table 2.19. PNL-31, Pin-1 four-group U-238 cross sections

Group	CENTRM cross sections (cm^{-1})			NITAWL cross sections (cm^{-1})		
	σ_a	$\langle\sigma_f$	σ_f	σ_a	$\langle\sigma_f$	σ_f
1	6.72455E-03	1.13885E-02	4.04980E-03	6.74729E-03	1.14467E-02	4.07385E-03
2	4.56936E-02	5.60056E-06	2.32029E-06	4.55851E-02	5.56831E-06	2.30692E-06
3	1.10516E-02	3.83036E-08	1.58698E-08	1.10407E-02	3.82095E-08	1.58309E-08
4	4.08111E-02	1.91551E-07	7.93633E-08	4.09499E-02	1.92215E-07	7.96381E-08

Table 2.20. PNL-31, Pin-1 four-group Pu-239 cross sections

Group	CENTRM cross sections (cm^{-1})			NITAWL cross sections (cm^{-1})		
	σ_a	$\langle\sigma_f$	σ_f	σ_a	$\langle\sigma_f$	σ_f
1	7.32515E-04	2.09589E-03	6.79949E-04	7.32859E-04	2.09690E-03	6.80273E-04
2	1.48948E-02	2.45228E-02	8.51540E-03	1.45238E-02	2.40236E-02	8.34210E-03
3	4.46260E-02	8.81024E-02	3.05931E-02	4.49138E-02	8.86079E-02	3.07687E-02
4	3.92873E-01	7.79195E-01	2.69624E-01	3.93098E-01	7.80112E-01	2.69936E-01

Table 2.21. PNL-31, Pin-109 four-group fluxes

Group	CENTRM $\overline{M}$ (cm^{-2} - s^{-1})	NITAWL $\overline{M}$ (cm^{-2} - s^{-1})
1	1.485E-04	1.486E-04
2	5.674E-05	5.667E-05
3	1.105E-05	1.126E-05
4	1.379E-05	1.412E-05

Table 2.22. PNL-31, Pin-109 four-group U-235 cross sections

Group	CENTRM cross sections (cm^{-1})			NITAWL cross sections (cm^{-1})		
	$\overline{\sigma_a}$	$\overline{\nu\sigma_f}$	$\overline{\sigma_f}$	$\overline{\sigma_a}$	$\overline{\nu\sigma_f}$	$\overline{\sigma_f}$
1	2.40011E-04	5.25238E-04	2.05020E-04	2.41044E-04	5.25948E-04	2.05500E-04
2	5.08433E-03	7.90435E-03	3.24387E-03	5.05763E-03	7.83928E-03	3.21717E-03
3	7.87603E-03	1.60055E-02	6.56854E-03	7.93289E-03	1.60894E-02	6.60295E-03
4	6.39052E-02	1.32666E-01	5.44450E-02	6.44026E-02	1.33734E-01	5.48830E-02

Table 2.23. PNL-31, Pin-109 four-group U-238 cross sections

Group	CENTRM cross sections (cm^{-1})			NITAWL cross sections (cm^{-1})		
	$\overline{\sigma_a}$	$\overline{\nu\sigma_f}$	$\overline{\sigma_f}$	$\overline{\sigma_a}$	$\overline{\nu\sigma_f}$	$\overline{\sigma_f}$
1	6.52904E-03	1.02652E-02	3.65253E-03	6.48723E-03	1.00441E-02	3.57473E-03
2	4.26228E-02	5.78745E-06	2.39771E-06	4.25107E-02	5.49843E-06	2.27798E-06
3	1.10023E-02	3.78561E-08	1.56844E-08	1.09805E-02	3.77877E-08	1.56562E-08
4	3.72074E-02	1.74257E-07	7.21979E-08	3.74882E-02	1.75595E-07	7.27521E-08

Table 2.24. PNL-31, Pin-109 four-group Pu-239 cross sections

Group	CENTRM cross sections (cm^{-1})			NITAWL cross sections (cm^{-1})		
	$\overline{\sigma_a}$	$\overline{\nu\sigma_f}$	$\overline{\sigma_f}$	$\overline{\sigma_a}$	$\overline{\nu\sigma_f}$	$\overline{\sigma_f}$
1	7.34579E-04	2.07331E-03	6.76047E-04	7.34616E-04	2.06809E-03	6.74966E-04
2	1.42795E-02	2.36502E-02	8.21241E-03	1.41529E-02	2.32927E-02	8.08827E-03
3	4.25902E-02	8.43169E-02	2.92786E-02	4.25863E-02	8.42498E-02	2.92554E-02
4	4.32807E-01	8.32922E-01	2.88390E-01	4.26617E-01	8.23669E-01	2.85166E-01

0	0	0	0	0	0	0	4.104	3.592	3.967	0	0	0	0	0	0	0
0	0	0	0	0	0	4.526	3.498	3.291	3.407	3.866	4.466	0	0	0	0	0
0	0	0	0	4.931	4.345	3.900	3.723	3.716	3.703	3.685	3.685	4.587	0	0	0	0
0	0	0	4.714	3.978	4.001	4.116	4.282	4.343	4.308	4.142	3.941	3.917	4.729	0	0	0
0	0	4.627	3.919	4.040	4.348	4.602	4.824	4.909	4.867	4.690	4.406	4.053	3.954	4.586	0	0
0	4.571	3.828	3.932	4.394	4.732	5.084	5.314	5.470	5.314	5.046	4.789	4.388	3.947	3.705	4.529	0
0	3.922	3.663	4.307	4.687	5.147	5.525	5.761	5.808	5.730	5.474	5.132	4.724	4.133	3.716	3.894	0
4.157	3.430	3.833	4.318	4.889	5.371	5.758	5.973	6.000	5.910	5.721	5.336	4.926	4.334	3.776	3.452	4.097
3.718	3.346	3.822	4.366	4.891	5.430	5.794	6.009	6.086	6.014	5.818	5.526	4.983	4.389	3.801	3.329	3.647
4.092	3.451	3.831	4.371	4.841	5.391	5.711	5.923	5.990	5.928	5.707	5.408	4.879	4.329	3.765	3.512	4.149
0	3.884	3.703	4.188	4.675	5.207	5.526	5.712	5.786	5.739	5.492	5.143	4.681	4.107	3.701	3.953	0
0	4.583	3.803	4.002	4.472	4.861	5.180	5.299	5.429	5.395	5.173	4.764	4.385	3.921	3.733	4.522	0
0	0	4.695	3.920	4.100	4.404	4.715	4.886	4.992	4.915	4.709	4.402	4.043	3.925	4.545	0	0
0	0	0	4.721	3.921	3.954	4.219	4.362	4.377	4.325	4.198	3.946	3.951	4.748	0	0	0
0	0	0	0	4.639	3.762	3.701	3.821	3.812	3.789	3.926	4.415	4.865	0	0	0	0
0	0	0	0	0	4.516	3.925	3.438	3.393	3.471	4.512	0	0	0	0	0	0
0	0	0	0	0	0	0	4.100	3.642	4.175	0	0	0	0	0	0	0

Fig. 2.9a. Pin-power distribution for CENTRM benchmark PNL-32 with standard deviation between 0.59 and 0.87% of the value.

0	0	0	0	0	0	0	4.193	3.696	4.139	0	0	0	0	0	0	0
0	0	0	0	0	0	4.568	3.565	3.354	3.466	3.987	4.530	0	0	0	0	0
0	0	0	0	4.902	4.409	3.981	3.841	3.804	3.753	3.706	3.767	4.624	0	0	0	0
0	0	0	4.739	3.971	4.071	4.190	4.304	4.352	4.301	4.177	3.952	3.930	4.705	0	0	0
0	0	4.625	3.956	4.080	4.417	4.773	4.884	4.914	4.907	4.720	4.427	4.010	3.991	4.684	0	0
0	4.612	3.769	4.039	4.470	4.913	5.191	5.404	5.433	5.357	5.142	4.790	4.319	3.940	3.779	4.489	0
0	3.884	3.700	4.150	4.792	5.200	5.595	5.759	5.763	5.729	5.484	5.192	4.683	4.164	3.727	3.874	0
4.153	3.500	3.842	4.455	4.989	5.431	5.783	5.974	5.974	5.953	5.726	5.346	4.840	4.324	3.784	3.470	4.059
3.735	3.352	3.825	4.417	4.978	5.524	5.756	6.026	6.099	5.988	5.801	5.425	4.969	4.412	3.818	3.329	3.711
4.211	3.533	3.823	4.416	4.969	5.395	5.781	5.929	5.958	5.856	5.731	5.360	4.817	4.315	3.757	3.404	4.099
0	3.894	3.705	4.182	4.755	5.208	5.492	5.682	5.749	5.595	5.475	5.095	4.677	4.078	3.680	3.876	0
0	4.558	3.742	4.015	4.413	4.846	5.195	5.336	5.383	5.265	5.059	4.737	4.377	3.944	3.712	4.465	0
0	0	4.614	3.980	4.088	4.380	4.731	4.941	4.880	4.853	4.659	4.358	4.024	3.882	4.574	0	0
0	0	0	4.789	3.910	3.973	4.142	4.350	4.423	4.348	4.130	3.973	3.904	4.683	0	0	0
0	0	0	0	4.625	3.768	3.664	3.837	3.803	3.735	3.920	4.301	4.912	0	0	0	0
0	0	0	0	0	4.516	3.907	3.442	3.317	3.414	4.463	0	0	0	0	0	0
0	0	0	0	0	0	0	4.045	3.626	4.106	0	0	0	0	0	0	0

Fig. 2.9b. Pin-power distribution for NITAWL benchmark PNL-32 with standard deviation between 0.57 and 0.90% of the values.

Table 2.25. PNL-32 CENTRM reaction rates and fluxes

Pin	Region	$\sigma_a \phi$ ($cm^{-3} - s^{-1}$)	$\langle \sigma_f \phi$ ($cm^{-3} - s^{-1}$)	$\sigma_f \phi$ ($cm^{-3} - s^{-1}$)	ϕ ($cm - s^{-1}$)	ϕ/ϕ_t
	Fuel	2.451E-05	4.086E-05	1.457E-05	2.060E-2	0.267
1	Clad	4.627E-07	0.0	0.0	3.943E-3	0.051
	Mod.	1.135E-06	0.0	0.0	5.259E-2	0.682
	Fuel	3.946E-05	6.076E-05	2.164E-05	4.729E-2	0.266
98	Clad	8.113E-07	0.0	0.0	9.173E-3	0.052
	Mod.	1.536E-06	0.0	0.0	1.121E-2	0.682

Table 2.26. PNL-32 NITAWL reaction rates and fluxes

Pin	Region	$\sigma_a \phi$ ($cm^{-3} - s^{-1}$)	$\langle \sigma_f \phi$ ($cm^{-3} - s^{-1}$)	$\sigma_f \phi$ ($cm^{-3} - s^{-1}$)	ϕ ($cm - s^{-1}$)	ϕ/ϕ_t
	Fuel	2.429E-05	4.063E-05	1.449E-05	2.033E-2	0.266
1	Clad	4.624E-07	0.0	0.0	3.930E-3	0.051
	Mod.	1.136E-06	0.0	0.0	5.223E-2	0.683
	Fuel	3.963E-05	6.092E-05	2.169E-05	4.753E-2	0.267
98	Clad	8.007E-07	0.0	0.0	9.195E-3	0.052
	Mod.	1.550E-06	0.0	0.0	1.214E-1	0.681

Table 2.27. PNL-32, Pin-1 four-group fluxes

Group	CENTRM Φ (cm^{-2} - s^{-1})	NITAWL Φ (cm^{-2} - s^{-1})
1	1.048E-04	1.029E-04
2	3.087E-05	3.073E-05
3	7.654E-06	7.310E-06
4	4.050E-05	4.057E-05

Table 2.28. PNL-32, Pin-1 four-group U-235 cross sections

Group	CENTRM cross sections (cm^{-1})			NITAWL cross sections (cm^{-1})		
	σ_a	$\langle\sigma_f$	σ_f	σ_a	$\langle\sigma_f$	σ_f
1	2.28226E-04	5.15645E-04	1.99145E-04	2.28198E-04	5.16018E-04	1.99123E-04
2	5.29819E-03	8.08102E-03	3.31639E-03	5.44312E-03	8.33186E-03	3.41933E-03
3	8.13381E-03	1.64731E-02	6.76041E-03	8.07192E-03	1.63713E-02	6.71862E-03
4	7.46578E-02	1.55396E-01	6.37731E-02	7.43303E-02	1.54714E-01	6.34932E-02

Table 2.29. PNL-32, Pin-1 four-group U-238 cross sections

Group	CENTRM cross sections (cm^{-1})			NITAWL cross sections (cm^{-1})		
	σ_a	$\langle\sigma_f$	σ_f	σ_a	$\langle\sigma_f$	σ_f
1	6.95603E-03	1.26008E-02	4.48409E-03	6.96190E-03	1.26902E-02	4.50424E-03
2	4.76213E-02	5.91756E-06	2.45162E-06	4.49401E-02	5.50696E-06	2.28152E-06
3	1.10199E-02	3.80020E-08	1.57448E-08	1.10245E-02	3.79821E-08	1.57367E-08
4	4.27798E-02	2.00991E-07	8.32743E-08	4.26310E-02	2.00282E-07	8.29805E-08

Table 2.30. PNL-32, Pin-1 four-group Pu-239 cross sections

Group	CENTRM cross sections (cm^{-1})			NITAWL cross sections (cm^{-1})		
	σ_a	$\langle\sigma_f$	σ_f	σ_a	$\langle\sigma_f$	σ_f
1	7.30986E-04	2.12139E-03	6.84695E-04	7.30230E-04	2.12081E-03	6.84023E-04
2	1.53809E-02	2.53859E-02	8.81516E-03	1.48494E-02	2.44809E-02	8.50088E-03
3	4.46591E-02	8.80834E-02	3.05866E-02	4.50509E-02	8.87866E-02	3.08308E-02
4	3.79625E-01	7.64299E-01	2.64388E-01	3.77128E-01	7.59495E-01	2.62726E-01

Table 2.31. PNL-32, Pin-98 four-group fluxes

Group	CENTRM Φ (cm^{-2} - s^{-1})	NITAWL Φ (cm^{-2} - s^{-1})
1	2.586E-04	2.586E-04
2	8.866E-05	8.976E-05
3	1.956E-05	2.042E-05
4	5.545E-05	5.552E-05

Table 2.32. PNL-32, Pin-98 four-group U-235 cross sections

Group	CENTRM cross sections (cm^{-1})			NITAWL cross sections (cm^{-1})		
	σ_a	$\langle\sigma_f$	σ_f	σ_a	$\langle\sigma_f$	σ_f
1	2.34086E-04	5.20599E-04	2.02092E-04	2.34329E-04	5.21021E-04	2.02251E-04
2	5.15153E-03	7.96071E-03	3.26701E-03	5.21152E-03	7.99933E-03	3.28285E-03
3	8.14944E-03	1.65985E-02	6.81186E-03	8.16239E-03	1.66200E-02	6.82071E-03
4	7.06334E-02	1.46886E-01	6.02804E-02	7.03727E-02	1.46337E-01	6.00555E-02

Table 2.33. PNL-32, Pin-98 four-group U-238 cross sections

Group	CENTRM cross sections (cm^{-1})			NITAWL cross sections (cm^{-1})		
	σ_a	$\langle\sigma_f$	σ_f	σ_a	$\langle\sigma_f$	σ_f
1	6.75406E-03	1.14805E-02	4.08322E-03	6.78241E-03	1.15393E-02	4.10572E-03
2	4.75024E-02	5.74765E-06	2.38123E-06	4.63517E-02	5.42737E-06	2.24854E-06
3	1.10577E-02	3.83380E-08	1.58842E-08	1.10567E-02	3.83610E-08	1.58937E-08
4	4.07001E-02	1.91006E-07	7.91378E-08	4.05670E-02	1.90373E-07	7.88750E-08

Table 2.34. PNL-32, Pin-98 four-group Pu-239 cross sections

Group	CENTRM cross sections (cm^{-1})			NITAWL cross sections (cm^{-1})		
	σ_a	$\langle\sigma_f$	σ_f	σ_a	$\langle\sigma_f$	σ_f
1	7.32645E-04	2.09793E-03	6.80410E-04	7.32954E-04	2.09852E-03	6.80530E-04
2	1.46368E-02	2.41261E-02	8.37768E-03	1.46065E-02	2.41771E-02	8.39539E-03
3	4.63098E-02	9.11738E-02	3.16598E-02	4.55958E-02	8.98849E-02	3.12122E-02
4	3.98803E-01	7.88748E-01	2.72941E-01	3.99072E-01	7.88716E-01	2.72936E-01

											2.024 (1.15)
										2.037 (0.53)	2.025 (0.53)
									1.958 (0.50)	2.001 (0.40)	2.009 (0.55)
								1.872 (0.50)	1.935 (0.32)	1.955 (0.40)	1.973 (0.54)
							1.783 (0.57)	1.848 (0.41)	1.869 (0.37)	1.905 (0.40)	1.904 (0.51)
						1.626 (0.54)	1.702 (0.39)	1.760 (0.37)	1.801 (0.37)	1.832 (0.41)	1.848 (0.47)
					1.461 (0.56)	1.539 (0.42)	1.624 (0.37)	1.661 (0.37)	1.707 (0.41)	1.721 (0.37)	1.746 (0.55)
				1.275 (0.64)	1.368 (0.47)	1.450 (0.43)	1.509 (0.45)	1.564 (0.43)	1.599 (0.37)	1.636 (0.40)	1.638 (0.55)
			1.065 (0.68)	1.155 (0.47)	1.251 (0.50)	1.341 (0.45)	1.403 (0.43)	1.448 (0.39)	1.485 (0.43)	1.512 (0.41)	1.518 (0.58)
		0.850 (0.79)	0.954 (0.52)	1.040 (0.51)	1.130 (051.)	1.204 (0.45)	1.258 (0.45)	1.323 (0.45)	1.358 (0.43)	1.373 (0.42)	1.386 (0.60)
	0.639 (0.83)	0.738 (0.57)	0.846 (0.54)	0.910 (0.58)	1.008 (0.49)	1.077 (0.48)	1.137 (0.49)	1.182 (0.53)	1.213 (0.50)	1.231 (0.48)	1.240 (0.72)
0.564 (1.07)	0.554 (0.78)	0.633 (0.62)	0.712 (0.59)	0.793 (0.58)	0.866 (0.60)	0.931 (0.48)	0.991 (0.45)	1.039 (0.53)	1.078 (0.48)	1.092 (0.54)	1.099 (0.62)
0	0.565 (0.69)	0.594 (0.73)	0.618 (0.63)	0.663 (0.64)	0.731 (0.57)	0.786 (0.54)	0.838 (0.57)	0.883 (0.53)	0.932 (0.52)	0.942 (0.51)	0.937 (0.74)
0	0	0	0.621 (0.69)	0.628 (0.59)	0.628 (0.52)	0.658 (0.61)	0.702 (0.63)	0.735 (0.62)	0.761 (0.54)	0.783 (0.62)	0.783 (0.86)
0	0	0	0	0	0.622 (0.64)	0.618 (0.65)	0.639 (0.63)	0.619 (0.63)	0.623 (0.66)	0.641 (0.63)	0.659 (0.97)
0	0	0	0	0	0	0	0	0.610 (0.66)	0.570 (0.66)	0.585 (0.75)	0.604 (0.90)

Fig. 2.10a. Pin-power distribution for CENTRM benchmark PNL-33. Value in parentheses is percent standard deviation.

											2.037 (0.95)
										2.052 (0.57)	2.057 (0.51)
									2.004 (0.50)	2.007 (0.40)	2.018 (0.53)
								1.884 (0.57)	1.950 (0.36)	1.981 (0.38)	1.981 (0.51)
							1.783 (0.53)	1.833 (0.41)	1.883 (0.35)	1.917 (0.38)	1.917 (0.54)
						1.646 (0.55)	1.711 (0.38)	1.772 (0.37)	1.804 (0.40)	1.823 (0.40)	1.827 (0.49)
					1.466 (0.59)	1.553 (0.39)	1.610 (0.40)	1.670 (0.43)	1.718 (0.41)	1.736 (0.37)	1.751 (0.50)
				1.245 (0.60)	1.362 (0.43)	1.456 (0.39)	1.527 (0.40)	1.572 (0.41)	1.604 (0.41)	1.643 (0.40)	1.638 (0.54)
			1.067 (0.72)	1.155 (0.45)	1.257 (0.46)	1.330 (0.48)	1.403 (0.43)	1.447 (0.43)	1.491 (0.43)	1.509 (0.42)	1.528 (0.55)
		0.839 (0.75)	0.943 (0.60)	1.050 (0.52)	1.135 (0.48)	1.220 (0.47)	1.283 (0.45)	1.321 (0.48)	1.371 (0.47)	1.393 (0.45)	1.391 (0.60)
	0.632 (0.82)	0.731 (0.65)	0.824 (0.57)	0.919 (0.50)	1.004 (0.50)	1.069 (0.49)	1.141 (0.47)	1.181 (0.52)	1.220 (0.44)	1.247 (0.44)	1.249 (063.)
0.565 (0.98)	0.561 (0.63)	0.631 (0.62)	0.703 (0.54)	0.788 (0.53)	0.880 (0.54)	0.938 (0.51)	0.990 (0.53)	1.042 (0.53)	1.071 (0.53)	1.099 (0.50)	1.088 (0.73)
0	0.566 (0.64)	0.586 (0.69)	0.617 (0.62)	0.672 (0.68)	0.729 (0.58)	0.795 (0.53)	0.845 (0.55)	0.886 (0.53)	0.922 (0.55)	0.941 (0.55)	0.947 (0.78)
0	0	0	0.619 (0.69)	0.618 (0.67)	0.625 (0.68)	0.665 (0.63)	0.708 (0.54)	0.737 (0.61)	0.763 (0.54)	0.776 (0.62)	0.797 (0.82)
0	0	0	0	0	0.621 (0.67)	0.619 (0.68)	0.637 (0.67)	0.618 (0.65)	0.629 (0.68)	0.634 (0.69)	0.642 (0.97)
0	0	0	0	0	0	0	0	0.608 (0.65)	0.579 (0.62)	0.588 (0.72)	0.590 (0.96)

Fig. 2.10b. Pin-power distribution for NITAWL benchmark PNL-33. Value in parentheses is percent standard deviation.

Table 2.35. PNL-33 CENTRM reaction rates and fluxes

Pin	Region	$\langle\sigma_a\phi\rangle$ (cm^{-3} - s^{-1})	$\langle\nu\sigma_f\phi\rangle$ (cm^{-3} - s^{-1})	$\langle\sigma_f\phi\rangle$ (cm^{-3} - s^{-1})	$\langle\phi\rangle$ (cm - s^{-1})	$\langle\phi\rangle/\langle\phi\rangle_t$
	Fuel	3.818E-06	6.043E-06	2.152E-06	3.853E-3	0.267
1	Clad	7.376E-08	0.0	0.0	7.423E-4	0.051
	Mod.	4.770E-07	0.0	0.0	9.836E-3	0.682
	Fuel	1.360E-05	2.034E-05	7.243E-06	1.705E-2	0.265
109	Clad	2.788E-07	0.0	0.0	3.401E-3	0.051
	Mod.	1.498E-06	0.0	0.0	4.516E-2	0.684

Table 2.36. PNL-33 NITAWL reaction rates and fluxes

Pin	Region	$\langle\sigma_a\phi\rangle$ (cm^{-3} - s^{-1})	$\langle\nu\sigma_f\phi\rangle$ (cm^{-3} - s^{-1})	$\langle\sigma_f\phi\rangle$ (cm^{-3} - s^{-1})	$\langle\phi\rangle$ (cm - s^{-1})	$\langle\phi\rangle/\langle\phi\rangle_t$
	Fuel	3.812E-06	6.048E-06	2.155E-06	3.867E-3	0.267
1	Clad	7.253E-08	0.0	0.0	7.426E-4	0.052
	Mod.	4.787E-07	0.0	0.0	9.858E-3	0.681
	Fuel	1.375E-05	2.067E-05	7.357E-06	1.779E-2	0.268
109	Clad	2.783E-07	0.0	0.0	3.442E-3	0.052
	Mod.	1.505E-06	0.0	0.0	4.521E-2	0.680

Table 2.37. PNL-33, Pin-1 four-group fluxes

Group	CENTRM Φ (cm^{-2} - s^{-1})	NITAWL Φ (cm^{-2} - s^{-1})
1	2.014E-05	2.016E-05
2	6.869E-06	6.908E-06
3	1.672E-06	1.719E-06
4	5.718E-06	5.745E-06

Table 2.38. PNL-33, Pin-1 four-group U-235 cross sections

Group	CENTRM cross sections (cm^{-1})			NITAWL cross sections (cm^{-1})		
	Σ_a	$\langle\Sigma_f$	Σ_f	Σ_a	$\langle\Sigma_f$	Σ_f
1	2.31933E-04	5.20055E-04	2.01129E-04	2.31159E-04	5.18686E-04	2.00672E-04
2	5.35943E-03	8.22495E-03	3.37546E-03	5.34155E-03	8.22719E-03	3.37636E-03
3	8.26154E-03	1.68721E-02	6.92416E-03	8.25026E-03	1.68098E-02	6.89860E-03
4	7.10700E-02	1.47828E-01	6.06675E-02	7.10641E-02	1.47819E-01	6.06639E-02

Table 2.39. PNL-33, Pin-1 four-group U-238 cross sections

Group	CENTRM cross sections (cm^{-1})			NITAWL cross sections (cm^{-1})		
	Σ_a	$\langle\Sigma_f$	Σ_f	Σ_a	$\langle\Sigma_f$	Σ_f
1	6.93024E-03	1.22507E-02	4.34474E-03	6.91791E-03	1.22576E-02	4.35689E-03
2	4.93469E-02	5.63616E-06	2.33504E-06	4.72956E-02	5.71788E-06	2.36889E-06
3	1.10965E-02	3.87293E-08	1.60462E-08	1.10697E-02	3.84758E-08	1.59412E-08
4	4.09384E-02	1.92170E-07	7.96200E-08	4.09467E-02	1.92207E-07	7.96350E-08

Table 2.40. PNL-33, Pin-1 four-group Pu-239 cross sections

Group	CENTRM cross sections (cm^{-1})			NITAWL cross sections (cm^{-1})		
	Σ_a	$\langle\Sigma_f$	Σ_f	Σ_a	$\langle\Sigma_f$	Σ_f
1	7.32468E-04	2.11213E-03	6.82512E-04	7.31890E-04	2.11186E-03	6.82669E-04
2	1.55242E-02	2.53875E-02	8.81569E-03	1.47320E-02	2.43541E-02	8.45686E-03
3	4.75761E-02	9.35353E-02	3.24798E-02	4.58342E-02	9.03415E-02	3.13708E-02
4	3.92576E-01	7.79160E-01	2.69612E-01	3.91025E-01	7.76590E-01	2.68717E-01

Table 2.41. PNL-33, Pin-109 four-group fluxes

Group	CENTRM Φ (cm^{-2} - s^{-1})	NITAWL Φ (cm^{-2} - s^{-1})
1	9.567E-05	9.796E-05
2	3.454E-05	3.486E-05
3	8.083E-06	7.903E-06
4	1.794E-05	1.809E-05

Table 2.42. PNL-33, Pin-109 four-group U-235 cross sections

Group	CENTRM cross sections (cm^{-1})			NITAWL cross sections (cm^{-1})		
	$\bar{\sigma}_a$	$\bar{\sigma}_f$	$\bar{\sigma}_f$	$\bar{\sigma}_a$	$\bar{\sigma}_f$	$\bar{\sigma}_f$
1	2.35819E-04	5.23015E-04	2.03090E-04	2.36391E-04	5.23032E-04	2.03334E-04
2	5.23295E-03	8.08842E-03	3.31943E-03	5.36724E-03	8.21076E-03	3.36962E-03
3	8.20877E-03	1.67738E-02	6.88382E-03	8.26627E-03	1.68900E-02	6.93152E-03
4	6.90920E-02	1.43635E-01	5.89465E-02	6.84549E-02	1.42274E-01	5.83881E-02

Table 2.43. PNL-33, Pin-109 four-group U-238 cross sections

Group	CENTRM cross sections (cm^{-1})			NITAWL cross sections (cm^{-1})		
	$\bar{\sigma}_a$	$\bar{\sigma}_f$	$\bar{\sigma}_f$	$\bar{\sigma}_a$	$\bar{\sigma}_f$	$\bar{\sigma}_f$
1	6.78959E-03	1.14474E-02	4.06739E-03	6.75365E-03	1.12640E-02	4.00886E-03
2	4.77122E-02	5.87328E-06	2.43327E-06	4.72083E-02	5.94071E-06	2.46121E-06
3	1.10759E-02	3.86960E-08	1.60324E-08	1.11162E-02	3.88436E-08	1.60936E-08
4	3.99038E-02	1.87192E-07	7.75574E-08	3.95563E-02	1.85520E-07	7.68646E-08

Table 2.44. PNL-33, Pin-109 four-group Pu-239 cross sections

Group	CENTRM cross sections (cm^{-1})			NITAWL cross sections (cm^{-1})		
	$\bar{\sigma}_a$	$\bar{\sigma}_f$	$\bar{\sigma}_f$	$\bar{\sigma}_a$	$\bar{\sigma}_f$	$\bar{\sigma}_f$
1	7.33828E-04	2.09652E-03	6.79997E-04	7.33983E-04	2.09254E-03	6.79479E-04
2	1.54018E-02	2.52039E-02	8.75191E-03	1.50735E-02	2.48369E-02	8.62447E-03
3	4.51535E-02	8.91184E-02	3.09459E-02	4.89102E-02	9.59904E-02	3.33323E-02
4	4.06251E-01	7.98367E-01	2.76308E-01	4.12182E-01	8.07020E-01	2.79323E-01

								7.799 (0.66)
							7.518 (0.37)	7.649 (0.35)
						6.835 (0.40)	7.190 (0.27)	7.306 (0.37)
					5.772 (0.44)	6.293 (0.30)	6.617 (0.26)	6.772 (0.35)
				4.766 (0.47)	5.125 (0.31)	5.558 (0.30)	5.878 (0.29)	5.991 (0.39)
			0	5.095 (0.29)	4.633 (0.33)	4.852 (0.31)	5.064 (0.30)	5.107 (0.46)
		0	0	0	5.015 (0.27)	4.688 (0.34)	4.382 (0.33)	4.282 (0.47)
	0	0	0	0	0	0	4.431 (0.34)	3.764 (0.52)
0	0	0	0	0	0	0	0	4.082 (0.48)

Fig. 2.11a. Pin-power distribution for CENTRM benchmark PNL-34. Value in parentheses is percent standard deviation.

								7.789 (0.58)
							7.559 (0.29)	7.692 (0.25)
						6.856 (0.30)	7.211 (0.20)	7.342 (0.28)
					5.778 (0.31)	6.319 (0.21)	6.661 (0.21)	6.794 (0.32)
				4.790 (0.33)	5.142 (0.25)	5.607 (0.23)	5.928 (0.22)	5.991 (0.32)
			0	5.108 (0.24)	4.634 (0.25)	4.865 (0.21)	5.047 (0.23)	5.134 (0.33)
		0	0	0	5.009 (0.25)	4.689 (0.24)	4.367 (0.26)	4.295 (0.36)
	0	0	0	0	0	0	4.412 (0.26)	3.775 (0.40)
0	0	0	0	0	0	0	0	4.055 (0.41)

Fig. 2.11b. Pin-power distribution for NITAWL benchmark PNL-34. Value in parentheses is percent standard deviation.

Table 2.45. PNL-34 CENTRM reaction rates and fluxes

Pin	Region	$\langle\sigma_a\phi\rangle$ (cm^{-3} - s^{-1})	$\langle\nu\sigma_f\phi\rangle$ (cm^{-3} - s^{-1})	$\langle\sigma_f\phi\rangle$ (cm^{-3} - s^{-1})	$\langle\phi\rangle$ (cm - s^{-1})	$\langle\phi\rangle/\langle\phi\rangle_t$
	Fuel	2.378E-05	4.072E-05	1.453E-05	1.638E-2	0.205
1	Clad	4.283E-07	0.0	0.0	3.115E-3	0.039
	Mod.	1.208E-06	0.0	0.0	6.042E-2	0.756
	Fuel	4.850E-05	7.778E-05	2.772E-05	4.812E-2	0.206
27	Clad	9.350E-07	0.0	0.0	9.315E-3	0.039
	Mod.	2.117E-06	0.0	0.0	1.767E-1	0.755

Table 2.46. PNL-34 NITAWL reaction rates and fluxes

Pin	Region	$\langle\sigma_a\phi\rangle$ (cm^{-3} - s^{-1})	$\langle\nu\sigma_f\phi\rangle$ (cm^{-3} - s^{-1})	$\langle\sigma_f\phi\rangle$ (cm^{-3} - s^{-1})	$\langle\phi\rangle$ (cm - s^{-1})	$\langle\phi\rangle/\langle\phi\rangle_t$
	Fuel	2.359E-05	4.048E-05	1.444E-05	1.632E-2	0.205
1	Clad	4.263E-07	0.0	0.0	3.103E-3	0.039
	Mod.	1.204E-06	0.0	0.0	6.010E-2	0.756
	Fuel	4.865E-05	7.795E-5	2.778E-05	4.833E-2	0.206
27	Clad	9.241E-07	0.0	0.0	9.314E-3	0.040
	Mod.	2.122E-06	0.0	0.0	1.768E-1	0.754

Table 2.47. PNL-34, Pin-1 four-group fluxes

Group	CENTRM Φ (cm^{-2} - s^{-1})	NITAWL Φ (cm^{-2} - s^{-1})
1	7.853E-05	7.833E-05
2	2.067E-05	2.085E-05
3	5.292E-06	5.285E-06
4	4.175E-05	4.127E-05

Table 2.48. PNL-34, Pin-1 four-group U-235 cross sections

Group	CENTRM cross sections (cm^{-1})			NITAWL cross sections (cm^{-1})		
	$\bar{\sigma}_a$	$\bar{\nu\sigma}_f$	$\bar{\sigma}_f$	$\bar{\sigma}_a$	$\bar{\nu\sigma}_f$	$\bar{\sigma}_f$
1	2.24131E-04	5.12577E-04	1.97109E-04	2.23704E-04	5.11854E-04	1.96816E-04
2	5.42283E-03	8.35085E-03	3.42710E-03	5.42556E-03	8.28643E-03	3.40068E-03
3	8.31740E-03	1.69753E-02	6.96653E-03	8.31298E-03	1.69590E-02	6.95981E-03
4	7.54771E-02	1.57143E-01	6.44898E-02	7.58120E-02	1.57838E-01	6.47754E-02

Table 2.49. PNL-34, Pin-1 four-group U-238 cross sections

Group	CENTRM cross sections (cm^{-1})			NITAWL cross sections (cm^{-1})		
	$\bar{\sigma}_a$	$\bar{\nu\sigma}_f$	$\bar{\sigma}_f$	$\bar{\sigma}_a$	$\bar{\nu\sigma}_f$	$\bar{\sigma}_f$
1	7.08275E-03	1.34026E-02	4.75965E-03	7.06095E-03	1.33747E-02	4.74910E-03
2	5.08244E-02	6.00968E-06	2.48979E-06	4.81132E-02	5.51775E-06	2.28598E-06
3	1.11012E-02	3.87466E-08	1.60534E-08	1.11191E-02	3.89584E-08	1.61412E-08
4	4.32220E-02	2.03118E-07	8.41557E-08	4.33792E-02	2.03865E-07	8.44652E-08

Table 2.50. PNL-34, Pin-1 four-group Pu-239 cross sections

Group	CENTRM cross sections (cm^{-1})			NITAWL cross sections (cm^{-1})		
	$\bar{\sigma}_a$	$\bar{\nu\sigma}_f$	$\bar{\sigma}_f$	$\bar{\sigma}_a$	$\bar{\nu\sigma}_f$	$\bar{\sigma}_f$
1	7.29345E-04	2.13767E-03	6.87363E-04	7.28644E-04	2.13663E-03	6.86999E-04
2	1.53106E-02	2.52664E-02	8.77363E-03	1.54151E-02	2.54295E-02	8.83026E-03
3	4.67356E-02	9.20261E-02	3.19556E-02	4.76683E-02	9.37614E-02	3.25584E-02
4	3.72031E-01	7.53188E-01	2.60517E-01	3.73795E-01	7.56765E-01	2.61754E-01

Table 2.51. PNL-34, Pin-27 four-group fluxes

Group	CENTRM Φ (cm^{-2} - s^{-1})	NITAWL Φ (cm^{-2} - s^{-1})
1	2.549E-04	2.550E-04
2	8.111E-05	8.287E-05
3	1.947E-05	1.947E-05
4	7.406E-05	7.415E-05

Table 2.52. PNL-34, Pin-27 four-group U-235 cross sections

Group	CENTRM cross sections (cm^{-1})			NITAWL cross sections (cm^{-1})		
	Σ_a	$\langle\Sigma_f$	Σ_f	Σ_a	$\langle\Sigma_f$	Σ_f
1	2.32268E-04	5.19584E-04	2.01251E-04	2.31678E-04	5.19278E-04	2.00931E-04
2	5.33129E-03	8.13383E-03	3.33805E-03	5.40039E-03	8.25888E-03	3.38937E-03
3	8.21787E-03	1.67382E-02	6.86918E-03	8.24787E-03	1.68440E-02	6.91263E-03
4	7.26200E-02	1.51090E-01	6.20057E-02	7.26900E-02	1.51227E-01	6.20624E-02

Table 2.53. PNL-34, Pin-27 four-group U-238 cross sections

Group	CENTRM cross sections (cm^{-1})			NITAWL cross sections (cm^{-1})		
	Σ_a	$\langle\Sigma_f$	Σ_f	Σ_a	$\langle\Sigma_f$	Σ_f
1	6.87156E-03	1.19877E-02	4.26261E-03	6.88984E-03	1.21250E-02	4.30392E-03
2	4.88942E-02	5.93992E-06	2.46088E-06	4.94199E-02	5.55323E-06	2.30068E-06
3	1.10643E-02	3.83905E-08	1.59059E-08	1.11102E-02	3.88583E-08	1.60997E-08
4	4.17166E-02	1.95887E-07	8.11600E-08	4.17541E-02	1.96065E-07	8.12334E-08

Table 2.54. PNL-34, Pin-27 four-group Pu-239 cross sections

Group	CENTRM cross sections (cm^{-1})			NITAWL cross sections (cm^{-1})		
	Σ_a	$\langle\Sigma_f$	Σ_f	Σ_a	$\langle\Sigma_f$	Σ_f
1	7.32585E-04	2.10845E-03	6.82303E-04	7.32086E-04	2.11047E-03	6.82341E-04
2	1.52932E-02	2.51849E-02	8.74535E-03	1.50659E-02	2.45838E-02	8.53662E-03
3	4.71772E-02	9.27560E-02	3.22091E-02	4.72429E-02	9.29723E-02	3.22843E-02
4	3.90512E-01	7.78732E-01	2.69434E-01	3.90550E-01	7.78815E-01	2.69459E-01

										2.316 (1.24)
									2.296 (0.53)	2.287 (0.52)
								2.231 (0.55)	2.256 (0.39)	2.273 (0.58)
							2.099 (0.52)	2.175 (0.40)	2.223 (0.43)	2.208 (0.54)
						1.961 (0.55)	2.034 (0.41)	2.098 (0.41)	2.134 (0.38)	2.135 (0.61)
					1.756 (0.64)	1.872 (0.43)	1.941 (0.42)	1.996 (0.39)	2.057 (0.38)	2.047 (0.55)
				1.554 (0.67)	1.667 (0.45)	1.768 (0.42)	1.831 (0.46)	1.888 (0.45)	1.915 (0.41)	1.936 (0.60)
			1.322 (0.73)	1.441 (0.50)	1.550 (0.43)	1.640 (0.45)	1.704 (0.46)	1.742 (0.40)	1.797 (0.43)	1.788 (0.57)
		1.050 (0.80)	1.196 (0.58)	1.301 (0.46)	1.414 (0.47)	1.498 (0.52)	1.567 (0.46)	1.606 (0.46)	1.640 (0.43)	1.640 (0.61)
	0.798 (0.83)	0.924 (0.60)	1.047 (0.60)	1.159 (0.53)	1.254 (0.49)	1.331 (0.51)	1.400 (0.49)	1.441 (0.49)	1.475 (0.45)	1.488 (0.64)
0.657 (0.98)	0.680 (0.66)	0.780 (0.67)	0.888 (0.60)	1.002 (0.60)	1.099 (0.58)	1.163 (0.52)	1.236 (0.55)	1.270 (0.55)	1.299 (0.48)	1.291 (0.76)
0	0.645 (0.64)	0.667 (0.70)	0.755 (0.71)	0.838 (0.66)	0.926 (0.58)	1.004 (0.57)	1.052 (0.58)	1.091 (0.50)	1.122 (0.56)	1.114 (0.73)
0	0	0.605 (0.73)	0.620 (0.71)	0.685 (0.66)	0.759 (0.64)	0.821 (0.68)	0.868 (0.53)	0.902 (0.62)	0.924 (0.56)	0.929 (0.81)
0	0	0	0.562 (0.81)	0.591 (0.78)	0.617 (0.75)	0.649 (0.79)	0.696 (0.66)	0.736 (0.69)	0.753 (0.64)	0.760 (0.98)
0	0	0	0	0	0.553 (0.78)	0.558 (0.83)	0.591 (0.70)	0.619 (0.71)	0.642 (0.75)	0.645 (1.12)

Fig. 2.12a. Pin-power distribution for CENTRM benchmark PNL-35. Value in parentheses is percent standard deviation.

										2.333 (0.98)
									2.308 (0.50)	2.324 (0.46)
								2.251 (0.49)	2.275 (0.36)	2.283 (0.54)
							2.133 (0.50)	2.193 (0..)36	2.202 (0.36)	2.210 (0.48)
						1.973 (0.50)	2.044 (0.36)	2.110 (0.35)	2.131 (0.37)	2.142 (0.54)
					1.790 (0.55)	1.887 (0.38)	1.950 (0.40)	2.004 (0.36)	2.038 (0.35)	2.050 (0.48)
				1.583 (0.60)	1.688 (0.41)	1.765 (0.40)	1.827 (0.40)	1.890 (0.38)	1.916 (0.37)	1.941 (0.52)
			1.329 (0.66)	1.460 (0.45)	1.552 (0.42)	1.636 (0.38)	1.692 (0.38)	1.766 (0.39)	1.772 (0.40)	1.802 (0.60)
		1.065 (0.73)	1.212 (0.48)	1.315 (0.50)	1.409 (0.45)	1.482 (0.42)	1.566 (0.44)	1.603 (0.42)	1.622 (0.42)	1.645 (0.59)
	8.130 (0.80)	9.340 (0.58)	1.060 (0.54)	1.164 (0.47)	1.252 (0.50)	1.329 (0.47)	1.391 (0.45)	1.433 (0.44)	1.479 (0.41)	1.488 (0.61)
6.750 (0.89)	6.790 (0.62)	7.980 (0.63)	9.02 (0.55)	1.011 (0.53)	1.095 (0.48)	1.159 (0.50)	1.220 (0.46)	1.258 (0.46)	1.301 (0.47)	1.315 (0.61)
0	0.651 (0.64)	0.663 (0.67)	0.742 (0.60)	0.837 (0.60)	0.927 (0.54)	0.994 (0.54)	1.033 (0.52)	1.087 (0.53)	1.101 (0.49)	1.123 (0.72)
0	0	0.607 (0.74)	0.616 (0.66)	0.677 (0.65)	0.765 (0.57)	0.819 (0.56)	0.870 (0.59)	0.900 (0.53)	0.920 (0.59)	0.921 (0.77)
0	0	0	0.565 (0.68)	0.591 (0.65)	0.606 (0.66)	0.653 (0.63)	0.686 (0.66)	0.717 (0.59)	0.744 (0.59)	0.755 (0.87)
0	0	0	0	0	0.557 (0.69)	0.554 (0.69)	0.600 (0.73)	0.615 (0.71)	0.640 (0.70)	0.650 (0.96)

Fig. 2.12b. Pin-power distribution for NITAWL benchmark PNL-35. Value in parentheses is percent standard deviation.

Table 2.55. PNL-35 CENTRM reaction rates and fluxes

Pin	Region	$\sigma_a\phi$ (cm^{-3} - s^{-1})	$\langle\sigma_f\phi$ (cm^{-3} - s^{-1})	$\sigma_f\phi$ (cm^{-3} - s^{-1})	ϕ (cm - s^{-1})	ϕ/ϕ_t
	Fuel	3.409E-06	5.555E-06	1.980E-06	3.018E-3	0.205
1	Clad	6.266E-08	0.0	0.0	5.795E-4	0.039
	Mod.	3.753E-07	0.0	0.0	1.113E-2	0.756
	Fuel	1.478E-05	2.314E-05	8.243E-06	1.578E-2	0.206
99	Clad	2.862E-07	0.0	0.0	3.049E-3	0.039
	Mod.	1.467E-06	0.0	0.0	5.794E-2	0.755

Table 2.56. PNL-35 NITAWL reaction rates and fluxes

Pin	Region	$\sigma_a\phi$ (cm^{-3} - s^{-1})	$\langle\sigma_f\phi$ (cm^{-3} - s^{-1})	$\sigma_f\phi$ (cm^{-3} - s^{-1})	ϕ (cm - s^{-1})	ϕ/ϕ_t
	Fuel	3.418E-06	5.589E-06	1.992E-06	3.030E-3	0.206
1	Clad	6.288E-08	0.0	0.0	5.820E-4	0.040
	Mod.	3.743E-07	0.0	0.0	1.107E-2	0.754
	Fuel	1.486E-05	2.341E-05	8.338E-06	1.603E-2	0.207
99	Clad	2.817E-07	0.0	0.0	3.073E-3	0.040
	Mod.	1.487E-06	0.0	0.0	5.834E-2	0.753

Table 2.57. PNL-35, Pin-1 four-group fluxes

Group	CENTRM Φ (cm^{-2} - s^{-1})	NITAWL Φ (cm^{-2} - s^{-1})
1	1.534E-05	1.545E-05
2	4.935E-06	4.897E-06
3	1.254E-06	1.264E-06
4	5.413E-06	5.443E-06

Table 2.58. PNL-35, Pin-1 four-group U-235 cross sections

Group	CENTRM cross sections (cm^{-1})			NITAWL cross sections (cm^{-1})		
	$\bar{\sigma}_a$	$\bar{\nu\sigma}_f$	$\bar{\sigma}_f$	$\bar{\sigma}_a$	$\bar{\nu\sigma}_f$	$\bar{\sigma}_f$
1	2.29059E-04	5.17093E-04	1.99589E-04	2.29390E-04	5.17691E-04	1.99788E-04
2	5.45929E-03	8.37664E-03	3.43769E-03	5.46541E-03	8.36718E-03	3.43382E-03
3	8.30534E-03	1.69238E-02	6.94538E-03	8.28758E-03	1.68623E-02	6.92012E-03
4	7.30078E-02	1.51919E-01	6.23460E-02	7.27680E-02	1.51408E-01	6.21367E-02

Table 2.59. PNL-35, Pin-1 four-group U-238 cross sections

Group	CENTRM cross sections (cm^{-1})			NITAWL cross sections (cm^{-1})		
	$\bar{\sigma}_a$	$\bar{\nu\sigma}_f$	$\bar{\sigma}_f$	$\bar{\sigma}_a$	$\bar{\nu\sigma}_f$	$\bar{\sigma}_f$
1	6.96200E-03	1.25983E-02	4.46724E-03	6.97774E-03	1.26269E-02	4.47453E-03
2	5.05345E-02	5.59431E-06	2.31769E-06	4.85328E-02	5.78528E-06	2.39681E-06
3	1.11140E-02	3.88695E-08	1.61043E-08	1.10876E-02	3.87287E-08	1.60460E-08
4	4.19366E-02	1.96955E-07	8.16021E-08	4.18109E-02	1.96348E-07	8.13505E-08

Table 2.60. PNL-35, Pin-1 four-group Pu-239 cross sections

Group	CENTRM cross sections (cm^{-1})			NITAWL cross sections (cm^{-1})		
	$\bar{\sigma}_a$	$\bar{\nu\sigma}_f$	$\bar{\sigma}_f$	$\bar{\sigma}_a$	$\bar{\nu\sigma}_f$	$\bar{\sigma}_f$
1	7.31004E-04	2.12002E-03	6.83898E-04	7.31003E-04	2.11949E-03	6.83599E-04
2	1.57027E-02	2.57978E-02	8.95814E-03	1.48272E-02	2.46432E-02	8.55722E-03
3	4.68010E-02	9.21946E-02	3.20143E-02	4.68134E-02	9.21519E-02	3.19994E-02
4	3.84903E-01	7.69989E-01	2.66394E-01	3.86636E-01	7.72458E-01	2.67253E-01

Table 2.61. PNL-35, Pin-99 four-group fluxes

Group	CENTRM Φ (cm^{-2} - s^{-1})	NITAWL Φ (cm^{-2} - s^{-1})
1	8.383E-05	8.501E-05
2	2.858E-05	2.911E-05
3	6.805E-06	7.098E-06
4	2.163E-05	2.187E-05

Table 2.62. PNL-35, Pin-99 four-group U-235 cross sections

Group	CENTRM cross sections (cm^{-1})			NITAWL cross sections (cm^{-1})		
	$\bar{\sigma}_a$	$\bar{\nu\sigma}_f$	$\bar{\sigma}_f$	$\bar{\sigma}_a$	$\bar{\nu\sigma}_f$	$\bar{\sigma}_f$
1	2.33860E-04	5.21028E-04	2.02116E-04	2.31754E-04	5.19152E-04	2.00942E-04
2	5.36679E-03	8.26977E-03	3.39384E-03	5.36675E-03	8.27252E-03	3.39496E-03
3	8.17348E-03	1.67070E-02	6.85640E-03	8.15523E-03	1.66066E-02	6.81524E-03
4	7.08756E-02	1.47418E-01	6.04988E-02	7.06159E-02	1.46859E-01	6.02693E-02

Table 2.63. PNL-35, Pin-99 four-group U-238 cross sections

Group	CENTRM cross sections (cm^{-1})			NITAWL cross sections (cm^{-1})		
	$\bar{\sigma}_a$	$\bar{\nu\sigma}_f$	$\bar{\sigma}_f$	$\bar{\sigma}_a$	$\bar{\nu\sigma}_f$	$\bar{\sigma}_f$
1	6.85097E-03	1.17780E-02	4.19479E-03	6.87710E-03	1.20714E-02	4.28595E-03
2	5.03681E-02	5.57278E-06	2.30878E-06	4.60701E-02	5.75479E-06	2.38419E-06
3	1.10871E-02	3.86935E-08	1.60313E-08	1.10723E-02	3.85789E-08	1.59839E-08
4	4.08300E-02	1.91640E-07	7.94004E-08	4.06994E-02	1.91015E-07	7.91408E-08

Table 2.64. PNL-35, Pin-99 four-group Pu-239 cross sections

Group	CENTRM cross sections (cm^{-1})			NITAWL cross sections (cm^{-1})		
	$\bar{\sigma}_a$	$\bar{\nu\sigma}_f$	$\bar{\sigma}_f$	$\bar{\sigma}_a$	$\bar{\nu\sigma}_f$	$\bar{\sigma}_f$
1	7.33474E-04	2.10363E-03	6.81678E-04	7.31953E-04	2.10893E-03	6.82076E-04
2	1.48751E-02	2.48097E-02	8.61505E-03	1.48705E-02	2.44772E-02	8.49959E-03
3	4.59681E-02	9.06342E-02	3.14723E-02	4.52842E-02	8.93873E-02	3.10394E-02
4	3.95694E-01	7.84138E-01	2.71343E-01	3.95679E-01	7.83429E-01	2.71097E-01

3. MIX-COMP-THERM-3 (SAXTON-1 TO SAXTON-6)

3.1 DESCRIPTION

This section describes a set of six critical experiments, each consisting of a square-pitched array of mixed plutonium-uranium fuel rods submerged in water surrounded by a water reflector. The fuel rods are identical in all cases. Criticality is controlled by varying the number of rods, rod pitch, boron in water, and water level. This set of experiments is contained in the *International Handbook of Evaluated Criticality Safety Benchmark Experiments*.[3]

This set of experiments was performed in 1965 at the in the Critical Reactor Experiment Facility at the Westinghouse Reactor Evaluation Center. The benchmark experiments are light-water-moderated critical assemblies consisting of a core array supported by upper, middle, and lower lattice plates. The lower and middle lattice plates are 0.635 cm thick. The upper lattice plate is 1.27 cm thick. The middle lattice plate was not included in the models to facilitate the accumulation of pin-power distributions. The reactor is brought to critical by raising the water level in the tank, thus avoiding the use of control rods. The fuel rods sit on a support plate above the bottom of the tank. The tank is wide enough to assume an infinite moderator on the sides and bottom (~30 cm of water).

All fuel rods have the same physical dimensions. A schematic diagram of the fuel rods and bottom reflector is given in Fig. 3.1. Each fuel rod has an active fuel length of 92.964 cm, a 1.905-cm-long cladding plug on the bottom and a 4.320-cm-long cladding plug on the top. The fuel has a diameter of 0.856996 cm. The cladding outside diameter is 0.99314 cm with a 0.059055-cm-thick wall. This leaves a 0.009017-cm gap between the fuel and cladding.

The bottom of the fuel rod and lower lattice plate rest on a 2.54-cm aluminum support plate. Between the bottom of the aluminum support plate and the top of a 5.08-cm aluminum slab is 6.35 cm of water. The space between the top of the lower lattice plate and bottom of the middle lattice plate is 46.99 cm. The space between the top of the middle lattice plate and bottom of the top lattice plate is 47.625 cm. To simplify the problem the middle lattice plate was removed and replaced with water. The water level varies with each problem but is always between the middle and upper lattice plates. The tank is large enough to assume an infinite water reflector on the sides and bottom. An infinite water reflector can be effectively modeled using 30 cm of water, which is used to model the reflector for this set of benchmarks.

The primary differences between the six benchmarks are lattice pitch, number of rods in the lattice, water level, and for problem 3, boron density in the water. The physical characteristics of each benchmark case, including moderator temperature, are given in Table 3.1. The atom densities for all the materials in the problem except B-10, B-11 H, and O in the moderator are contained in Table 3.2. The atom densities in Table 3.2 are constant for all benchmarks. Table 3.3 contain the atom densities of B-10, B-11, H, and O in the moderator for each benchmark.

The lattice is filled from the 1/8th or 1/4th section by inserting additional pins in a mirror image. Figures 3.2 through 3.6 show the lattice map for each problem. Figure 3.2 shows a 1/4th lattice mapping while the other figures contain only 1/8th lattices. This difference exists because SAXTON-1 contains a different number of pins in the X and Y directions.

Table 3.1. Lattice description for SAXTON benchmark cases

Benchmark No.	Boron con. (ppm)	Lattice	Lattice pitch (cm)	Water level from bottom of fuel (cm)	Water temp. (^{o}C)
1	0.0	22 × 23	1.3208	82.90	25.8
2	0.0	19 × 19	1.4224	80.80	17.0
3	337	21 × 21	1.4224	88.06	18.0
4	0.0	13 × 13	1.86789	68.41	24.1
5	0.0	12 × 12	2.01158	76.76	16.1
6	0.0	11 × 11	2.6416	79.50	19.9

Table 3.2. Constant benchmark atom densities

Material	Isotope	Atom density (atoms/barn-cm)	Material	Isotope	Atom density (atoms/barn-cm)
Fuel UO_2-PuO_2	U-234	4.6590×10^{-6}	Cladding and end plugs	Sn	4.6590×10^{-4}
	U-235	1.5301×10^{-4}		Fe	1.4148×10^{-4}
	U-238	2.1097×10^{-2}		Cr	7.5977×10^{-5}
	Pu-239	1.3526×10^{-3}		O	2.9630×10^{-4}
	Pu-240	1.2759×10^{-4}		Zr	4.2517×10^{-2}
	Pu-241	1.1407×10^{-5}	Al lattice plate, Al support plate, Al slab (2.69 gm/cc)	Al	6.0039×10^{-2}
	Pu-242	6.0318×10^{-7}			
	Am-241	1.7783×10^{-6}			
	O-16	4.3779×10^{-2}			

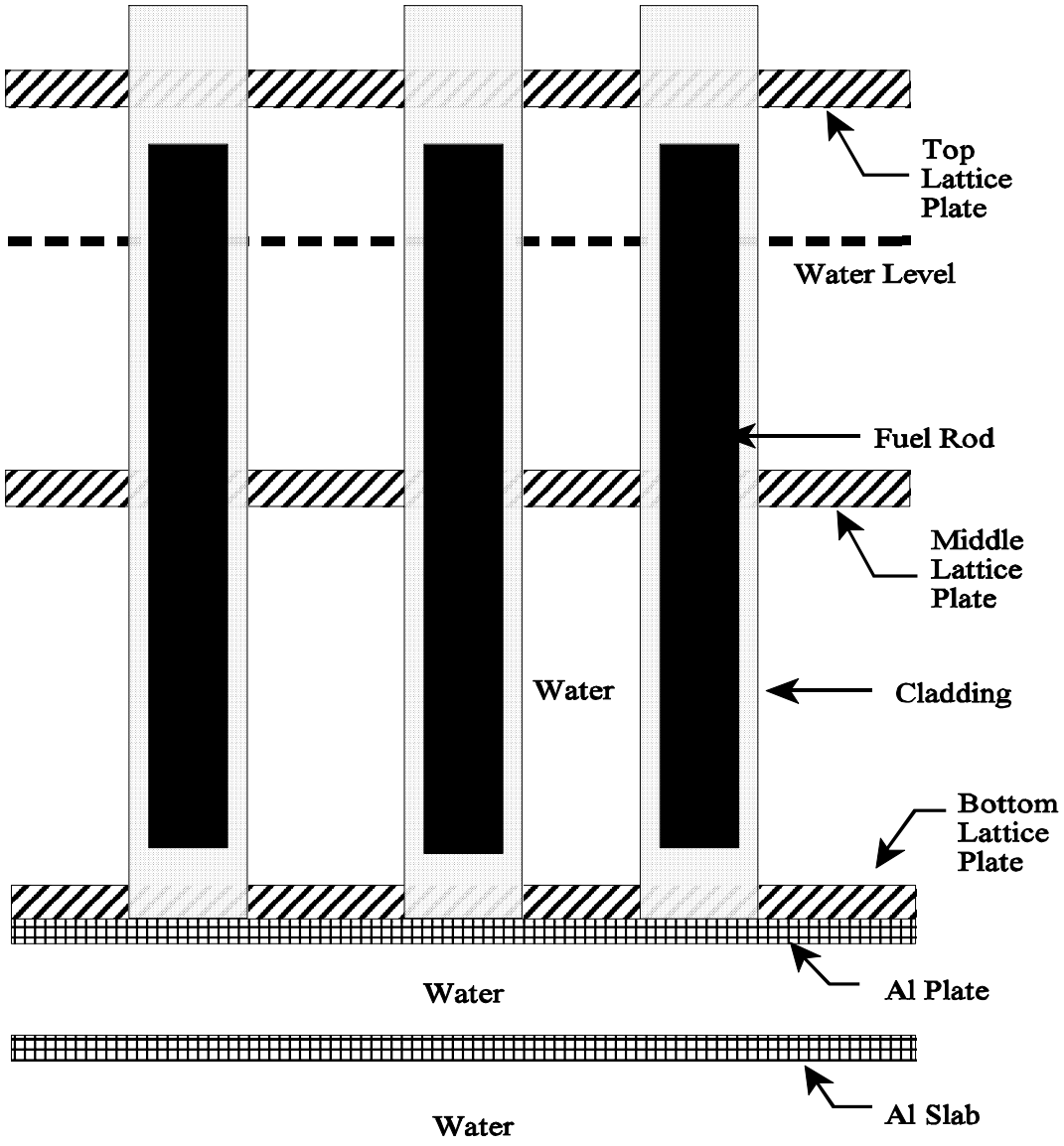

Fig. 3.1. Schematic of the SAXTON fuel rods with reflector.

Table 3.3. Moderator atom densities

Benchmark No.	Atom densities (atoms/barn-cm)			
	H	O	B-10	B-11
SAXTON-1	6.6643×10^{-2}	3.3322×10^{-2}	0.0	0.0
SAXTON-2	6.6781×10^{-2}	3.3390×10^{-2}	0.0	0.0
SAXTON-3	6.6751×10^{-2}	3.3404×10^{-2}	3.7338×10^{-6}	1.5029×10^{-5}
SAXTON-4	6.6673×10^{-2}	3.3336×10^{-2}	0.0	0.0
SAXTON-5	6.6783×10^{-2}	3.3392×10^{-2}	0.0	0.0
SAXTON-6	6.6737×10^{-2}	3.3368×10^{-2}	0.0	0.0

3.2 ANALYSIS

All six computational benchmarks in this section were processed twice using SCALE 5.0. The set labeled NITAWL uses the NITAWL resonance processor to self-shield the resolved resonance region for all nuclides in the unit cell. An identical set, labeled CENTRM, replaces NITAWL with the CENTRM/PMC code sequence. The NITAWL and CENTRM results are then compared.

Table 3.4 contains the k_{eff} and Energy of the Average Lethargy Causing Fission (EALCF). The k_{eff} values for all the benchmark cases are very close to 1.0, the worst NITAWL benchmark being 0.68% high and the worst CENTRM case being 0.59% high. There appears to be a small negative bias between NITAWL and CENTRM, the CENTRM cases being about 0.3% lower on average than the NITAWL cases. The EALCF values listed are from the CENTRM cases. For all cases, the difference between this value for CENTRM and NITAWL was less than 0.1%. Both CENTRM and NITAWL produce excellent results for the k_{eff} and EALCF for this set of problems.

Also, calculated for each problem are the pin-power distributions; absorption, σ_a, and fission reaction rates and fluxes in the pin fuel, clad, and moderator; and four group cross sections and fluxes for a corner outside pin and the center pin. Each set of data is calculated using both CENTRM and NITAWL. All the data for each case are contained in the following Figs. 3.7a through 3.12b and Tables 2.5 through 3.64.

The pin-power distributions for the first problem assume 1/4th core symmetry, the pin-power distributions for the remaining problems assume 1/8th core symmetry, with a surrounding reflector in all problems. The pin-power data consist of a value and a standard deviation for each pin. The values for the pin power are actually in units of fissions per cm^3-source particle $\times 10^{-5}$. The value in parentheses is the percent standard deviation of the pin-power value. The pin-power distributions in the 1/8th or full-core representations are the portion of the pin covered by water. The value off to the side in the pin-power distributions represents all the fuel not covered by water. Separating the fuel rod was necessary to model this in KENO-V.a.

In most cases the CENTRM and NITAWL results for each benchmark case agree within 2 standard deviations. The peak-to-low power changes with respect to pitch. The peak-to-low power ratio initially decreased with increasing pitch, starting with a high of 2.6 for SAXTON-1 and decreasing to a low of 1.8 for SAXTON-5. A further increase in pitch, as shown in SAXTON-6,

increases the ratio to 2.5. The small pitch in SAXTON-1 and -2 cause the array to be under moderated. This under moderation results in the highest power pin being on the edge of the array and the lowest power pin being several pins in from the edge where the thermal flux is low due to lack of moderator and the fast flux is also low because it is not deep within the array.

The total fluxes, and flux ratios for the CENTRM and NITAWL cases of each benchmark case, are also in good agreement, seldom varying by more than 1%. These values are included for a corner pin and the center pin for each case. The reaction rates in the fuel and cladding are also in good agreement. However, the reaction rates for the moderator appear to be significantly different, with the CENTRM value being almost a factor of 2 higher for all cases.

Finally, four-group fluxes and cross sections were calculated for selected nuclides in the fuel region of the same corner and center pins. The macroscopic cross sections listed include the radiative capture, fission, and nu*fission cross sections for U-235, U-238, and Pu-239. The four groups are collapsed from the 238-group multigroup cross-section set using the flux profile calculated in KENO-V.a as follows: group 1 is from 20 Mev to 9.5 keV, group 2 is from 9.5 keV to 3.0 eV, group 3 is from 3 eV to 0.4 eV, and group 4 is from 0.4 eV to 10^{-5} eV. The 0.4 eV was chosen as a boundary because it is the cadmium cutoff energy. Groups 2 and 3 contain the resolved resonance regions for most of the nuclides used in these cases. Most of the cross-section data for the CENTRM and NITAWL cases of a given benchmark case agree within 1%.

3.3 CONCLUSIONS

For this set of benchmark cases using either NITAWL and CENTRM as the resonance region processor produces acceptable results of the k_{eff} values. All other values produced using CENTRM and NITAWL are also consistent with each. For all cases, the k_{eff}*'s* produced using CENTRM are slightly lower (~0.3%) than those produced using NITAWL to do the resonance self-shielding. As a result the average k_{eff} of all the CENTRM cases is closer to 1.0 than the average k_{eff} of all the NITAWL cases for this set of benchmarks. The pin-power distributions, fluxes, most reactions rates, and macroscopic cross sections generally agree to approximately 1% between CENTRM and NITAWL. The only significant discrepancy is the absorption reaction rate for the moderator. CENTRM calculates a value that is about a factor of 2 higher than the same value using NITAWL.

Table 3.4 Comparison of k_{eff} and EALCF from CENTRM and NITAWL[a]

CASE MIX-COMP-THERM-3	NITAWL k_{eff} (±F)	CENTRM k_{eff} (±F)	% DIFF	EALCF (eV)
SAXTON-1	1.0046 (0.0005)	1.0007 (0.0004)	-0.39	0.881
SAXTON-2	1.0058 (0.0004)	1.0012 (0.0004)	-0.46	0.537
SAXTON-3	1.0054 (0.0004)	1.0017 (0.0004)	-0.37	0.633
SAXTON-4	1.0056 (0.0004)	1.0029 (0.0004)	-0.27	0.186
SAXTON-5	1.0062 (0.0004)	1.0035 (0.0004)	-0.27	0.154
SAXTON-6	1.0068 (0.0005)	1.0059 (0.0004)	-0.09	0.100

[a] Value in parentheses is percent standard deviation.

121	122	123	124	125	126	127	128	129	130	131	132
109	110	111	112	113	114	115	116	117	118	119	120
97	98	99	100	101	102	103	104	105	106	107	108
85	86	87	88	89	90	91	92	93	94	95	96
73	74	75	76	77	78	79	80	81	82	83	84
61	62	63	64	65	66	67	68	69	70	71	72
49	50	51	52	53	54	55	56	57	58	59	60
37	38	39	40	41	42	43	44	45	46	47	48
25	26	27	28	29	30	31	32	33	34	35	36
13	14	15	16	17	18	19	20	21	22	23	24
1	2	3	4	5	6	7	8	9	10	11	12

Fig.3.2. Pin layout of benchmark case SAXTON-1.

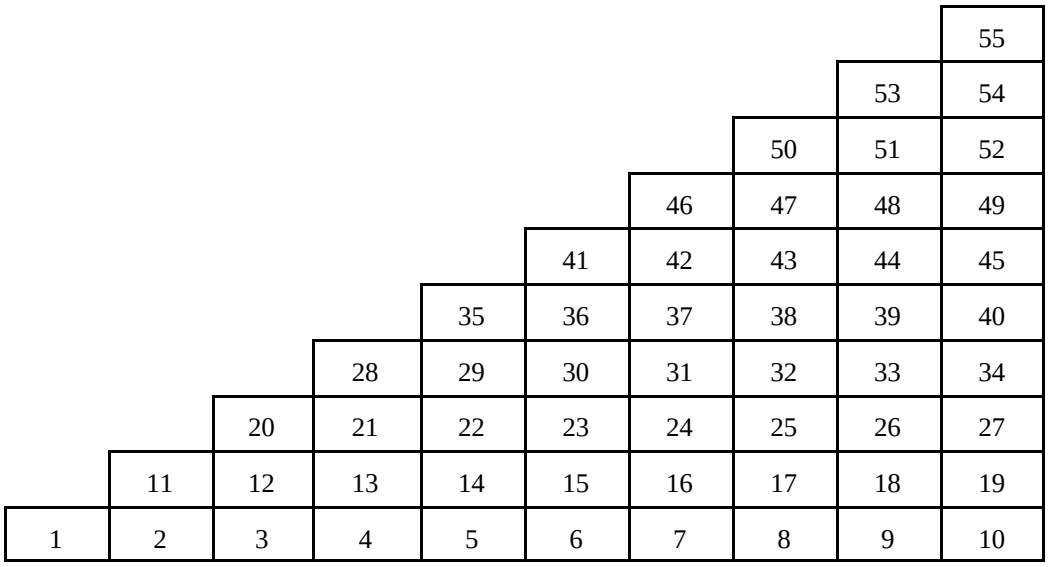

Fig. 3.3. Pin layout of benchmark case SAXTON-2.

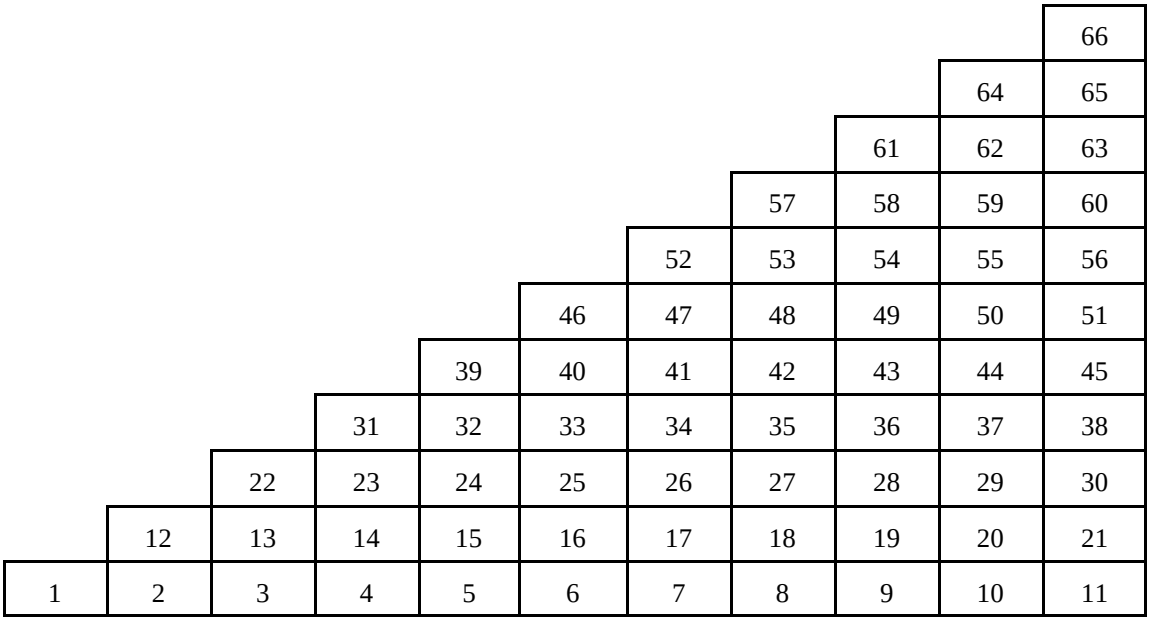

Fig. 3.4. Pin layout of benchmark case SAXTON-3.

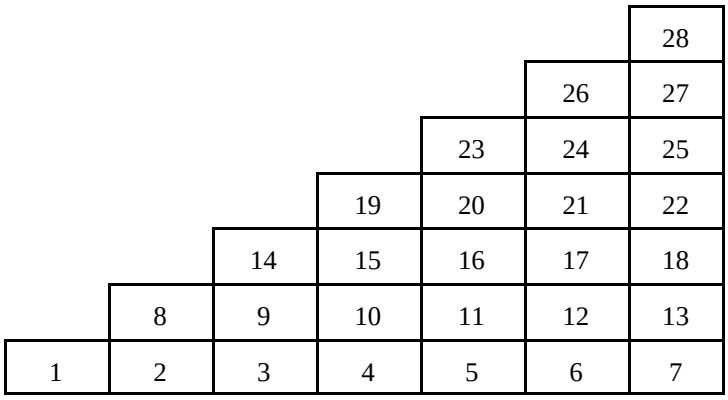

Fig. 3.5. Pin layout of benchmark case SAXTON-4.

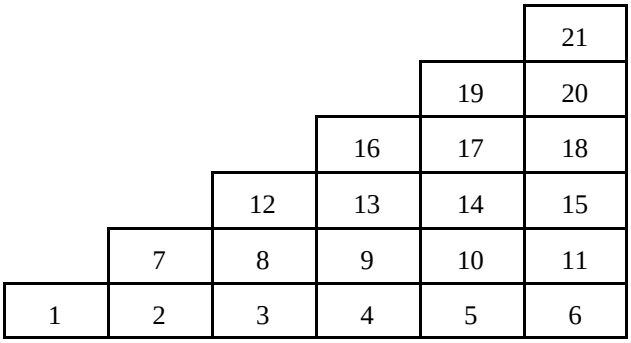

Fig. 3.6. Pin layout of benchmark cases SAXTON-5 and 6.

						0.150 (0.73)					
6.485 (0.53)	3.658 (0.59)	3.513 (0.64)	3.704 (0.60)	3.968 (0.55)	4.199 (0.57)	4.486 (0.55)	4.633 (0.49)	4.770 (0.54)	4.894 (0.55)	4.914 (0.50)	4.971 (0.73)
6.446 (0.50)	3.716 (0.58)	3.461 (0.61)	3.693 (0.61)	3.957 (0.59)	4.222 (0.55)	4.421 (0.57)	4.570 (0.57)	4.687 (0.51)	4.871 (0.51)	4.858 (0.53)	4.962 (0.66)
6.319 (0.48)	3.630 (0.63)	3.434 (0.62)	3.601 (0.61)	3.837 (0.54)	4.133 (0.57)	4.381 (0.56)	4.493 (0.49)	4.664 (0.56)	4.782 (0.56)	4.846 (0.52)	4.847 (0.71)
6.148 (0.50)	3.531 (0.62)	3.368 (0.59)	3.524 (0.66)	3.729 (0.56)	3.986 (0.58)	4.175 (0.52)	4.397 (0.55)	4.503 (0.50)	4.649 (0.51)	4.680 (0.52)	4.705 (0.75)
5.884 (0.49)	3.410 (0.63)	3.176 (0.67)	3.433 (0.59)	3.686 (0.59)	3.876 (0.58)	4.087 (0.61)	4.247 (0.55)	4.338 (0.54)	4.491 (0.54)	4.514 (0.53)	4.556 (0.75)
5.635 (0.50)	3.234 (0.67)	3.058 (0.64)	3.231 (0.66)	3.496 (0.60)	3.668 (0.54)	3.879 (0.60)	4.029 (0.57)	4.171 (0.52)	4.254 (0.57)	4.283 (0.51)	4.344 (0.75)
5.340 (0.53)	3.066 (0.66)	2.898 (0.63)	3.037 (0.71)	3.280 (0.62)	3.477 (0.56)	3.662 (0.61)	3.794 (0.59)	3.908 (0.61)	4.018 (0.57)	4.067 (0.56)	4.085 (0.75)
4.988 (0.55)	2.822 (0.70)	2.693 (0.72)	2.864 (0.66)	3.054 (0.70)	3.264 (0.61)	3.412 (0.61)	3.552 (0.61)	3.652 (0.59)	3.747 (0.59)	3.772 (0.58)	3.830 (0.84)
4.609 (0.58)	4.609 (0.67)	2.520 (0.72)	2.716 (0.71)	2.878 (0.67)	3.057 (0.67)	3.187 (0.62)	3.360 (0.58)	3.473 (0.62)	3.531 (0.59)	3.574 (0.70)	3.571 (0.88)
4.611 (0.62)	2.773 (0.75)	2.701 (0.67)	2.827 (0.68)	3.079 (0.65)	3.255 (0.69)	3.427 (0.66)	3.557 (0.63)	3.717 (0.60)	3.757 (0.54)	3.81 (0.62)	3.815 (0.88)
6.090 (0.50)	4.599 (0.56)	4.683 (0.52)	5.010 (0.56)	5.313 (0.51)	5.712 (0.53)	5.943 (0.52)	6.227 (0.49)	6.425 (0.51)	6.539 (0.50)	6.636 (0.48)	6.635 (0.67)

Fig. 3.7a. Pin-power distribution for CENTRM benchmark SAXTON-1. Value in parentheses is the percent standard deviation.

						4.967 (0.78)					
6.502 (0.50)	3.746 (0.64)	3.555 (0.60)	3.711 (0.62)	4.013 (0.54)	4.274 (0.56)	4.457 (0.58)	4.689 (0.54)	4.801 (0.55)	4.913 (0.55)	4.997 (0.49)	4.967 (0.78)
6.441 (0.49)	3.706 (0.59)	3.493 (0.67)	3.699 (0.65)	3.939 (0.63)	4.244 (0.56)	4.422 (0.53)	4.641 (0.55)	4.780 (0.55)	4.840 (0.51)	4.917 (0.49)	4.912 (0.74)
6.347 (0.45)	3.634 (0.54)	3.368 (0.65)	3.599 (0.59)	3.884 (0.61)	4.115 (0.57)	4.390 (0.51)	4.502 (0.52)	4.684 (0.54)	4.757 (0.56)	4.854 (0.51)	4.879 (0.78)
6.197 (0.52)	3.522 (0.63)	3.356 (0.64)	3.356 (0.59)	3.836 (0.60)	4.052 (0.56)	4.279 (0.57)	4.446 (0.54)	4.547 (0.54)	4.614 (0.55)	4.711 (0.49)	4.737 (0.76)
5.882 (0.52)	3.391 (0.62)	3.212 (0.63)	3.408 (0.64)	3.685 (0.61)	3.868 (0.56)	4.112 (0.57)	4.229 (0.55)	4.343 (049.)	4.500 (0.54)	4.497 (0.57)	4.520 (0.76)
5.619 (0.54)	3.243 (0.70)	3.060 (0.66)	3.260 (0.61)	3.477 (0.64)	3.708 (0.59)	3.880 (0.57)	4.050 (0.60)	4.189 (0.60)	4.265 (0.55)	4.321 (0.58)	4.305 (0.71)
5.353 (0.51)	3.065 (0.67)	2.880 (0.64)	3.041 (0.64)	3.296 (0.66)	3.479 (0.62)	3.650 (0.59)	3.879 (0.60)	3.922 (0.67)	3.990 (0.52)	4.087 (0.54)	4.126 (0.78)
4.982 (0.54)	2.844 (0.73)	2.673 (0.69)	2.857 (0.73)	3.063 (0.66)	3.264 (0.62)	3.422 (0.68)	3.577 (0.62)	3.698 (0.59)	3.787 (0.62)	3.847 (0.59)	3.823 (0.83)
4.689 (0.60)	2.684 (0.76)	2.526 (0.71)	2.697 (0.68)	2.904 (0.69)	3.064 (0.68)	3.243 (0.65)	3.361 (0.64)	3.478 (0.62)	3.538 (0.61)	3.578 (0.63)	3.626 (0.89)
4.621 (0.58)	2.801 (0.72)	2.677 (0.75)	2.839 (0.78)	3.079 (0.61)	3.258 (0.64)	3.417 (0.65)	3.558 (0.61)	3.735 (0.53)	3.801 (0.60)	3.882 (0.63)	3.872 (0.86)
6.047 (0.48)	4.602 (0.56)	4.618 (0.58)	4.932 (0.58)	5.360 (0.51)	5.681 (0.53)	6.037 (0.46)	6.282 (0.44)	6.440 (0.48)	6.562 (0.47)	6.694 (0.48)	6.750 (0.68)

Fig. 3.7b. Pin-power distribution for NITAWL benchmark SAXTON-1. Value in parentheses is the percent standard deviation.

Table 3.5. SAXTON-1 CENTRM reaction rates and fluxes

Pin	Region	$\langle\sigma_a\phi\rangle$ (cm^{-3} - s^{-1})	$\langle\sigma_f\phi\rangle$ (cm^{-3} - s^{-1})	$\langle\sigma_f\phi\rangle$ (cm^{-3} - s^{-1})	$\langle\phi\rangle$ (cm - s^{-1})	$\langle\phi\rangle/\langle\phi\rangle_t$
	Fuel	3.400E-05	6.075E-05	2.123E-05	7.209E-03	0.344
1	Clad	3.137E-07	0.0	0.0	2.114E-03	0.101
	Mod.	1.303E-06	0.0	0.0	1.162E-02	0.555
	Fuel	3.446E-05	5.001E-05	1.747E-05	1.905E-02	0.339
132	Clad	5.304E-07	0.0	0.0	5.690E-03	0.101
	Mod.	9.171E-07	0.0	0.0	3.141E-02	0.559

Table 3.6. SAXTON-1 NITAWL reaction rates and fluxes

Pin	Region	$\langle\sigma_a\phi\rangle$ (cm^{-3} - s^{-1})	$\langle\sigma_f\phi\rangle$ (cm^{-3} - s^{-1})	$\langle\sigma_f\phi\rangle$ (cm^{-3} - s^{-1})	$\langle\phi\rangle$ (cm - s^{-1})	$\langle\phi\rangle/\langle\phi\rangle_t$
	Fuel	3.407E-05	6.097E-05	2.131E-05	7.160E-03	0.344
1	Clad	3.038E-07	0.0	0.0	2.102E-03	0.101
	Mod.	6.505E-07	0.0	0.0	1.157E-02	0.556
	Fuel	3.445E-05	4.998E-05	1.746E-05	1.895E-02	0.338
132	Clad	5.131E-07	0.0	0.0	5.682E-03	0.101
	Mod.	4.648E-07	0.0	0.0	3.143E-02	0.561

Table 3.7. SAXTON-1, Pin-1 four-group fluxes

Group	CENTRM M (cm^{-2} - s^{-1})	NITAWL M (cm^{-2} - s^{-1})
1	9.920E-05	9.850E-05
2	2.598E-05	2.555E-05
3	5.448E-06	5.416E-06
4	2.012E-05	2.026E-05

Table 3.8. SAXTON-1, Pin-1 four-group U-235 cross sections

Group	CENTRM cross sections (cm^{-1})			NITAWL cross sections (cm^{-1})		
	Σ_a	$\nu\Sigma_f$	Σ_f	Σ_a	$\nu\Sigma_f$	Σ_f
1	2.32297E-04	5.28702E-04	2.03588E-04	2.31560E-04	5.28129E-04	2.03214E-04
2	5.36940E-03	8.29315E-03	3.40344E-03	5.43045E-03	8.32423E-03	3.41618E-03
3	7.84363E-03	1.58948E-02	6.52311E-03	7.88612E-03	1.60166E-02	6.57304E-03
4	7.43305E-02	1.54727E-01	6.34985E-02	7.41841E-02	1.54426E-01	6.33751E-02

Table 3.9. SAXTON-1, Pin-1 four-group U-238 cross sections

Group	CENTRM cross sections (cm^{-1})			NITAWL cross sections (cm^{-1})		
	Σ_a	$\nu\Sigma_f$	Σ_f	Σ_a	$\nu\Sigma_f$	Σ_f
1	7.21435E-03	1.34429E-02	4.77316E-03	7.22446E-03	1.35539E-02	4.80883E-03
2	5.31239E-02	5.82914E-06	2.41498E-06	5.09276E-02	5.71143E-06	2.36622E-06
3	1.12361E-02	3.85156E-08	1.59577E-08	1.12440E-02	3.86270E-08	1.60039E-08
4	4.26642E-02	2.00382E-07	8.30224E-08	4.25934E-02	2.00045E-07	8.28825E-08

Table 3.10. SAXTON-1, Pin-1 four-group Pu-239 cross sections

Group	CENTRM cross sections (cm^{-1})			NITAWL cross sections (cm^{-1})		
	Σ_a	$\nu\Sigma_f$	Σ_f	Σ_a	$\nu\Sigma_f$	Σ_f
1	2.51521E-03	7.34395E-03	2.36412E-03	2.51413E-03	7.35233E-03	2.36542E-03
2	4.31528E-02	7.26582E-02	2.52301E-02	4.23284E-02	7.17029E-02	2.48984E-02
3	1.42157E-01	2.82164E-01	9.79800E-02	1.43048E-01	2.83783E-01	9.85430E-02
4	1.26177E+00	2.54082E+00	8.78966E-01	1.25963E+00	2.53651E+00	8.77483E-01

Table 3.11. SAXTON-1, Pin-132 four-group fluxes

Group	CENTRM Φ (cm^{-2} - s^{-1})	NITAWL Φ (cm^{-2} - s^{-1})
1	2.750E-04	2.726E-04
2	9.570E-05	9.640E-05
3	1.651E-05	1.607E-05
4	1.110E-05	1.112E-05

Table 3.12. SAXTON-1, Pin-132 four-group U-235 cross sections

Group	CENTRM cross sections (cm^{-1})			NITAWL cross sections (cm^{-1})		
	Σ_a	$\langle\Sigma_f\rangle$	Σ_f	Σ_a	$\langle\Sigma_f\rangle$	Σ_f
1	2.45122E-04	5.39109E-04	2.10038E-04	2.44993E-04	5.38844E-04	2.09938E-04
2	5.15441E-03	7.97880E-03	3.27443E-03	5.09111E-03	7.85028E-03	3.22168E-03
3	7.58571E-03	1.52693E-02	6.26638E-03	7.63367E-03	1.54170E-02	6.32701E-03
4	6.21247E-02	1.28918E-01	5.29069E-02	6.23526E-02	1.29385E-01	5.30985E-02

Table 3.13. SAXTON-1, Pin-132 four-group U-238 cross sections

Group	CENTRM cross sections (cm^{-1})			NITAWL cross sections (cm^{-1})		
	Σ_a	$\langle\Sigma_f\rangle$	Σ_f	Σ_a	$\langle\Sigma_f\rangle$	Σ_f
1	6.80382E-03	1.10027E-02	3.91622E-03	6.78188E-03	1.09576E-02	3.89839E-03
2	4.89435E-02	6.26429E-06	2.59527E-06	4.75272E-02	6.04762E-06	2.50550E-06
3	1.11343E-02	3.75412E-08	1.55540E-08	1.11699E-02	3.77752E-08	1.56510E-08
4	3.63750E-02	1.70185E-07	7.05107E-08	3.64831E-02	1.70704E-07	7.07262E-08

Table 3.14. SAXTON-1, Pin-132 four-group Pu-239 cross sections

Group	CENTRM cross sections (cm^{-1})			NITAWL cross sections (cm^{-1})		
	Σ_a	$\langle\Sigma_f\rangle$	Σ_f	Σ_a	$\langle\Sigma_f\rangle$	Σ_f
1	2.52991E-03	7.17411E-03	2.33467E-03	2.52913E-03	7.17146E-03	2.33393E-03
2	4.10734E-02	6.89915E-02	2.39569E-02	3.95781E-02	6.68722E-02	2.32210E-02
3	1.30973E-01	2.61059E-01	9.06517E-02	1.35790E-01	2.70087E-01	9.37866E-02
4	1.45288E+00	2.78304E+00	9.63703E-01	1.45769E+00	2.79201E+00	9.66808E-01

									7.032 (0.91)
	0.171 (0.75)							7.088 (0.42)	7.085 (0.46)
							6.809 (0.46)	6.904 (0.32)	6.960 (0.49)
						6.408 (0.49)	6.587 (0.33)	6.701 (0.33)	6.721 (0.48)
					5.874 (0.49)	6.137 (0.35)	6.268 (0.37)	6.459 (0.35)	6.431 (0.48)
				5.267 (0.53)	5.498 (0.34)	5.807 (0.36)	5.922 (0.34)	6.082 (0.36)	6.127 (0.49)
			4.501 (0.61)	4.877 (0.40)	5.169 (0.39)	5.362 (0.37)	5.580 (0.37)	5.629 (0.38)	5.695 (0.52)
		3.937 (0.61)	4.239 (0.41)	4.533 (0.40)	4.826 (0.42)	5.017 (0.39)	5.191 (0.39)	5.256 (0.37)	5.308 (0.56)
	4.056 (0.65)	4.036 (0.42)	4.308 (0.40)	4.628 (0.40)	4.898 (0.37)	5.101 (0.39)	5.261 (0.38)	5.374 (0.35)	5.422 (0.51)
7.779 (0.47)	6.169 (0.37)	6.394 (0.34)	6.876 (0.36)	7.378 (0.34)	7.815 (0.30)	8.167 (0.33)	8.417 (0.30)	8.574 (0.31)	8.669 (0.41)

Fig. 3.8a. Pin-power distribution for CENTRM benchmark SAXTON-2. Value in parentheses is percent standard deviation.

0.172 (0.72)									7.111 (0.85)
								7.073 (0.45)	7.107 (0.46)
							6.803 (0.46)	6.929 (0.32)	7.015 (0.47)
						6.476 (0.49)	6.655 (0.35)	6.786 (0.34)	6.773 (0.44)
					5.890 (0.52)	6.194 (0.36)	6.362 (0.34)	6.449 (0.34)	6.504 (0.46)
				5.255 (0.53)	5.527 (0.39)	5.826 (0.36)	5.985 (0.35)	6.159 (0.37)	6.139 (0.50)
			4.556 (0.57)	4.871 (0.39)	5.198 (0.36)	5.449 (0.38)	5.562 (0.37)	5.690 (0.38)	5.706 (0.48)
		3.988 (0.57)	4.229 (0.40)	4.534 (0.40)	4.839 (040.)	5.022 (0.42)	5.209 (0.39)	5.298 (0.39)	5.338 (054.)
	4.073 (0.62)	3.989 (0.46)	4.314 (0.38)	4.651 (0.40)	4.909 (0.36)	5.172 (0.39)	5.260 (040.)	5.401 (0.36)	5.401 (048.)
7.878 (0.40)	6.193 (0.34)	6.355 (0.33)	6.870 (0.34)	7.353 (0.32)	7.839 (0.32)	8.201 (0.30)	8.457 (0.29)	8.657 (0.29)	8.684 (0.44)

Fig. 3.8b. Pin-power distribution for NITAWL benchmark SAXTON-2. Value in parentheses is percent standard deviation.

Table 3.15. SAXTON-2 CENTRM reaction rates and fluxes

Pin	Region	$\langle\sigma_a\phi\rangle$ (cm^{-3} - s^{-1})	$\langle\nu\sigma_f\phi\rangle$ (cm^{-3} - s^{-1})	$\langle\sigma_f\phi\rangle$ (cm^{-3} - s^{-1})	$\langle\phi\rangle$ (cm - s^{-1})	$\langle\phi\rangle/\langle\phi\rangle_t$
	Fuel	4.361E-05	7.811E-05	2.729E-05	8.590E-03	0.296
1	Clad	3.882E-07	0.0	0.0	2.531E-03	0.087
	Mod.	1.731E-06	0.0	0.0	1.793E-02	0.617
	Fuel	4.675E-05	7.033E-05	2.457E-05	2.148E-02	0.293
55	Clad	6.310E-07	0.0	0.0	6.403E-03	0.087
	Mod.	1.351E-06	0.0	0.0	4.552E-02	0.620

Table 3.16. SAXTON-2 NITAWL reaction rates and fluxes

Pin	Region	$\langle\sigma_a\phi\rangle$ (cm^{-3} - s^{-1})	$\langle\nu\sigma_f\phi\rangle$ (cm^{-3} - s^{-1})	$\langle\sigma_f\phi\rangle$ (cm^{-3} - s^{-1})	$\langle\phi\rangle$ (cm - s^{-1})	$\langle\phi\rangle/\langle\phi\rangle_t$
	Fuel	4.393E-05	7.895E-05	2.759E-05	8.596E-03	0.296
1	Clad	3.874E-07	0.0	0.0	2.523E-03	0.087
	Mod.	8.732E-07	0.0	0.0	1.790E-02	0.617
	Fuel	4.723E-05	7.130E-05	2.491E-05	2.145E-02	0.292
55	Clad	6.079E-07	0.0	0.0	6.411E-03	0.087
	Mod.	6.803E-07	0.0	0.0	4.565E-02	0.621

Table 3.17. SAXTON-2, Pin-1 four-group fluxes

Group	CENTRM Φ (cm^{-2} - s^{-1})	NITAWL Φ (cm^{-2} - s^{-1})
1	1.210E-04	1.209E-04
2	3.068E-05	3.075E-05
3	6.650E-06	6.426E-06
4	2.598E-05	2.635E-05

Table 3.18. SAXTON-2, Pin-1 four-group U-235 cross sections

Group	CENTRM cross sections (cm^{-1})			NITAWL cross sections (cm^{-1})		
	Σ_a	$\langle\Sigma_f$	Σ_f	Σ_a	$\langle\Sigma_f$	Σ_f
1	2.31295E-04	5.28168E-04	2.03137E-04	2.31046E-04	5.27611E-04	2.02942E-04
2	5.50818E-03	8.46995E-03	3.47598E-03	5.34062E-03	8.20683E-03	3.36800E-03
3	7.88307E-03	1.60481E-02	6.58600E-03	7.88335E-03	1.59830E-02	6.55932E-03
4	7.48945E-02	1.55911E-01	6.39846E-02	7.47985E-02	1.55708E-01	6.39009E-02

Table 3.19. SAXTON-2, Pin-1 four-group U-238 cross sections

Group	CENTRM cross sections (cm^{-1})			NITAWL cross sections (cm^{-1})		
	Σ_a	$\langle\Sigma_f$	Σ_f	Σ_a	$\langle\Sigma_f$	Σ_f
1	7.27299E-03	1.37200E-02	4.87017E-03	7.25772E-03	1.36913E-02	4.86098E-03
2	5.45685E-02	6.04055E-06	2.50257E-06	5.15366E-02	5.85011E-06	2.42368E-06
3	1.12498E-02	3.86744E-08	1.60235E-08	1.12126E-02	3.84197E-08	1.59180E-08
4	4.29376E-02	2.01691E-07	8.35643E-08	4.28896E-02	2.01461E-07	8.34691E-08

Table 3.20. SAXTON-2, Pin-1 four-group Pu-239 cross sections

Group	CENTRM cross sections (cm^{-1})			NITAWL cross sections (cm^{-1})		
	Σ_a	$\langle\Sigma_f$	Σ_f	Σ_a	$\langle\Sigma_f$	Σ_f
1	2.51538E-03	7.36394E-03	2.36798E-03	2.51302E-03	7.35725E-03	2.36609E-03
2	4.36441E-02	7.27138E-02	2.52495E-02	4.25694E-02	7.20315E-02	2.50126E-02
3	1.44153E-01	2.85821E-01	9.92499E-02	1.40219E-01	2.78403E-01	9.66744E-02
4	1.26117E+00	2.54337E+00	8.79827E-01	1.26115E+00	2.54272E+00	8.79601E-01

Table 3.21. SAXTON-2, Pin-55 four-group fluxes

Group	CENTRM Φ (cm^{-2} - s^{-1})	NITAWL Φ (cm^{-2} - s^{-1})
1	3.168E-04	3.145E-04
2	1.074E-04	1.086E-04
3	1.945E-05	1.953E-05
4	1.722E-05	1.751E-05

Table 3.22 SAXTON-2, Pin-55 four-group U-235 cross sections

Group	CENTRM cross sections (cm^{-1})			NITAWL cross sections (cm^{-1})		
	Σ_a	$\langle\Sigma_f$	Σ_f	Σ_a	$\langle\Sigma_f$	Σ_f
1	2.42818E-04	5.37235E-04	2.08871E-04	2.42331E-04	5.36480E-04	2.08578E-04
2	5.28301E-03	8.16913E-03	3.35254E-03	5.21227E-03	8.02944E-03	3.29521E-03
3	7.65558E-03	1.53980E-02	6.31918E-03	7.58530E-03	1.53401E-02	6.29544E-03
4	6.42364E-02	1.33386E-01	5.47403E-02	6.47836E-02	1.34511E-01	5.52022E-02

Table 3.23. SAXTON-2, Pin-55 four-group U-238 cross sections

Group	CENTRM cross sections (cm^{-1})			NITAWL cross sections (cm^{-1})		
	Σ_a	$\langle\Sigma_f$	Σ_f	Σ_a	$\langle\Sigma_f$	Σ_f
1	6.89564E-03	1.14866E-02	4.08747E-03	6.87320E-03	1.14586E-02	4.07844E-03
2	5.10445E-02	5.98081E-06	2.47782E-06	5.07872E-02	5.96084E-06	2.46955E-06
3	1.11261E-02	3.76231E-08	1.55879E-08	1.11419E-02	3.76606E-08	1.56035E-08
4	3.74682E-02	1.75440E-07	7.26882E-08	3.77212E-02	1.76632E-07	7.31816E-08

Table 3.24. SAXTON-2, Pin-55 four-group Pu-239 cross sections

Group	CENTRM cross sections (cm^{-1})			NITAWL cross sections (cm^{-1})		
	Σ_a	$\langle\Sigma_f$	Σ_f	Σ_a	$\langle\Sigma_f$	Σ_f
1	2.52700E-03	7.20417E-03	2.33954E-03	2.52549E-03	7.20372E-03	2.33961E-03
2	4.23034E-02	7.11892E-02	2.47201E-02	4.01978E-02	6.76656E-02	2.34965E-02
3	1.33769E-01	2.66117E-01	9.24077E-02	1.31144E-01	2.61407E-01	9.07727E-02
4	1.41690E+00	2.73612E+00	9.47311E-01	1.43265E+00	2.76589E+00	9.57596E-01

0.186 (0.99)										5.900 (0.99)
									5.929 (0.48)	5.958 (0.50)
								5.672 (0.51)	5.819 (0.31)	5.884 (0.49)
							5.436 (0.48)	5.585 (0.33)	5.666 (0.33)	5.630 (0.49)
						5.000 (0.54)	5.206 (0.35)	5.373 (0.33)	5.425 (0.33)	5.486 (0.55)
					4.473 (0.49)	4.718 (0.35)	4.935 (0.37)	5.060 (0.34)	5.148 (0.34)	5.191 (0.)55
				3.921 (0.58)	4.189 (0.42)	4.440 (0.38)	4.590 (0.38)	4.750 (0.36)	4.833 (0.34)	4.836 (0.52)
			3.331 (0.66)	3.599 (0.45)	3.842 (0.38)	4.096 (0.43)	4.271 (0.41)	4.357 (0.41)	4.399 (0.42)	4.447 (0.52)
		2.821 (0.75)	3.029 (0.47)	3.314 (0.50)	3.555 (0.43)	3.722 (0.39)	3.898 (0.40)	3.976 (0.39)	4.078 (0.39)	4.096 (0.57)
	2.693 (0.80)	2.750 (0.51)	2.987 (0.44)	3.235 (0.47)	3.464 (0.40)	3.672 (0.41)	3.860 (0.41)	3.906 (0.40)	3.977 (0.41)	3.972 (0.56)
4.495 (0.57)	3.726 (0.48)	3.956 (0.41)	4.320 (0.37)	4.667 (0.37)	5.028 (0.37)	5.272 (0.37)	5.506 (0.38)	5.679 (0.38)	5.763 (0.36)	5.781 (0.51)

Fig. 3.9a. Pin-power distribution for CENTRM benchmark SAXTON-3. Value in parentheses is percent standard deviation.

0.187 (1.06)										5.920 (1.07)
									5.932 (0.47)	5.983 (0.45)
								5.779 (0.48)	5.826 (0.33)	5.906 (0.48)
							5.446 (0.46)	5.598 (0.33)	5.704 (0.33)	5.705 (0.45)
						5.019 (0.56)	5.257 (0.36)	5.406 (0.36)	5.478 (0.36)	5.496 (0.47)
					4.482 (0.54)	4.743 (0.40)	4.946 (0.34)	5.088 (0.35)	5.205 (0.34)	5.195 (0.51)
				3.988 (0.58)	4.209 (0.38)	4.447 (0.36)	4.582 (0.37)	4.738 (0.36)	4.822 (0.36)	4.866 (0.54)
			3.317 (0.60)	3.625 (0.44)	3.856 (0.39)	4.081 (0.38)	4.245 (0.37)	4.400 (0.36)	4.439 (0.34)	4.515 (0.51)
		2.787 (0.67)	3.058 (0.48)	3.340 (0.44)	3.557 (0.45)	3.734 (0.42)	3.912 (0.43)	4.022 (0.39)	4.049 (0.41)	4.134 (0.59)
	2.676 (0.74)	2.740 (0.51)	3.007 (0.46)	3.254 (0.49)	3.491 (0.42)	3.663 (0.47)	3.821 (0.42)	3.954 (0.42)	4.004 (0.43)	4.050 (0.61)
4.515 (0.53)	3.758 (0.45)	3.949 (0.41)	4.335 (0.40)	4.695 (0.39)	5.019 (0.36)	5.313 (0.36)	5.493 (0.38)	5.685 (0.38)	5.746 (0.34)	5.823 (0.46)

Fig. 3.9b. Pin-power distribution for NITAWL benchmark SAXTON-3. Value in parentheses is percent standard deviation.

Table 3.25. SAXTON-3 CENTRM reaction rates and fluxes

Pin	Region	$\langle\sigma_a\phi\rangle$ (cm^{-3} - s^{-1})	$\langle\nu\sigma_f\phi\rangle$ (cm^{-3} - s^{-1})	$\langle\sigma_f\phi\rangle$ (cm^{-3} - s^{-1})	$\langle\phi\rangle$ (cm - s^{-1})	$\langle\phi\rangle/\langle\phi\rangle_t$
	Fuel	2.543E-05	4.469E-05	1.562E-05	6.051E-03	0.295
1	Clad	2.340E-07	0.0	0.0	1.781E-03	0.087
	Mod.	1.588E-06	0.0	0.0	1.266E-02	0.618
	Fuel	3.944E-05	5.901E-05	2.061E-05	1.985E-02	0.292
66	Clad	5.323E-07	0.0	0.0	5.950E-03	0.087
	Mod.	1.782E-06	0.0	0.0	4.227E-02	0.621

Table 3.26. SAXTON-3 NITAWL reaction rates and fluxes

Pin	Region	$\langle\sigma_a\phi\rangle$ (cm^{-3} - s^{-1})	$\langle\nu\sigma_f\phi\rangle$ (cm^{-3} - s^{-1})	$\langle\sigma_f\phi\rangle$ (cm^{-3} - s^{-1})	$\langle\phi\rangle$ (cm - s^{-1})	$\langle\phi\rangle/\langle\phi\rangle_t$
	Fuel	2.574E-05	4.529E-05	1.589E-05	6.060E-03	0.295
1	Clad	2.313E-07	0.0	0.0	1.785E-03	0.087
	Mod.	7.923E-07	0.0	0.0	1.270E-02	0.618
	Fuel	3.956E-05	5.952E-05	2.079E-05	1.999E-02	0.293
66	Clad	5.281E-07	0.0	0.0	5.968E-03	0.087
	Mod.	8.857E-07	0.0	0.0	4.235E-02	0.620

Table 3.27. SAXTON-3, Pin-1 four-group fluxes

Group	CENTRM Φ (cm^{-2} - s^{-1})	NITAWL Φ (cm^{-2} - s^{-1})
1	7.796E-05	7.800E-05
2	2.181E-05	2.192E-05
3	4.829E-06	4.689E-06
4	1.453E-05	1.470E-05

Table 3.28. SAXTON-3, Pin-1 four-group U-235 cross sections

Group	CENTRM cross sections (cm^{-1})			NITAWL cross sections (cm^{-1})		
	σ_a	$\langle\sigma_f\rangle$	σ_f	σ_a	$\langle\sigma_f\rangle$	σ_f
1	2.32521E-04	5.28612E-04	2.03658E-04	2.32862E-04	5.29454E-04	2.03931E-04
2	5.50005E-03	8.43228E-03	3.46053E-03	5.39193E-03	8.28878E-03	3.40165E-03
3	7.92452E-03	1.60789E-02	6.59865E-03	7.90441E-03	1.60146E-02	6.57223E-03
4	7.31686E-02	1.52279E-01	6.24939E-02	7.33599E-02	1.52663E-01	6.26517E-02

Table 3.29. SAXTON-3, Pin-1 four-group U-238 cross sections

Group	CENTRM cross sections (cm^{-1})			NITAWL cross sections (cm^{-1})		
	σ_a	$\langle\sigma_f\rangle$	σ_f	σ_a	$\langle\sigma_f\rangle$	σ_f
1	7.20136E-03	1.33762E-02	4.75174E-03	7.23290E-03	1.34483E-02	4.77628E-03
2	5.41784E-02	5.69922E-06	2.36116E-06	5.29886E-02	5.86670E-06	2.43054E-06
3	1.12448E-02	3.86080E-08	1.59959E-08	1.12161E-02	3.84319E-08	1.59231E-08
4	4.20736E-02	1.97550E-07	8.18486E-08	4.21529E-02	1.97922E-07	8.20034E-08

Table 3.30. SAXTON-3, Pin-1 four-group Pu-239 cross sections

Group	CENTRM cross sections (cm^{-1})			NITAWL cross sections (cm^{-1})		
	σ_a	$\langle\sigma_f\rangle$	σ_f	σ_a	$\langle\sigma_f\rangle$	σ_f
1	2.51444E-03	7.33436E-03	2.36219E-03	2.51691E-03	7.34278E-03	2.36421E-03
2	4.43213E-02	7.47680E-02	2.59628E-02	4.17771E-02	7.10830E-02	2.46832E-02
3	1.44573E-01	2.86496E-01	9.94842E-02	1.40383E-01	2.78776E-01	9.68036E-02
4	1.27177E+00	2.55010E+00	8.82257E-01	1.28214E+00	2.56855E+00	8.88646E-01

Table 3.31. SAXTON-3, Pin-66 four-group fluxes

Group	CENTRM Φ (cm^{-2} - s^{-1})	NITAWL Φ (cm^{-2} - s^{-1})
1	2.666E-04	2.684E-04
2	9.313E-05	9.364E-05
3	1.707E-05	1.685E-05
4	1.407E-05	1.456E-05

Table 3.32. SAXTON-3, Pin-66 four-group U-235 cross sections

Group	CENTRM cross sections (cm^{-1})			NITAWL cross sections (cm^{-1})		
	Σ_a	$\langle\Sigma_f\rangle$	Σ_f	Σ_a	$\langle\Sigma_f\rangle$	Σ_f
1	2.42733E-04	5.37472E-04	2.08870E-04	2.43387E-04	5.37876E-04	2.09178E-04
2	5.30011E-03	8.16540E-03	3.35100E-03	5.27422E-03	8.12879E-03	3.33598E-03
3	7.70943E-03	1.55532E-02	6.38289E-03	7.67703E-03	1.54383E-02	6.33579E-03
4	6.52259E-02	1.35439E-01	5.55832E-02	6.49576E-02	1.34906E-01	5.53641E-02

Table 3.33. SAXTON-3, Pin-66 four-group U-238 cross sections

Group	CENTRM cross sections (cm^{-1})			NITAWL cross sections (cm^{-1})		
	Σ_a	$\langle\Sigma_f\rangle$	Σ_f	Σ_a	$\langle\Sigma_f\rangle$	Σ_f
1	6.92119E-03	1.15793E-02	4.11808E-03	6.86967E-03	1.13727E-02	4.04314E-03
2	5.09692E-02	6.02439E-06	2.49588E-06	4.92231E-02	6.08021E-06	2.51901E-06
3	1.11677E-02	3.78609E-08	1.56865E-08	1.11602E-02	3.77671E-08	1.56476E-08
4	3.79241E-02	1.77598E-07	7.35821E-08	3.78323E-02	1.77181E-07	7.34093E-08

Table 3.34. SAXTON-3, Pin-66 four-group Pu-239 cross sections

Group	CENTRM cross sections (cm^{-1})			NITAWL cross sections (cm^{-1})		
	Σ_a	$\langle\Sigma_f\rangle$	Σ_f	Σ_a	$\langle\Sigma_f\rangle$	Σ_f
1	2.52720E-03	7.21032E-03	2.34053E-03	2.52750E-03	7.19788E-03	2.33835E-03
2	4.12518E-02	6.95573E-02	2.41534E-02	4.03271E-02	6.74581E-02	2.34245E-02
3	1.37500E-01	2.73101E-01	9.48330E-02	1.37757E-01	2.73564E-01	9.49941E-02
4	1.43800E+00	2.77757E+00	9.61635E-01	1.41120E+00	2.73126E+00	9.45577E-01

0.218 (0.73)						18.89 (0.69)
					18.60 (0.33)	18.82 (0.36)
				17.23 (0.35)	17.81 (0.24)	18.18 (0.33)
			14.90 (0.35)	16.09 (0.26)	1.6.9 (0.26)	16.95 (0.35)
		12.39 (0.38)	13.62 (0.29)	14.58 (0.24)	15.18 (0.25)	15.37 (0.38)
	10.54 (0.30)	11.44 (0.28)	12.55 (0.28)	13.40 (0.26)	13.91 (0.27)	14.11 (0.40)
13.71 (0.41)	12.57 (0.29)	13.86 (0.29)	15.06 (0.26)	16.18 (0.25)	16.83 (0.25)	17.04 (0.30)

Fig. 3.10a. Pin-power distribution for CENTRM benchmark SAXTON-4. Value in parentheses is percent standard deviation.

0.216 (0.71)						19.22 (0.63)
					18.69 (0.34)	18.74 (0.33)
				17.22 (0.35)	17.97 (0.23)	18.11 (0.32)
			15.01 (0.37)	16.06 (0.26)	16.70 (0.24)	16.94 (0.35)
		12.38 (0.42)	13.63 (0.29)	14.56 (0.25)	15.19 (0.26)	15.46 (0.37)
	10.58 (0.45)	11.45 (0.28)	12.55 (0.30)	13.47 (0.29)	14.02 (0.27)	14.19 (0.39)
13.72 (0.38)	12.61 (0.27)	13.89 (0.27)	15.18 (0.25)	16.16 (0.28)	16.86 (0.24)	17.12 (0.33)

Fig. 3.10b. Pin-power distribution for NITAWL benchmark SAXTON-4. Value in parentheses is percent standard deviation.

Table 3.35. SAXTON-4 CENTRM reaction rates and fluxes

Pin	Region	$\langle\sigma_a\phi\rangle$ (cm^{-3} - s^{-1})	$\langle\nu\sigma_f\phi\rangle$ (cm^{-3} - s^{-1})	$\langle\sigma_f\phi\rangle$ (cm^{-3} - s^{-1})	$\langle\phi\rangle$ (cm - s^{-1})	$\langle\phi\rangle/\langle\phi\rangle_t$
	Fuel	7.531E-05	1.363E-04	4.765E-05	1.085E-02	0.172
1	Clad	6.208E-07	0.0	0.0	3.159E-03	0.050
	Mod.	3.325E-06	0.0	0.0	4.911E-02	0.778
	Fuel	1.133E-04	1.888E-04	6.597E-05	2.644E-02	0.170
28	Clad	1.093E-06	0.0	0.0	7.857E-03	0.051
	Mod.	4.152E-06	0.0	0.0	1.212E-01	0.779

Table 3.36. SAXTON-4 NITAWL reaction rates and fluxes

Pin	Region	$\langle\sigma_a\phi\rangle$ (cm^{-3} - s^{-1})	$\langle\nu\sigma_f\phi\rangle$ (cm^{-3} - s^{-1})	$\langle\sigma_f\phi\rangle$ (cm^{-3} - s^{-1})	$\langle\phi\rangle$ (cm - s^{-1})	$\langle\phi\rangle/\langle\phi\rangle_t$
	Fuel	7.555E-05	1.372E-04	4.796E-05	1.091E-02	0.172
1	Clad	6.298E-07	0.0	0.0	3.186E-03	0.050
	Mod.	1.677E-06	0.0	0.0	4.926E-02	0.778
	Fuel	1.153E-04	1.923E-04	6.721E-05	2.661E-02	0.171
28	Clad	1.090E-06	0.0	0.0	7.874E-03	0.050
	Mod.	2.076E-06	0.0	0.0	1.214E-01	0.779

Table 3.37. SAXTON-4, Pin-1 four-group fluxes

Group	CENTRM Φ (cm^{-2} - s^{-1})	NITAWL Φ (cm^{-2} - s^{-1})
1	1.767E-04	1.772E-04
2	4.238E-05	4.314E-05
3	9.788E-06	9.606E-06
4	4.606E-05	4.644E-05

Table 3.38. SAXTON-4, Pin-1 four-group U-235 cross sections

Group	CENTRM cross sections (cm^{-1})			NITAWL cross sections (cm^{-1})		
	σ_a	$\langle\sigma_f\rangle$	σ_f	σ_a	$\langle\sigma_f\rangle$	σ_f
1	2.28768E-04	5.25936E-04	2.01824E-04	2.28888E-04	5.26218E-04	2.01905E-04
2	5.58388E-03	8.56052E-03	3.51317E-03	5.50211E-03	8.45190E-03	3.46859E-03
3	8.12596E-03	1.65337E-02	6.78529E-03	8.00644E-03	1.62619E-02	6.67374E-03
4	7.52875E-02	1.56735E-01	6.43226E-02	7.54139E-02	1.57003E-01	6.44324E-02

Table 3.39. SAXTON-4, Pin-1 four-group U-238 cross sections

Group	CENTRM cross sections (cm^{-1})			NITAWL cross sections (cm^{-1})		
	σ_a	$\langle\sigma_f\rangle$	σ_f	σ_a	$\langle\sigma_f\rangle$	σ_f
1	7.34533E-03	1.41658E-02	5.02602E-03	7.35536E-03	1.41852E-02	5.03150E-03
2	5.77836E-02	6.06902E-06	2.51437E-06	5.53505E-02	5.94471E-06	2.46287E-06
3	1.12800E-02	3.90072E-08	1.61613E-08	1.12638E-02	3.87636E-08	1.60605E-08
4	4.31348E-02	2.02633E-07	8.39546E-08	4.31960E-02	2.02927E-07	8.40764E-08

Table 3.40. SAXTON-4, Pin-1 four-group Pu-239 cross sections

Group	CENTRM cross sections (cm^{-1})			NITAWL cross sections (cm^{-1})		
	σ_a	$\langle\sigma_f\rangle$	σ_f	σ_a	$\langle\sigma_f\rangle$	σ_f
1	2.51088E-03	7.39032E-03	2.37191E-03	2.51148E-03	7.39283E-03	2.37221E-03
2	4.48570E-02	7.50776E-02	2.60703E-02	4.28458E-02	7.19822E-02	2.49954E-02
3	1.48740E-01	2.94317E-01	1.02200E-01	1.46544E-01	2.90227E-01	1.00780E-01
4	1.25958E+00	2.54316E+00	8.79726E-01	1.25886E+00	2.54285E+00	8.79615E-01

Table 3.41. SAXTON-4, Pin-28 four-group fluxes

Group	CENTRM Φ (cm^{-2} - s^{-1})	NITAWL Φ (cm^{-2} - s^{-1})
1	4.435E-04	4.456E-04
2	1.401E-04	1.409E-04
3	2.995E-05	2.997E-05
4	5.644E-05	5.789E-05

Table 3.42. SAXTON-4, Pin-28 four-group U-235 cross sections

Group	CENTRM cross sections (cm^{-1})			NITAWL cross sections (cm^{-1})		
	Σ_a	$\langle\Sigma_f\rangle$	Σ_f	Σ_a	$\langle\Sigma_f\rangle$	Σ_f
1	2.37576E-04	5.33610E-04	2.06345E-04	2.36654E-04	5.32933E-04	2.05880E-04
2	5.42624E-03	8.34946E-03	3.42656E-03	5.49204E-03	8.44613E-03	3.46621E-03
3	8.00180E-03	1.62249E-02	6.65856E-03	7.91521E-03	1.60134E-02	6.57174E-03
4	7.09472E-02	1.47553E-01	6.05542E-02	7.02795E-02	1.46150E-01	5.99789E-02

Table 3.43. SAXTON-4, Pin-28 four-group U-238 cross sections

Group	CENTRM cross sections (cm^{-1})			NITAWL cross sections (cm^{-1})		
	Σ_a	$\langle\Sigma_f\rangle$	Σ_f	Σ_a	$\langle\Sigma_f\rangle$	Σ_f
1	7.11109E-03	1.26244E-02	4.48453E-03	7.14856E-03	1.28317E-02	4.55624E-03
2	5.52425E-02	5.99818E-06	2.48502E-06	5.40680E-02	5.89807E-06	2.44355E-06
3	1.12522E-02	3.86845E-08	1.60276E-08	1.12054E-02	3.82593E-08	1.58516E-08
4	4.09068E-02	1.91933E-07	7.95213E-08	4.05719E-02	1.90337E-07	7.88606E-08

Table 3.44. SAXTON-4, Pin-28 four-group Pu-239 cross sections

Group	CENTRM cross sections (cm^{-1})			NITAWL cross sections (cm^{-1})		
	Σ_a	$\langle\Sigma_f\rangle$	Σ_f	Σ_a	$\langle\Sigma_f\rangle$	Σ_f
1	2.52286E-03	7.28582E-03	2.35416E-03	2.52139E-03	7.29800E-03	2.35595E-03
2	4.55287E-02	7.65767E-02	2.65909E-02	4.36759E-02	7.33527E-02	2.54713E-02
3	1.45672E-01	2.88541E-01	1.00195E-01	1.41609E-01	2.80817E-01	9.75128E-02
4	1.32655E+00	2.62741E+00	9.09199E-01	1.32947E+00	2.62807E+00	9.09471E-01

0.274 (0.94)					20.09 (0.35)
				18.84 (0.33)	19.55 (0.23)
			16.65 (0.35)	17.71 (0.21)	18.36 (0.23)
		13.79 (0.34)	15.16 (0.22)	16.11 (0.24)	16.66 (0.24)
	11.35 (0.40)	12.45 (0.27)	13.69 (0.26)	14.59 (0.26)	15.00 (0.23)
13.36 (0.35)	12.75 (0.28)	14.14 (0.23)	15.59 (0.23)	16.47 (0.23)	17.04 (0.24)

Fig. 3.11a. Pin-power distribution for CENTRM benchmark SAXTON-5. Value in parentheses is percent standard deviation.

0.273 (0.90)					20.26 (0.30)
				19.04 (0.33)	19.51 (0.21)
			16.69 (0.35)	17.88 (0.23)	18.32 (0.22)
		13.84 (0.38)	15.25 (0.24)	16.23 (0.23)	16.66 (0.23)
	11.26 (0.44)	12.43 (0.29)	13.78 (0.25)	14.67 (0.26)	15.07 (0.25)
13.29 (0.34)	12.74 (0.26)	14.20 (0.24)	15.58 (0.22)	16.46 (0.22)	17.07 (0.24)

Fig. 3.11b. Pin-power distribution for NITAWL Benchmark SAXTON-5. Value in parentheses is percent standard deviation.

Table 3.45. SAXTON-5 CENTRM reaction rates and fluxes

Pin	Region	$\langle \sigma_a \phi \rangle$ ($cm^{-3} - s^{-1}$)	$\langle \nu\sigma_f \phi \rangle$ ($cm^{-3} - s^{-1}$)	$\langle \sigma_f \phi \rangle$ ($cm^{-3} - s^{-1}$)	ϕ ($cm - s^{-1}$)	ϕ/ϕ_t
	Fuel	7.340E-05	1.334E-04	4.665E-05	1.142E-02	0.148
1	Clad	6.001E-07	0.0	0.0	3.327E-03	0.043
	Mod.	3.369E-06	0.0	0.0	6.246E-02	0.809
	Fuel	1.175E-04	2.005E-04	7.008E-05	2.753E-02	0.147
21	Clad	1.081E-06	0.0	0.0	8.169E-03	0.043
	Mod.	4.571E-06	0.0	0.0	1.519E-01	0.810

Table 3.46. SAXTON-5 NITAWL reaction rates and fluxes

Pin	Region	$\langle \sigma_a \phi \rangle$ ($cm^{-3} - s^{-1}$)	$\langle \nu\sigma_f \phi \rangle$ ($cm^{-3} - s^{-1}$)	$\langle \sigma_f \phi \rangle$ ($cm^{-3} - s^{-1}$)	ϕ ($cm - s^{-1}$)	ϕ/ϕ_t
	Fuel	7.276E-05	1.326E-04	4.636E-05	1.134E-02	0.147
1	Clad	5.939E-07	0.0	0.0	3.314E-03	0.043
	Mod.	1.683E-06	0.0	0.0	6.233E-02	0.810
	Fuel	1.185E-04	2.024E-04	7.072E-05	2.776E-02	0.147
21	Clad	1.081E-06	0.0	0.0	8.220E-03	0.044
	Mod.	2.306E-06	0.0	0.0	1.528E-01	0.809

Table 3.47. SAXTON-5, Pin-1 four-group fluxes

Group	CENTRM Φ (cm^{-2} - s^{-1})	NITAWL Φ (cm^{-2} - s^{-1})
1	1.642E-04	1.632E-04
2	3.938E-05	3.897E-05
3	9.086E-06	8.830E-06
4	4.517E-05	4.505E-05

Table 3.48. SAXTON-5, Pin-1 four-group U-235 cross sections

Group	CENTRM cross sections (cm^{-1})			NITAWL cross sections (cm^{-1})		
	$\bar{\sigma}_a$	$\bar{\nu\sigma}_f$	$\bar{\sigma}_f$	$\bar{\sigma}_a$	$\bar{\nu\sigma}_f$	$\bar{\sigma}_f$
1	2.28516E-04	5.26334E-04	2.01776E-04	2.28104E-04	5.25678E-04	2.01507E-04
2	5.57692E-03	8.53438E-03	3.50244E-03	5.57593E-03	8.52166E-03	3.49720E-03
3	8.00912E-03	1.62733E-02	6.67842E-03	7.98496E-03	1.61621E-02	6.63276E-03
4	7.58687E-02	1.57957E-01	6.48244E-02	7.56584E-02	1.57516E-01	6.46433E-02

Table 3.49. SAXTON-5, Pin-1 four-group U-238 cross sections

Group	CENTRM cross sections (cm^{-1})			NITAWL cross sections (cm^{-1})		
	$\bar{\sigma}_a$	$\bar{\nu\sigma}_f$	$\bar{\sigma}_f$	$\bar{\sigma}_a$	$\bar{\nu\sigma}_f$	$\bar{\sigma}_f$
1	7.40499E-03	1.43721E-02	5.09562E-03	7.36961E-03	1.43170E-02	5.07374E-03
2	6.01938E-02	6.08276E-06	2.52006E-06	5.60690E-02	5.89946E-06	2.44412E-06
3	1.12744E-02	3.88600E-08	1.61004E-08	1.12557E-02	3.87165E-08	1.60410E-08
4	4.34215E-02	2.04004E-07	8.45229E-08	4.33185E-02	2.03512E-07	8.43190E-08

Table 3.50. SAXTON-5, Pin-1 four-group Pu-239 cross sections

Group	CENTRM cross sections (cm^{-1})			NITAWL cross sections (cm^{-1})		
	$\bar{\sigma}_a$	$\bar{\nu\sigma}_f$	$\bar{\sigma}_f$	$\bar{\sigma}_a$	$\bar{\nu\sigma}_f$	$\bar{\sigma}_f$
1	2.51193E-03	7.40536E-03	2.37431E-03	2.51011E-03	7.40294E-03	2.37356E-03
2	4.59985E-02	7.75008E-02	2.69116E-02	4.40523E-02	7.41950E-02	2.57639E-02
3	1.50511E-01	2.97520E-01	1.03313E-01	1.47223E-01	2.91456E-01	1.01207E-01
4	1.25860E+00	2.54527E+00	8.80429E-01	1.25753E+00	2.54209E+00	8.79338E-01

Table 3.51. SAXTON-5, Pin-21 four-group fluxes

Group	CENTRM Φ (cm^{-2} - s^{-1})	NITAWL Φ (cm^{-2} - s^{-1})
1	4.092E-04	4.112E-04
2	1.239E-04	1.261E-04
3	2.677E-05	2.696E-05
4	6.193E-05	6.260E-05

Table 3.52. SAXTON-5, Pin-21 four-group U-235 cross sections

Group	CENTRM cross sections (cm^{-1})			NITAWL cross sections (cm^{-1})		
	σ_a	$\langle\sigma_f$	σ_f	σ_a	$\langle\sigma_f$	σ_f
1	2.36162E-04	5.32867E-04	2.05677E-04	2.35623E-04	5.32179E-04	2.05354E-04
2	5.48935E-03	8.40097E-03	3.44768E-03	5.44674E-03	8.35559E-03	3.42905E-03
3	7.96989E-03	1.61823E-02	6.64109E-03	7.98750E-03	1.62231E-02	6.65779E-03
4	7.21016E-02	1.49992E-01	6.15555E-02	7.19091E-02	1.49587E-01	6.13891E-02

Table 3.53. SAXTON-5, Pin-21 four-group U-238 cross sections

Group	CENTRM cross sections (cm^{-1})			NITAWL cross sections (cm^{-1})		
	σ_a	$\langle\sigma_f$	σ_f	σ_a	$\langle\sigma_f$	σ_f
1	7.19130E-03	1.30115E-02	4.61767E-03	7.19283E-03	1.30642E-02	4.63670E-03
2	5.75995E-02	6.14358E-06	2.54525E-06	5.55646E-02	6.04202E-06	2.50319E-06
3	1.12575E-02	3.87725E-08	1.60642E-08	1.12617E-02	3.87641E-08	1.60607E-08
4	4.14883E-02	1.94726E-07	8.06790E-08	4.13946E-02	1.94278E-07	8.04931E-08

Table 3.54. SAXTON-5, Pin-21 four-group Pu-239 cross sections

Group	CENTRM cross sections (cm^{-1})			NITAWL cross sections (cm^{-1})		
	σ_a	$\langle\sigma_f$	σ_f	σ_a	$\langle\sigma_f$	σ_f
1	2.52182E-03	7.31114E-03	2.35818E-03	2.52033E-03	7.31286E-03	2.35814E-03
2	4.59107E-02	7.65671E-02	2.65875E-02	4.38622E-02	7.38489E-02	2.56436E-02
3	1.46728E-01	2.90546E-01	1.00891E-01	1.47469E-01	2.91907E-01	1.01364E-01
4	1.31306E+00	2.61230E+00	9.03898E-01	1.31380E+00	2.61230E+00	9.03907E-01

0.349 (1.00)					26.71 (0.54)
				25.24 (0.26)	26.06 (0.27)
			22.18 (0.30)	23.68 (0.19)	24.15 (0.28)
		17.62 (0.35)	19.75 (0.21)	21.10 (0.19)	21.46 (0.29)
	12.89 (0.35)	15.03 (0.22)	16.85 (0.22)	17.95 (0.20)	18.30 (0.31)
10.69 (0.39)	11.87 (0.28)	13.89 (0.26)	15.51 (0.25)	16.58 (0.23)	16.92 (0.35)

Fig. 3.12a. Pin-power distribution for CENTRM benchmark SAXTON-6. Value in parentheses is percent standard deviation.

0.341 (1.01)					26.34 (0.53)
				25.27 (0.28)	25.86 (0.27)
			22.14 (0.31)	23.68 (0.20)	24.16 (0.27)
		17.65 (0.32)	19.77 (0.21)	21.15 (0.19)	21.58 (0.30)
	12.84 (0.40)	15.03 (0.24)	16.86 (0.23)	17.98 (0.20)	18.46 (0.31)
10.75 (0.42)	11.84 (0.27)	13.94 (0.26)	15.58 (0.24)	16.62 (0.23)	16.94 (0.30)

Fig. 3.12b. Pin-power distribution for NITAWL benchmark SAXTON-6. Value in parentheses is percent standard deviation.

Table 3.55. SAXTON-6 CENTRM reaction rates and fluxes

Pin	Region	$\langle\sigma_a\phi\rangle$ (cm^{-3} - s^{-1})	$\langle\nu\sigma_f\phi\rangle$ (cm^{-3} - s^{-1})	$\langle\sigma_f\phi\rangle$ (cm^{-3} - s^{-1})	$\langle\phi\rangle$ (cm - s^{-1})	$\langle\phi\rangle/\langle\phi\rangle_t$
	Fuel	5.801E-05	1.068E-04	3.734E-05	8.227E-03	0.085
1	Clad	4.571E-07	0.0	0.0	2.381E-03	0.024
	Mod.	2.974E-06	0.0	0.0	8.646E-02	0.891
	Fuel	1.483E-04	2.649E-04	9.259E-05	2.605E-02	0.085
21	Clad	1.224E-06	0.0	0.0	7.665E-03	0.025
	Mod.	6.914E-06	0.0	0.0	2.718E-01	0.890

Table 3.56. SAXTON-6 NITAWL reaction rates and fluxes

Pin	Region	$\langle\sigma_a\phi\rangle$ (cm^{-3} - s^{-1})	$\langle\nu\sigma_f\phi\rangle$ (cm^{-3} - s^{-1})	$\langle\sigma_f\phi\rangle$ (cm^{-3} - s^{-1})	$\langle\phi\rangle$ (cm - s^{-1})	$\langle\phi\rangle/\langle\phi\rangle_t$
	Fuel	5.849E-05	1.078E-04	3.768E-05	8.318E-03	0.085
1	Clad	4.597E-07	0.0	0.0	2.405E-03	0.025
	Mod.	1.489E-06	0.0	0.0	8.696E-02	0.890
	Fuel	1.484E-04	2.656E-04	9.284E-05	2.592E-02	0.085
21	Clad	1.212E-06	0.0	0.0	7.589E-03	0.025
	Mod.	3.439E-06	0.0	0.0	2.708E-01	0.890

Table 3.57. SAXTON-6, Pin-1 four-group fluxes

Group	CENTRM Φ (cm^{-2} - s^{-1})	NITAWL Φ (cm^{-2} - s^{-1})
1	1.127E-04	1.136E-04
2	2.431E-05	2.487E-05
3	5.596E-06	5.708E-06
4	3.680E-05	3.720E-05

Table 3.58. SAXTON-6, Pin-1 four-group U-235 cross sections

Group	CENTRM cross sections (cm^{-1})			NITAWL cross sections (cm^{-1})		
	σ_a	$\langle\sigma_f\rangle$	σ_f	σ_a	$\langle\sigma_f\rangle$	σ_f
1	2.25419E-04	5.23524E-04	2.00192E-04	2.25627E-04	5.23460E-04	2.00250E-04
2	5.64554E-03	8.59223E-03	3.52618E-03	5.66043E-03	8.68922E-03	3.56598E-03
3	8.10920E-03	1.64809E-02	6.76363E-03	8.14676E-03	1.65761E-02	6.80268E-03
4	7.66356E-02	1.59575E-01	6.54883E-02	7.61884E-02	1.58640E-01	6.51043E-02

Table 3.59. SAXTON-6, Pin-1 four-group U-238 cross sections

Group	CENTRM cross sections (cm^{-1})			NITAWL cross sections (cm^{-1})		
	σ_a	$\langle\sigma_f\rangle$	σ_f	σ_a	$\langle\sigma_f\rangle$	σ_f
1	7.46961E-03	1.48484E-02	5.26453E-03	7.45908E-03	1.47830E-02	5.24259E-03
2	6.30267E-02	6.27162E-06	2.59830E-06	5.76920E-02	5.74105E-06	2.37850E-06
3	1.12849E-02	3.89762E-08	1.61485E-08	1.13126E-02	3.92234E-08	1.62510E-08
4	4.38120E-02	2.05877E-07	8.52986E-08	4.35935E-02	2.04834E-07	8.48667E-08

Table 3.60. SAXTON-6, Pin-1 four-group Pu-239 cross sections

Group	CENTRM cross sections (cm^{-1})			NITAWL cross sections (cm^{-1})		
	σ_a	$\langle\sigma_f\rangle$	σ_f	σ_a	$\langle\sigma_f\rangle$	σ_f
1	2.50829E-03	7.44201E-03	2.38103E-03	2.50741E-03	7.43347E-03	2.37922E-03
2	4.78379E-02	8.01259E-02	2.78233E-02	4.63764E-02	7.75412E-02	2.69258E-02
3	1.52214E-01	3.00611E-01	1.04386E-01	1.54150E-01	3.04373E-01	1.05692E-01
4	1.24949E+00	2.53488E+00	8.76780E-01	1.24891E+00	2.53120E+00	8.75527E-01

Table 3.61. SAXTON-6, Pin-21 four-group fluxes

Group	CENTRM Φ (cm^{-2} - s^{-1})	NITAWL Φ (cm^{-2} - s^{-1})
1	3.626E-04	3.592E-04
2	9.528E-05	9.575E-05
3	2.230E-05	2.206E-05
4	8.798E-05	8.816E-05

Table 3.62. SAXTON-6, Pin-21 four-group U-235 cross sections

Group	CENTRM cross sections (cm^{-1})			NITAWL cross sections (cm^{-1})		
	Σ_a	$\langle\Sigma_f\rangle$	Σ_f	Σ_a	$\langle\Sigma_f\rangle$	Σ_f
1	2.30565E-04	5.27350E-04	2.02688E-04	2.30477E-04	5.28068E-04	2.02763E-04
2	5.63375E-03	8.59935E-03	3.52909E-03	5.56879E-03	8.53534E-03	3.50283E-03
3	8.06789E-03	1.64302E-02	6.74278E-03	8.03178E-03	1.64159E-02	6.73694E-03
4	7.49118E-02	1.55931E-01	6.39925E-02	7.47374E-02	1.55564E-01	6.38420E-02

Table 3.63. SAXTON-6, Pin-21 four-group U-238 cross sections

Group	CENTRM cross sections (cm^{-1})			NITAWL cross sections (cm^{-1})		
	Σ_a	$\langle\Sigma_f\rangle$	Σ_f	Σ_a	$\langle\Sigma_f\rangle$	Σ_f
1	7.31139E-03	1.38701E-02	4.92308E-03	7.34112E-03	1.40133E-02	4.96478E-03
2	6.04901E-02	6.16474E-06	2.55402E-06	5.89630E-02	6.22799E-06	2.58023E-06
3	1.12898E-02	3.90791E-08	1.61912E-08	1.12885E-02	3.90972E-08	1.61987E-08
4	4.29311E-02	2.01652E-07	8.35480E-08	4.28370E-02	2.01200E-07	8.33613E-08

Table 3.64. SAXTON-6, Pin-21 four-group Pu-239 cross sections

Group	CENTRM cross sections (cm^{-1})			NITAWL cross sections (cm^{-1})		
	Σ_a	$\langle\Sigma_f\rangle$	Σ_f	Σ_a	$\langle\Sigma_f\rangle$	Σ_f
1	2.51210E-03	7.36437E-03	2.36645E-03	2.51355E-03	7.37904E-03	2.36928E-03
2	4.63848E-02	7.74581E-02	2.68969E-02	4.49666E-02	7.52761E-02	2.61392E-02
3	1.47063E-01	2.91411E-01	1.01191E-01	1.47665E-01	2.92500E-01	1.01570E-01
4	1.27191E+00	2.56133E+00	8.86051E-01	1.27598E+00	2.56709E+00	8.88067E-01

4. MIX-COMP-THERM-4 (TCA-1 TO TCA-11)

4.1 DESCRIPTION

This section describes a set of 11 critical experiments, each consisting of a square-pitched array of mixed Plutonium-Uranium fuel rods partially submerged in water surrounded by a water reflector. The water-to-fuel ratios for the arrays range from 2.4 to 5.6. This set of experiments is contained in the *International Handbook of Evaluated Criticality Safety Benchmark Experiments*.[3]

This set of experiments was performed between 1972 and 1975 at the Tokai Research Establishment of JAERI. The Tank-Type Critical Assembly (TCA) benchmark cases are light-water moderated critical assemblies, consisting of a core array supported by upper, middle, and lower grid plates. The grid plates do not pass through the fuel region. The fuel is sufficiently long such that the water level is below the top of the fuel region in all cases. The reactor is brought to critical by raising the water level in the tank, thus avoiding the use of control rods. The fuel rods sit on a support plate above the bottom of the tank. The tank is wide enough to assume an infinite moderator on the sides (~30 cm of water).

All fuel rods have the same physical dimensions. A schematic diagram of the fuel rods and bottom reflector is given in Fig. 4.1. Each fuel rod has an active fuel length of 70.6 cm and a 16.83-cm-long bottom aluminum end plug that sits on a 1.27-cm-thick aluminum support plate. The fuel has a radius of 0.5325 cm. The cladding has an outside radius of 0.6115 cm. For the calculation, the cladding is extended 9.97 cm above the active fuel to the bottom of the middle grid plate. The middle grid plate and everything above are assumed to be insignificant and thus excluded from the model. The fuel lattice is surrounded by 30 cm of water on the four sides from the bottom of the tank to the top of the critical water level.

From the top of the aluminum support plate is a 4.445-cm water gap and 0.601-cm lower aluminum grid plate. Below the aluminum support plate is a 2.2-cm-thick stainless steel (SS) support plate, a 13.8-cm water gap, 0.5-cm-thick SS tank liner and 37.0 cm of concrete.

The primary differences between the 11 benchmarks are lattice pitch, number of rods in the lattice, water level, and Pu-241 and Am-241 number densities. All other benchmark characteristics are constant. The 11 benchmarks are divided into four different lattice pitches: 1.825 cm, 1.956 cm, 2.225 cm, and 2.474 cm. For a given pitch, the number of pins in the lattice is given. The fuel is arranged in a square-pitched square lattice. The characteristics of each of the four lattices are given in Table 4.1. The critical fuel height variations are due to the changes in Pu-241 and Am-241 atom densities. Table 4.2 contains the atom densities for all the materials in the problem except Pu-241 and Am-241. The atom densities in Table 4.2 are constant for all benchmarks. Table 4.3 contains the atom densities for Pu-241 and Am-241 for each benchmark. All material temperatures are assumed to be 20°C.

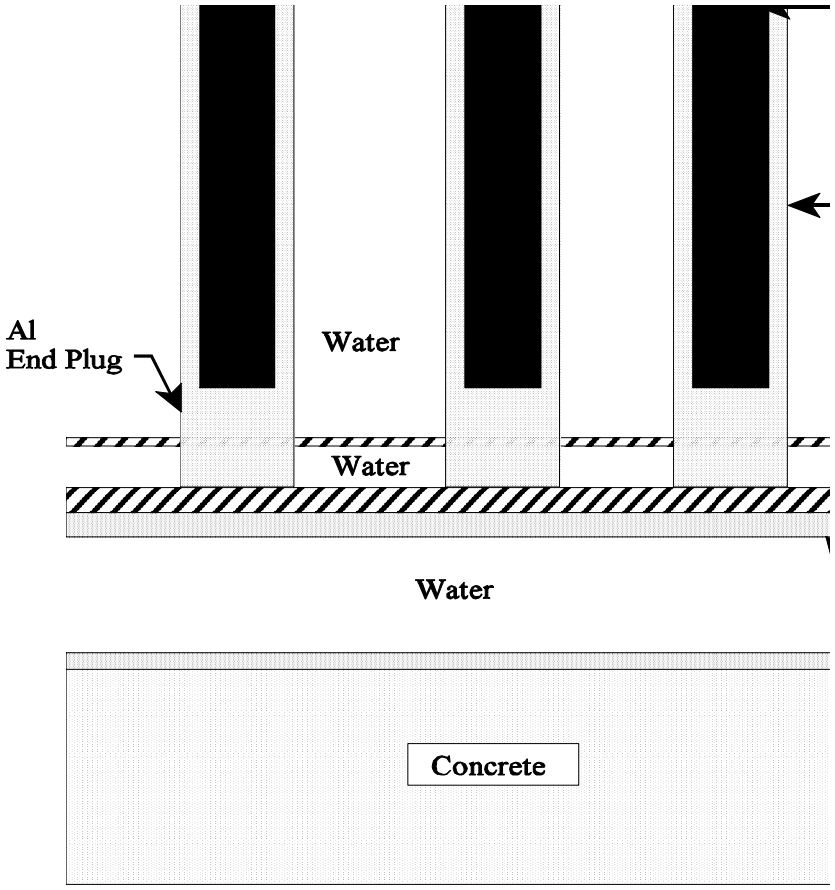

Fig. 4.1. Schematic of the TCA fuel rods and bottom reflector.

Table 4.1. Lattice description for benchmarks

Benchmark No.	Water/Fuel volume ratio (H/Pu ratio)	Lattice pitch (cm)	Number of rods on a Side	Lattice side dimension (cm)	Critical water level (cm)
1	2.42 (402)	1.825	23	41.975	59.5
2					91.90
3					64.06
4	2.98 (494)	1.956	21	41.076	61.50
5					64.40
6					69.40
7	4.24 (703)	p2.225	20	44.500	60.32
8					62.99
9					65.63
10	5.55 (921)	2.474	21	51.954	62.05
11					64.53

The first three benchmarks; TCA-1, TCA-2, and TCA-3 have a pitch of 1.825 cm and 23 × 23 pin lattice. This pitch produces a water-to-fuel volume ratio of 2.42 cm and a H/Pu ratio of 402. To simplify the production of the lattice pin-power distribution and improve the statistics, the lattice advantage is taken of the lattice symmetry. Only 1/8th of the lattice needs to be modeled precisely to produce the pin-power distribution. The lattice is then filled from the 1/8th section by inserting additional pins in a mirror image. Figure 4.2 is a lattice map of the pin locations.

The same approach is used for the next three benchmarks: TCA-4, TCA-5, and TCA-6. These benchmarks have a pitch of 1.956 cm and 21 × 21 pin lattice. This pitch produces a water-to-fuel volume ratio of 2.98 cm and a H/Pu ratio of 494. The symmetry of the lattice is used in the same way it was used in the first three benchmarks. One-eighth of the lattice is filled, and the remaining lattice is filled assuming a mirror image. Figure 4.3 is a lattice map of the pin locations.

The next three benchmark problems**C**TCA-7, TCA-8, and TCA-9**C**again use the same approach. These benchmarks have a pitch of 2.225 cm and a 20 × 20 pin lattice. This pitch produces a water-to-fuel volume ratio of 4.24 cm and a H/Pu ratio of 703. Figure 4.4 is a lattice map of the pin locations.

The last benchmark problems**C**TCA-10 and TCA-11**C**have the same lattice arrangement as the second set of benchmarks (see Fig. 4.3). However, these benchmarks have of pitch of 2.474 cm which produces a water-to-fuel volume ratio of 5.55 cm and a H/Pu ratio of 921. The input files for each of the benchmark problems can be found in Appendix C.

4.2 ANALYSIS

All 11 computational benchmarks in this section were processed twice using SCALE 5.0. The set labeled NITAWL uses the NITAWL resonance processor to self-shield the resolved resonance region for all nuclides in the fuel and clad. An identical set, labeled CENTRM, replaces NITAWL with the CENTRM/PMC code sequence. The NITAWL and CENTRM results are then compared.

Table 4.4 contains the k_{eff} and Energy of the Average Lethargy Causing Fission (EALCF). The k_{eff} values for all the benchmark cases are very close to 1.0: the worst NITAWL benchmark is 0.26% high, and the worst CENTRM case is 0.37% low. There does appear to be a small negative bias between NITAWL and CENTRM, the CENTRM cases being about 0.2% lower on average than the NITAWL cases. The EALCF values listed are from the CENTRM cases. For all cases the difference between this value for CENTRM and NITAWL was less than 0.1%. Both CENTRM and NITAWL produce excellent results for the k_{eff} and fission energy for this set of problems.

Also, calculated for each problem is the: pin-power distributions; absorption, σ_f, and fission reaction rates and fluxes in the pin fuel, clad, and moderator; and four group cross sections and fluxes for a corner outside pin and the innermost pin. Each of these sets of data are calculated using both CENTRM and NITAWL. The data for each case are contained in Figs. 4.5a through 4.15b and Tables 4.114 through 4.5.

The pin-power distributions for this problem assumed 1/8th core symmetry with a surrounding reflector. The pin-power data consist of a value and a standard deviation for each pin. The values for the pin-powers are actually in units of fissions per cm^3-s-source particle $\times 10^{-5}$. The value in parentheses is the percent standard deviation of the pin-power value. In most cases, the CENTRM and NITAWL results for each benchmark case agree within 2 standard deviations. The pin-power distributions represent that portion of the pin covered by water. The value off to the side in the pin-power distributions represents all the fuel not covered by water. The peak-to-low power changed with respect to pitch. The peak-to-low-power ratio changed from a low of 2.7 for the smallest pitch to a high of 4.9 at the largest pitch.

The reaction rates, total fluxes, and flux ratios for the CENTRM and NITAWL cases of each benchmark case are also in good agreement, seldom varying by more than 1%. These values are included for a corner pin and the center pin for each case. The flux ratios over the fuel, clad, and moderator stay relatively constant for a given pitch. However, as the pitch increases the proportion of the total pin flux in the moderator increases.

Finally, four-group fluxes and cross sections were calculated for selected nuclides in the fuel region of the same corner and center pins. The macroscopic cross sections include the radiative capture, fission, and nu*fission cross sections for U-235, U-238, and Pu-239. The four groups are collapsed from the 238-group multigroup cross-section set using the flux profile calculated in KENO-V.a as follows: group 1 is from 20 Mev to 9.5 keV, group 2 is from 9.5 keV to 3.0 eV, Group 3 is from 3 eV to 0.4 eV, and group 4 is from 0.4 eV to 10^{-5} eV. The 0.4 eV was chosen as a boundary because it is the cadmium cutoff energy. Groups 2 and 3 contain the resolved resonance regions for most of the nuclides used in these cases. Most of the cross-section data for the CENTRM and NITAWL cases of a given benchmark case agree within 1%.

4.3 CONCLUSIONS

For this set of benchmark cases, using either NITAWL and CENTRM as the resonance region processor produces acceptable results of the k_{eff} values. All other values produced using CENTRM and NITAWL are also consistent with each. The k_{eff} values are slightly lower, ~0.2%, for all CENTRM cases. The pin-power distributions, fluxes, reaction rates, and macroscopic cross sections generally agree within approximately 1% between CENTRM and NITAWL. No significant differences were identified between the results produced by NITAWL and CENTRM for these benchmark cases.

Table 4.2. Benchmark atom densities

Material	Isotope	Atom density (atoms/barn-cm)	Material	Isotope	Atom density (atoms/barn-cm)
Fuel	U-234	7.1749×10^{-7}	Ordinary concrete	H	1.3742×10^{-2}
	U-235	9.3926×10^{-5}		O	4.5919×10^{-2}
	U-238	1.2951×10^{-2}		C	1.1532×10^{-4}
	Pu-238	2.0003×10^{-6}		Na	9.6395×10^{-4}
	Pu-239	2.7491×10^{-4}		Mg	1.2388×10^{-4}
	Pu-240	8.8417×10^{-5}		Al	1.7409×10^{-3}
	Pu-241	(See Table 3.3)		Si	1.6617×10^{-2}
	Pu-242	8.1234×10^{-6}		K	4.6052×10^{-4}
	Am-241	(See Table 3.3)		Ca	1.5025×10^{-3}
	O-16	2.7837×10^{-2}		Fe	3.4492×10^{-4}
	B-10	6.0418×10^{-8}			
	B-11	2.4319×10^{-7}			
Cladding + Air gap	Zr	3.7772×10^{-2}	Stainless steel (SS-304L)	C	1.1928×10^{-4}
	Sn	4.3737×10^{-4}		Si	1.7003×10^{-3}
	Fe	8.8570×10^{-5}		Mn	1.7385×10^{-3}
	Cr	6.6119×10^{-5}		P	6.9381×10^{-5}
	Ni	3.5864×10^{-5}		S	4.4673×10^{-5}
				Ni	8.9506×10^{-3}
				Cr	1.7450×10^{-2}
				Fe	5.7202×10^{-2}
Water (20° C) 0.9982 g/cc	H	6.6735×10^{-2}	Aluminum	Al	6.0224×10^{-2}
	O	3.3368×10^{-2}			

Table 4.3. Pu-241 and Am-241 atom densities

Benchmark No.	Atom densities (atoms/barn-cm)	
	Pu-241	Am-241
1	2.7923×10^{-5}	1.3531×10^{-6}
2	2.6701×10^{-5}	2.5812×10^{-6}
3	2.5447×10^{-5}	3.8361×10^{-6}
4	2.8003×10^{-5}	1.2793×10^{-6}
5	2.6670×10^{-5}	2.6129×10^{-6}
6	2.4228×10^{-5}	5.0543×10^{-6}
7	2.8133×10^{-5}	1.1498×10^{-6}
8	2.6649×10^{-5}	2.6340×10^{-6}
9	2.5373×10^{-5}	3.9098×10^{-6}
10	2.8077×10^{-5}	1.2053×10^{-6}
11	2.6617×10^{-5}	2.6656×10^{-6}

Table 4.4. Comparison of k_{eff} and EALCF from CENTRM and NITAWL[a]

Benchmark identification	CENTRM k_{eff} (±F)	NITAWL k_{eff} (±F)	EALF (eV)	k_{eff} % DIFF
TCA-1	0.9963 (0.0005)	0.9993 (0.0004)	0.145	-0.3
TCA-2	0.9969 (0.0004)	1.0001 (0.0004)	0.144	-0.32
TCA-3	0.9985 (0.0005)	1.0002 (0.0004)	0.143	-0.17
TCA-4	0.9973 (0.0004)	0.9995 (0.0004)	0.119	-0.22
TCA-5	0.9982 (0.0004)	1.0008 (0.0004)	0.118	-0.26
TCA-6	0.9988 (0.0004)	1.0003 (0.0003)	0.117	-0.15
TCA-7	0.9994 (0.0004)	1.0016 (0.0004)	0.0927	-0.22
TCA-8	1.0002 (0.0004)	1.0017 (0.0003)	0.0923	-0.15
TCA-9	1.0009 (0.0004)	1.0024 (0.0004)	0.0916	-0.15
TCA-10	1.0003 (0.0003)	1.0020 (0.0004)	0.0797	-0.17
TCA-11	1.0010 (0.0004)	1.0026 (0.0004)	0.0792	-0.16

[a] Value in parentheses is percent standard deviation.

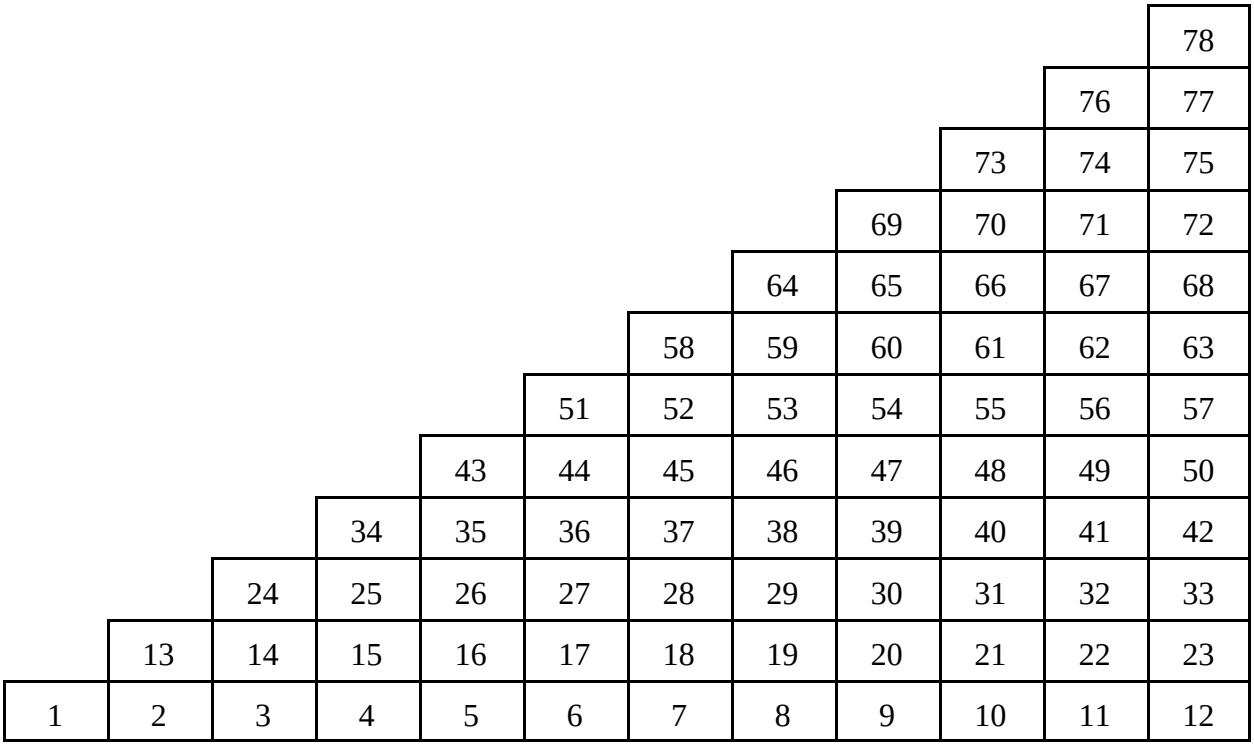

Fig. 4.2. Pin layout of benchmark cases TCA-1, TCA-2, and TCA-3.

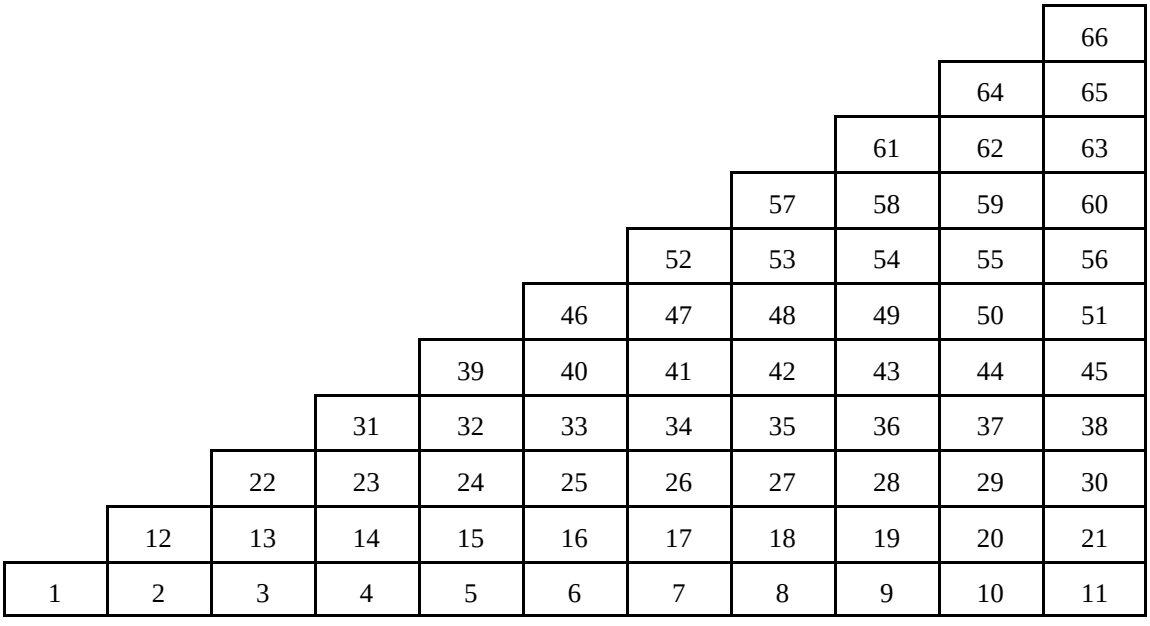

Fig. 4.3. Pin layout of benchmark cases TCA-4, TCA-5 ,TCA-6, TCA-10, and TCA-11.

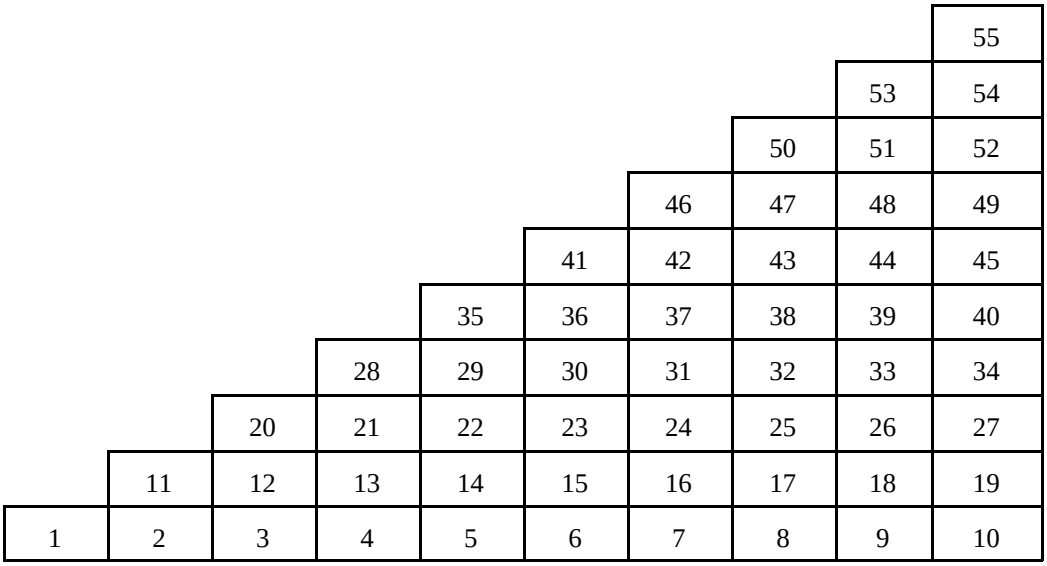

Fig. 4.4. Pin layout of benchmark cases TCA-7, TCA-8, and TCA-9.

											5.299 (0.91)
	0.131 (0.59)									5.191 (0.46)	5.175 (0.48)
									4.954 (0.48)	5104 (0.36)	5.242 (0.48)
								4.722 (0.51)	4.871 (0.33)	4.971 (0.34)	4.937 (0.48)
							4.426 (0.51)	4.601 (0.33)	4.697 (0.36)	4.759 (0.36)	4.815 (0.54)
						3.982 (0.50)	4.212 (0.39)	4.340 (0.37)	4.479 0.36)	4.554 (0.33)	4.551 (0.44)
					3.535 (0.54)	3.766 (0.44)	3.934 (0.40)	4.068 (0.40)	4.184 (0.38)	4.252 (0.38)	4.286 (0.53)
				3.058 (060)	3.295 (0.43)	3.456 (0.45)	3.650 (0.35)	3.781 (0.36)	3.895 (0.37)	3.942 (0.39)	3.989 (0.53)
			2.518 (0.75)	2.769 (0.48)	2.963 (0.45)	3.180 (0.44)	3.354 (0.46)	3.457 (0.41)	3.555 (0.38)	3.617 (0.40)	3.640 (0.56)
		2.104 (0.83)	2.321 (0.51)	2.533 (0.48)	2.736 (0.45)	2.893 (0.47)	3.058 (0.39)	3.159 (0.41)	3.257 (0.42)	3.271 (0.41)	3.331 (0.58)
	1.889 (0.78)	1.980 (0.57)	2.223 (0.55)	2.402 (0.51)	2.624 (0.50)	2.789 (0.41)	2.917 (0.41)	3.037 (0.47)	3.092 (0.45)	3.150 (0.42)	3.184 (0.65)
2.329 (0.66)	2.178 (0.54)	2.356 (0.50)	2.589 (0.47)	2.844 (0.47)	3.066 (0.41)	3.258 (0.42)	3.398 (0.43)	3.576 (0.39)	3.644 (0.44)	3.710 (0.40)	3.729 (0.57)

Fig. 4.5a. Pin-power distribution for CENTRM benchmark TCA-1. Value in parentheses is percent standard deviation.

											5.219 (0.86)
	0.131 (0.53)									5.153 (0.50)	5.235 (0.47)
									5.022 (0.49)	5.083 (0.36)	5.140 (0.46)
								4.775 (0.48)	4.893 (0.35)	4.968 (0.38)	5.010 (0.49)
							4.453 (0.54	4.607 (0.35)	4.712 (0.36)	4.779 (0.33)	4.840 (0.50)
						4.006 (0.55)	4.225 (0.41)	4.384 (0.36)	4.474 (0.36)	4.594 (0.35)	4.547 (0.53)
					3.541 (0.55)	3.807 (0.39)	3.978 (0.41)	4.086 (0.36)	4.200 (0.39)	4.270 (0.37)	4.341 (0.47)
				3.013 (0.60)	3.298 (0.40)	3.496 (0.39)	3.645 (0.42)	3.821 (0.38)	3.921 (0.43)	3.981 (0.37)	3.948 (0.55)
			2.552 (0.65)	2.767 (0.46)	2.999 (0.44)	3.200 (0.40)	3.362 (0.36)	3.471 (0.38)	3.581 (0.41)	3.631 (0.41)	3.624 (0.59)
		2.113 (0.73)	2.284 (0.48)	2.509 0.50)	2.749 (0.46)	2.906 (0.47)	3.036 (0.42)	3.153 (0.42)	3.238 (0.41)	3.276 (0.44)	3.329 (0.53)
	1.911 (0.77)	1.997 (0.47)	2.202 (0.57)	2.417 (0.51)	2.623 (0.44)	2.768 (0.46)	2.927 (0.46)	3.029 (0.40)	3.071 (0.44)	3.176 (0.41)	3.180 (0.65)
2.279 (0.69)	2.171 (0.53)	2.347 (0.50)	2.571 (0.48)	2.845 (0.43)	3.066 (0.47)	3.274 (0.39)	3.446 (0.41)	3.601 (0.38)	3.673 (0.38)	3.729 (0.41)	3.776 (0.55)

Fig. 4.5b. Pin-power distribution for NITAWL benchmark TCA-1. Value in parentheses is percent standard deviation.

Table 4.5. Selected reaction rates for CENTRM case TCA-1

Pin	Region	$\langle \sigma_a \phi \rangle$ ($cm^{-3} - s^{-1}$)	$\langle \nu\sigma_f \phi \rangle$ ($cm^{-3} - s^{-1}$)	$\langle \sigma_f \phi \rangle$ ($cm^{-3} - s^{-1}$)	$\langle \phi \rangle$ ($cm - s^{-1}$)	$\langle \phi \rangle / \langle \phi \rangle_t$
	Fuel	1.400E-05	2.320E-05	8.219E-06	5.406E-03	0.271
1	Clad	2.686E-07	0.0	0.0	1.687E-03	0.085
	Mod.	7.396E-07	0.0	0.0	1.285E-02	0.644
	Fuel	3.547E-05	5.287E-05	1.869E-05	2.162E-02	0.270
78	Clad	7.404E-07	0.0	0.0	6.840E-03	0.085
	Mod.	1.542E-06	0.0	0.0	5.169E-02	0.645

Table 4.6. Selected reaction rates for NITAWL case TCA-1

Pin	Region	$\langle \sigma_a \phi \rangle$ ($cm^{-3} - s^{-1}$)	$\langle \nu\sigma_f \phi \rangle$ ($cm^{-3} - s^{-1}$)	$\langle \sigma_f \phi \rangle$ ($cm^{-3} - s^{-1}$)	$\langle \phi \rangle$ ($cm - s^{-1}$)	$\langle \phi \rangle / \langle \phi \rangle_t$
	Fuel	1.386E-05	2.292E-05	8.121E-06	5.354E-03	0.271
1	Clad	2.641E-07	0.0	0.0	1.665E-03	0.084
	Mod.	7.348E-07	0.0	0.0	1.277E-02	0.645
	Fuel	3.457E-05	5.164E-05	1.827E-05	2.134E-02	0.268
78	Clad	7.151E-07	0.0	0.0	6.771E-03	0.085
	Mod.	1.529E-06	0.0	0.0	5.146E-02	0.647

Table 4.7. TCA-1, Pin-1 four-group fluxes

Group	CENTRM Φ (cm^{-2} - s^{-1})	NITAWL Φ (cm^{-2} - s^{-1})
1	5.205E-05	5.150E-05
2	1.550E-05	1.533E-05
3	3.677E-06	3.705E-06
4	3.068E-05	3.040E-05

Table 4.8. TCA-1, Pin-1 four-group U-235 cross sections

Group	CENTRM cross sections (cm^{-1})			NITAWL cross sections (cm^{-1})		
	σ_a	$\langle\sigma_f$	σ_f	σ_a	$\langle\sigma_f$	σ_f
1	1.43276E-04	3.25948E-04	1.25443E-04	1.43133E-04	3.25491E-04	1.25308E-04
2	3.47383E-03	5.32334E-03	2.18465E-03	3.41501E-03	5.21704E-03	2.14103E-03
3	5.07797E-03	1.03603E-02	4.25178E-03	5.13482E-03	1.05164E-02	4.31584E-03
4	4.86542E-02	1.01291E-01	4.15691E-02	4.83612E-02	1.00680E-01	4.13181E-02

Table 4.9. TCA-1, Pin-1 four-group U-238 cross sections

Group	CENTRM cross sections (cm^{-1})			NITAWL cross sections (cm^{-1})		
	σ_a	$\langle\sigma_f$	σ_f	σ_a	$\langle\sigma_f$	σ_f
1	4.48868E-03	8.37908E-03	2.97182E-03	4.45235E-03	8.27583E-03	2.93388E-03
2	3.79279E-02	3.70803E-06	1.53622E-06	3.78200E-02	3.60508E-06	1.49357E-06
3	6.96274E-03	2.42790E-08	1.00592E-08	6.99725E-03	2.45979E-08	1.01914E-08
4	2.76422E-02	1.29929E-07	5.38321E-08	2.75005E-02	1.29251E-07	5.35513E-08

Table 4.10. TCA-1, Pin-1 four-group Pu-239 cross sections

Group	CENTRM cross sections (cm^{-1})			NITAWL cross sections (cm^{-1})		
	σ_a	$\langle\sigma_f$	σ_f	σ_a	$\langle\sigma_f$	σ_f
1	5.12119E-04	1.49477E-03	4.80859E-04	5.11680E-04	1.49305E-03	4.80499E-04
2	1.13759E-02	1.87090E-02	6.49658E-03	1.06255E-02	1.76083E-02	6.11439E-03
3	3.27337E-02	6.44523E-02	2.23808E-02	3.35760E-02	6.60534E-02	2.29368E-02
4	2.66846E-01	5.40163E-01	1.86831E-01	2.66855E-01	5.39595E-01	1.86638E-01

Table 4.11. TCA-1, Pin-78 four-group fluxes

Group	CENTRM $\overline{M}$ (cm^{-2} - s^{-1})	NITAWL $\overline{M}$ (cm^{-2} - s^{-1})
1	2.399E-04	2.360E-04
2	8.524E-05	8.507E-05
3	1.867E-05	1.851E-05
4	6.380E-05	6.276E-05

Table 4.12. TCA-1, Pin-78 four-group U-235 cross sections

Group	CENTRM cross sections (cm^{-1})			NITAWL cross sections (cm^{-1})		
	$\overline{G_a}$	$\overline{\nu G_f}$	$\overline{G_f}$	$\overline{G_a}$	$\overline{\nu G_f}$	$\overline{G_f}$
1	1.48131E-04	3.30102E-04	1.27921E-04	1.47652E-04	3.28787E-04	1.27540E-04
2	3.33968E-03	5.12318E-03	2.10251E-03	3.40930E-03	5.23865E-03	2.14990E-03
3	5.10391E-03	1.04015E-02	4.26869E-03	5.13030E-03	1.04663E-02	4.29526E-03
4	4.54602E-02	9.45345E-02	3.87961E-02	4.53139E-02	9.42388E-02	3.86748E-02

Table 4.13. TCA-1, Pin-78 four-group U-238 cross sections

Group	CENTRM cross sections (cm^{-1})			NITAWL cross sections (cm^{-1})		
	$\overline{G_a}$	$\overline{\nu G_f}$	$\overline{G_f}$	$\overline{G_a}$	$\overline{\nu G_f}$	$\overline{G_f}$
1	4.34327E-03	7.48462E-03	2.65627E-03	4.30530E-03	7.37008E-03	2.62250E-03
2	3.98175E-02	3.68536E-06	1.52683E-06	3.74190E-02	3.60909E-06	1.49523E-06
3	6.98275E-03	2.43235E-08	1.00777E-08	6.98957E-03	2.44139E-08	1.01151E-08
4	2.59889E-02	1.21997E-07	5.05458E-08	2.59301E-02	1.21719E-07	5.04304E-08

Table 4.14. TCA-1, Pin-78 four-group Pu-239 cross sections

Group	CENTRM cross sections (cm^{-1})			NITAWL cross sections (cm^{-1})		
	$\overline{G_a}$	$\overline{\nu G_f}$	$\overline{G_f}$	$\overline{G_a}$	$\overline{\nu G_f}$	$\overline{G_f}$
1	5.14181E-04	1.47485E-03	4.77461E-04	5.13292E-04	1.47159E-03	4.76847E-04
2	1.06372E-02	1.75772E-02	6.10359E-03	1.08006E-02	1.79107E-02	6.21938E-03
3	3.42975E-02	6.73203E-02	2.33768E-02	3.44553E-02	6.76072E-02	2.34764E-02
4	2.85886E-01	5.65284E-01	1.95610E-01	2.82398E-01	5.59148E-01	1.93483E-01

											4.965 (0.99)
	0.139 (0.64)									4.937 (0.46)	4.994 (0.49)
									4.776 (0.50)	4.866 (0.34)	4.932 (0.47)
								4.569 (0.53)	4.688 (0.32)	4.750 (0.35)	4.781 (0.47)
							4.283 (0.57)	4.402 (0.38)	4.527 (0.36)	4.600 (0.35)	4.677 (0.48)
						3.846 (0.55)	4.048 (0.38)	4.205 (0.37)	4.302 (0.36)	4.359 (0.34)	4.376 (0.50)
					3.405 (0.57)	3.636 (0.43)	3.795 (0.37)	3.946 (0.36)	4.058 (0.34)	4.111 (0.39)	4.125 (0.49)
				2.910 (0.64)	3.171 (0.47)	3.388 (0.42)	3.532 (0.36)	3.649 (0.41)	3.739 (0.41)	3.822 (0.40)	3.849 (0.55)
			2.455 (0.64)	2.666 (0.48)	2.882 (0.43)	3.063 (0.42)	3.207 (0.41)	3.324 (0.42)	3.449 (0.41)	3.489 (0.42)	3.486 (0.55)
		2.021 (0.74)	2.222 (0.54)	2.433 0.46)	2.634 (0.46)	2.808 (0.47)	2.906 (0.42)	3.043 (0.45)	3.141 (0.44)	3.166 (0.45)	3.189 (0.61)
	1.841 (0.80)	1.935 (0.54)	2.120 (0.48)	2.324 (0.52)	2.503 (0.44)	2.645 (0.46)	2.825 (0.44)	2.902 (0.43)	2.982 (0.43)	3.040 (0.46)	3.036 (0.61)
2.226 (0.69)	2.099 (0.51)	2.276 (0.50)	2.506 (0.50)	2.739 (0.44)	2.952 (0.41)	3.138 (0.43)	3.341 (0.35)	3.425 (0.39)	3.533 (0.37)	3.606 (0.40)	3.590 (0.59)

Fig. 4.6a. Pin-power distribution for CENTRM benchmark TCA-2. Value in parentheses is percent standard deviation.

											5.023 (0.99)
	0.139 (0.63)									4.960 (0.46)	5.042 (0.47)
									4.835 (0.48)	4.922 (0.33)	4.929 (0.47)
								4.569 (0.52)	4.721 (0.32)	4.780 (0.36)	4.776 (0.48)
							4.250 (0.50)	4.420 (0.35)	4.521 (0.36)	4.608 (0.35)	4.612 (0.50)
						3.803 (0.58)	4.057 (0.34)	4.179 (0.39)	4.303 (0.35)	4.406 (0.35)	4.409 (0.51)
					3.430 (0.58)	3.641 (0.41)	3.836 (0.39)	3.972 (0.37)	4.049 (0.39)	4.121 (0.37)	4.127 (0.54)
				2.949 (0.66)	3.164 (0.42)	3.374 (0.41)	3.549 (0.43)	3.649 (0.40)	3.775 (0.38)	3.806 (0.42)	3.858 (0.53)
			2.447 (0.66)	2.659 (0.43)	2.876 (0.44)	3.101 (0.45)	3.229 (0.44)	3.359 (0.40)	3.459 (0.38)	3.487 (0.43)	3.504 (0.59)
		2.029 (0.71)	2.232 (0.51)	2.431 0.48)	2.644 (0.45)	2.793 (0.49)	2.940 (0.44)	3.042 (0.45)	3.132 (0.39)	3.194 (0.43)	3.205 (0.58)
	1.837 (0.75)	1.930 (0.56)	2.140 (0.51)	2.325 (0.53)	2.522 (0.47)	2.677 (0.44)	2.816 (0.44)	2.936 (0.40)	3.008 (0.44)	3.035 (0.40)	3.064 (0.61)
2.222 (0.68)	2.106 (0.51)	2.274 (0.52)	2.527 (0.47)	2.756 (0.43)	2.976 (0.41)	3.149 (0.44)	3.323 (0.39)	3.477 (0.38)	3.562 (0.38)	3.583 (0.41)	3.598 (0.59)

Fig. 4.6b. Pin-power distribution for NITAWL benchmark TCA-2. Value in parentheses is percent standard deviation.

Table 4.15. Selected reaction rates for CENTRM case TCA-2

Pin	Region	$\sigma_a \phi$ ($cm^{-3} - s^{-1}$)	$\nu\sigma_f \phi$ ($cm^{-3} - s^{-1}$)	$\sigma_f \phi$ ($cm^{-3} - s^{-1}$)	ϕ ($cm - s^{-1}$)	ϕ/ϕ_t
1	Fuel	1.356E-05	2.236E-05	7.923E-06	5.453E-03	0.270
	Clad	2.613E-07	0.0	0.0	1.705E-03	0.085
	Mod.	7.206E-07	0.0	0.0	1.301E-02	0.645
78	Fuel	3.394E-05	5.051E-05	1.786E-05	2.155E-02	0.269
	Clad	7.023E-07	0.0	0.0	6.812E-03	0.085
	Mod.	1.495E-06	0.0	0.0	5.179E-02	0.646

Table 4.16. Selected reaction rates for NITAWL case TCA-2

Pin	Region	$\sigma_a \phi$ ($cm^{-3} - s^{-1}$)	$\nu\sigma_f \phi$ ($cm^{-3} - s^{-1}$)	$\sigma_f \phi$ ($cm^{-3} - s^{-1}$)	ϕ ($cm - s^{-1}$)	ϕ/ϕ_t
1	Fuel	1.356E-05	2.241E-05	7.942E-06	5.429E-03	0.271
	Clad	2.591E-07	0.0	0.0	1.693E-03	0.084
	Mod.	7.211E-07	0.0	0.0	1.293E-02	0.645
78	Fuel	3.354E-05	5.009E-05	1.771E-05	2.137E-02	0.268
	Clad	6.772E-07	0.0	0.0	6.756E-03	0.084
	Mod.	1.478E-06	0.0	0.0	5.172E-02	0.648

Table 4.17. TCA-2, Pin-1 four-group fluxes

Group	CENTRM Φ (cm^{-2} - s^{-1})	NITAWL Φ (cm^{-2} - s^{-1})
1	5.046E-05	5.017E-05
2	1.503E-05	1.485E-05
3	3.705E-06	3.620E-06
4	2.970E-05	2.981E-05

Table 4.18. TCA-2, Pin-1 four-group U-235 cross sections

Group	CENTRM cross sections (cm^{-1})			NITAWL cross sections (cm^{-1})		
	σ_a	$\langle\sigma_f$	σ_f	σ_a	$\langle\sigma_f$	σ_f
1	1.43119E-04	3.25379E-04	1.25277E-04	1.42796E-04	3.25595E-04	1.25157E-04
2	3.53013E-03	5.42307E-03	2.22558E-03	3.53101E-03	5.37976E-03	2.20780E-03
3	5.06839E-03	1.03472E-02	4.24642E-03	5.21793E-03	1.06593E-02	4.37445E-03
4	4.85643E-02	1.01103E-01	4.14919E-02	4.86105E-02	1.01201E-01	4.15317E-02

Table 4.19. TCA-2, Pin-1 four-group U-238 cross sections

Group	CENTRM cross sections (cm^{-1})			NITAWL cross sections (cm^{-1})		
	σ_a	$\langle\sigma_f$	σ_f	σ_a	$\langle\sigma_f$	σ_f
1	4.44405E-03	8.24665E-03	2.92378E-03	4.49711E-03	8.46895E-03	2.99705E-03
2	3.85408E-02	3.81629E-06	1.58108E-06	3.63117E-02	3.48554E-06	1.44405E-06
3	6.97263E-03	2.42518E-08	1.00480E-08	6.99494E-03	2.45706E-08	1.01801E-08
4	2.75966E-02	1.29711E-07	5.37418E-08	2.76225E-02	1.29835E-07	5.37930E-08

Table 4.20. TCA-2, Pin-1 four-group Pu-239 cross sections

Group	CENTRM cross sections (cm^{-1})			NITAWL cross sections (cm^{-1})		
	σ_a	$\langle\sigma_f$	σ_f	σ_a	$\langle\sigma_f$	σ_f
1	5.11583E-04	1.49239E-03	4.80303E-04	5.11437E-04	1.49567E-03	4.80666E-04
2	1.10651E-02	1.80525E-02	6.26864E-03	1.07872E-02	1.76378E-02	6.12465E-03
3	3.33360E-02	6.55390E-02	2.27581E-02	3.37318E-02	6.63232E-02	2.30304E-02
4	2.67093E-01	5.40384E-01	1.86909E-01	2.66605E-01	5.39661E-01	1.86656E-01

Table 4.21. TCA-2, Pin-78 four-group fluxes

Group	CENTRM Φ (cm^{-2} - s^{-1})	NITAWL Φ (cm^{-2} - s^{-1})
1	2.302E-04	2.272E-04
2	8.173E-05	8.176E-05
3	1.759E-05	1.791E-05
4	6.122E-05	6.071E-05

Table 4.22. TCA-2, Pin-78 four-group U-235 cross sections

Group	CENTRM cross sections (cm^{-1})			NITAWL cross sections (cm^{-1})		
	Σ_a	$\nu\Sigma_f$	Σ_f	Σ_a	$\nu\Sigma_f$	Σ_f
1	1.47775E-04	3.29361E-04	1.27654E-04	1.47727E-04	3.29384E-04	1.27666E-04
2	3.40270E-03	5.23267E-03	2.14744E-03	3.44284E-03	5.28022E-03	2.16695E-03
3	5.19904E-03	1.06173E-02	4.35723E-03	5.12518E-03	1.04631E-02	4.29398E-03
4	4.56001E-02	9.48282E-02	3.89167E-02	4.54184E-02	9.44484E-02	3.87607E-02

Table 4.23. TCA-2, Pin-78 four-group U-238 cross sections

Group	CENTRM cross sections (cm^{-1})			NITAWL cross sections (cm^{-1})		
	Σ_a	$\nu\Sigma_f$	Σ_f	Σ_a	$\nu\Sigma_f$	Σ_f
1	4.32970E-03	7.46321E-03	2.65044E-03	4.32945E-03	7.46893E-03	2.65359E-03
2	3.93173E-02	3.71651E-06	1.53973E-06	3.66084E-02	3.70903E-06	1.53663E-06
3	7.00819E-03	2.46566E-08	1.02156E-08	6.99481E-03	2.44808E-08	1.01429E-08
4	2.60606E-02	1.22341E-07	5.06882E-08	2.59687E-02	1.21901E-07	5.05058E-08

Table 4.24. TCA-2, Pin-78 four-group Pu-239 cross sections

Group	CENTRM cross sections (cm^{-1})			NITAWL cross sections (cm^{-1})		
	Σ_a	$\nu\Sigma_f$	Σ_f	Σ_a	$\nu\Sigma_f$	Σ_f
1	5.13614E-04	1.47354E-03	4.77076E-04	5.13794E-04	1.47461E-03	4.77474E-04
2	1.10415E-02	1.82425E-02	6.33460E-03	1.06940E-02	1.76497E-02	6.12879E-03
3	3.48073E-02	6.83161E-02	2.37224E-02	3.39004E-02	6.66510E-02	2.31443E-02
4	2.84748E-01	5.63652E-01	1.95041E-01	2.85625E-01	5.64792E-01	1.95441E-01

											4.889 (1.00)
	0.143 (0.72)									4.823 (0.45)	4.841 (0.48)
									4.680 (0.49)	4.775 (0.35)	4.801 (0.51)
								4.418 (0.49)	4.556 (0.35)	4.662 (0.34)	4.671 (0.44)
							4.131 (0.53)	4.290 (0.37)	4.381 (0.40)	4.473 (0.37)	4.486 (0.50)
						3.736 (0.54)	3.929 (0.37)	4.067 (0.37)	4.181 (0.37)	4.232 (0.35)	4.253 (0.47)
					3.282 (0.51)	3.485 (0.38)	3.672 (0.38)	3.812 (0.35)	3.911 (0.36)	3.997 (0.36)	4.014 (0.57)
				2.803 (0.63)	3.040 (0.42)	3.236 (0.40)	3.429 (0.41)	3.556 (0.41)	3.634 (0.40)	3.682 (0.39)	3.716 (0.53)
			2.356 (0.60)	2.576 (0.50)	2.763 (0.42)	2.948 (0.40)	3.121 (0.39)	3.244 (0.43)	3.319 (0.40)	3.364 (0.43)	3.384 (0.59)
		1.962 (0.81)	2.133 (0.49)	2.338 0.47)	2.571 (0.43)	2.695 (0.42)	2.838 (0.44)	2.947 (0.47)	3.038 (0.46)	3.085 (0.43)	3.097 (0.55)
	1.782 (0.78)	1.874 (0.52)	2.046 (0.52)	2.263 (0.47)	2.423 (0.44)	2.573 (0.48)	2.708 (0.46)	2.819 (0.40)	2.891 (0.44)	2.907 (0.42)	2.936 (0.54)
2.156 (0.74)	2.021 (0.52)	2.204 (0.50)	2.429 (0.49)	2.663 (0.44)	2.876 (0.42)	3.083 (0.41)	3.215 (0.40)	3.338 (0.42)	3.414 (0.40)	3.474 (0.33)	3.480 (0.59)

Fig. 4.7a. Pin-power distribution for CENTRM benchmark TCA-3. Value in parentheses is percent standard deviation.

											4.857 (1.00)
	0.143 (0.73)									4.845 (0.46)	4.826 (0.50)
									4.692 (0.49)	4.713 (0.37)	4.814 (0.46)
								4.430 (0.53)	4.565 (0.34)	4.635 (0.34)	4.646 (0.48)
							4.145 (0.54)	4.284 (0.39)	4.400 (0.36)	4.464 (0.36)	4.512 (0.50)
						3.718 (0.51)	3.929 (0.35)	4.066 (0.38)	4.195 (0.37)	4.262 (0.33)	4.242 (0.50)
					3.318 (0.57)	3.525 (0.36)	3.701 (0.40)	3.836 (0.37)	3.934 (0.37)	3.997 (0.35)	4.006 (0.51)
				2.807 (0.61)	3.095 (0.41)	3.287 (0.39)	3.406 (0.41)	3.538 (0.40)	3.646 (0.36)	3.714 (0.36)	3.704 (0.49)
			2.365 (0.67)	2.589 (0.48)	2.799 (0.44)	2.975 (0.41)	3.132 (0.41)	3.230 (0.40)	3.314 (0.41)	3.391 (0.39)	3.396 (0.59)
		1.949 (0.76)	2.150 (0.51)	2.363 0.47)	2.541 (0.48)	2.706 (0.45)	2.838 (0.44)	2.977 (0.42)	3.035 (0.43)	3.082 (0.43)	3.092 (0.55)
	1.762 (0.77)	1.861 (0.58)	2.063 (0.49)	2.238 (0.53)	2.433 (0.47)	2.572 (0.46)	2.729 (0.48)	2.840 (0.40)	2.894 (0.44)	2.944 (0.42)	2.962 (0.59)
2.155 (0.76)	2.037 (0.53)	2.194 (0.47	2.420 (0.50)	2.654 (0.46)	2.866 (0.42)	3.058 (0.41)	3.225 (0.40)	3.315 (0.41)	3.430 (0.39)	3.480 (0.37)	3.483 (0.58)

Fig. 4.7b. Pin-power distribution for NITAWL benchmark TCA-3. Value in parentheses is percent standard deviation.

Table 4.25. Selected reaction rates for CENTRM case TCA-3

Pin	Region	$\langle\sigma_a\phi\rangle$ (cm^{-3} - s^{-1})	$\langle\nu\sigma_f\phi\rangle$ (cm^{-3} - s^{-1})	$\langle\sigma_f\phi\rangle$ (cm^{-3} - s^{-1})	$\langle\phi\rangle$ (cm - s^{-1})	$\langle\phi\rangle/\langle\phi_t\rangle$
	Fuel	1.307E-05	2.156E-05	7.643E-06	5.476E-03	0.271
1	Clad	2.496E-07	0.0	0.0	1.701E-03	0.085
	Mod.	6.938E-07	0.0	0.0	1.300E-02	0.644
	Fuel	3.318E-05	4.938E-05	1.747E-05	2.182E-02	0.269
78	Clad	6.794E-07	0.0	0.0	6.875E-03	0.085
	Mod.	1.442E-06	0.0	0.0	5.233E-02	0.646

Table 4.26. Selected reaction rates for NITAWL case TCA-3

Pin	Region	$\langle\sigma_a\phi\rangle$ (cm^{-3} - s^{-1})	$\langle\nu\sigma_f\phi\rangle$ (cm^{-3} - s^{-1})	$\langle\sigma_f\phi\rangle$ (cm^{-3} - s^{-1})	$\langle\phi\rangle$ (cm - s^{-1})	$\langle\phi\rangle/\langle\phi_t\rangle$
	Fuel	1.296E-05	2.142E-05	7.591E-06	5.418E-03	0.272
1	Clad	2.463E-07	0.0	0.0	1.676E-03	0.084
	Mod.	6.886E-07	0.0	0.0	1.285E-02	0.644
	Fuel	3.290E-05	4.896E-05	1.732E-05	2.172E-02	0.269
78	Clad	6.746E-07	0.0	0.0	6.861E-03	0.085
	Mod.	1.449E-06	0.0	0.0	5.222E-02	0.646

Table 4.27. TCA-3, Pin-1 four-group fluxes

Group	CENTRM Φ (cm^{-2} - s^{-1})	NITAWL Φ (cm^{-2} - s^{-1})
1	4.915E-05	4.860E-05
2	1.453E-05	1.440E-05
3	3.519E-06	3.300E-06
4	2.876E-05	2.864E-05

Table 4.28. TCA-3, Pin-1 four-group U-235 cross sections

Group	CENTRM cross sections (cm^{-1})			NITAWL cross sections (cm^{-1})		
	Σ_a	$\langle\Sigma_f\rangle$	Σ_f	Σ_a	$\langle\Sigma_f\rangle$	Σ_f
1	1.42818E-04	3.25054E-04	1.25124E-04	1.43107E-04	3.25739E-04	1.25325E-04
2	3.36929E-03	5.19745E-03	2.13299E-03	3.46178E-03	5.31513E-03	2.18128E-03
3	5.17928E-03	1.05930E-02	4.34726E-03	5.19818E-03	1.06224E-02	4.35933E-03
4	4.86050E-02	1.01190E-01	4.15275E-02	4.84951E-02	1.00958E-01	4.14323E-02

Table 4.29. TCA-3, Pin-1 four-group U-238 cross sections

Group	CENTRM cross sections (cm^{-1})			NITAWL cross sections (cm^{-1})		
	Σ_a	$\langle\Sigma_f\rangle$	Σ_f	Σ_a	$\langle\Sigma_f\rangle$	Σ_f
1	4.44993E-03	8.27601E-03	2.93516E-03	4.47772E-03	8.36366E-03	2.96352E-03
2	3.65872E-02	3.54715E-06	1.46957E-06	3.65101E-02	3.54449E-06	1.46847E-06
3	7.01523E-03	2.46279E-08	1.02038E-08	7.00700E-03	2.46391E-08	1.02084E-08
4	2.76173E-02	1.29810E-07	5.37830E-08	2.75642E-02	1.29555E-07	5.36770E-08

Table 4.30. TCA-3, Pin-1 four-group Pu-239 cross sections

Group	CENTRM cross sections (cm^{-1})			NITAWL cross sections (cm^{-1})		
	Σ_a	$\langle\Sigma_f\rangle$	Σ_f	Σ_a	$\langle\Sigma_f\rangle$	Σ_f
1	5.11491E-04	1.49361E-03	4.80637E-04	5.11798E-04	1.49459E-03	4.80689E-04
2	1.09264E-02	1.82048E-02	6.32153E-03	1.06379E-02	1.74194E-02	6.04882E-03
3	3.56962E-02	6.99270E-02	2.42818E-02	3.44527E-02	6.76673E-02	2.34972E-02
4	2.66921E-01	5.40191E-01	1.86841E-01	2.66795E-01	5.39735E-01	1.86684E-01

Table 4.31. TCA-3, Pin-78 four-group fluxes

Group	CENTRM Φ (cm^{-2} - s^{-1})	NITAWL Φ (cm^{-2} - s^{-1})
1	2.243E-04	2.215E-04
2	8.038E-05	8.190E-05
3	1.810E-05	1.765E-05
4	5.962E-05	5.956E-05

Table 4.32. TCA-3, Pin-78 four-group U-235 cross sections

Group	CENTRM cross sections (cm^{-1})			NITAWL cross sections (cm^{-1})		
	Σ_a	$\langle\Sigma_f$	Σ_f	Σ_a	$\langle\Sigma_f$	Σ_f
1	1.47728E-04	3.29228E-04	1.27610E-04	1.47738E-04	3.29429E-04	1.27667E-04
2	3.36825E-03	5.14716E-03	2.11235E-03	3.40828E-03	5.21512E-03	2.14023E-03
3	5.12983E-03	1.04660E-02	4.29517E-03	5.13172E-03	1.04717E-02	4.29747E-03
4	4.59777E-02	9.56112E-02	3.92380E-02	4.54550E-02	9.45238E-02	3.87918E-02

Table 4.33. TCA-3, Pin-78 four-group U-238 cross sections

Group	CENTRM cross sections (cm^{-1})			NITAWL cross sections (cm^{-1})		
	Σ_a	$\langle\Sigma_f$	Σ_f	Σ_a	$\langle\Sigma_f$	Σ_f
1	4.31758E-03	7.42746E-03	2.63695E-03	4.34475E-03	7.50781E-03	2.66748E-03
2	3.69603E-02	3.91179E-06	1.62064E-06	3.60504E-02	3.75949E-06	1.55755E-06
3	6.98884E-03	2.44361E-08	1.01243E-08	6.98652E-03	2.44809E-08	1.01429E-08
4	2.62422E-02	1.23201E-07	5.10444E-08	2.59876E-02	1.21988E-07	5.05418E-08

Table 4.34. TCA-3, Pin-78 four-group Pu-239 cross sections

Group	CENTRM cross sections (cm^{-1})			NITAWL cross sections (cm^{-1})		
	Σ_a	$\langle\Sigma_f$	Σ_f	Σ_a	$\langle\Sigma_f$	Σ_f
1	5.13304E-04	1.47258E-03	4.76835E-04	5.13774E-04	1.47465E-03	4.77404E-04
2	1.08802E-02	1.78741E-02	6.20669E-03	1.05497E-02	1.73471E-02	6.02371E-03
3	3.36764E-02	6.62210E-02	2.29950E-02	3.26723E-02	6.44142E-02	2.23675E-02
4	2.87561E-01	5.69182E-01	1.96949E-01	2.86127E-01	5.65714E-01	1.95759E-01

										6.107 (0.90)
	0.155 (0.61)								6.067 (0.43)	6.093 (0.43)
								5.865 (0.43)	5.933 (0.35)	5.977 (0.46)
							5.480 (0.46)	5.673 (0.35)	5.759 (0.31)	5.797 (0.43)
						4.989 (0.43)	5.244 (0.34)	5.447 (0.34)	5.513 (0.35)	5.571 (0.47)
					4.464 (0.56)	4.722 (0.35)	4.957 (0.33)	5.109 (0.36)	5.207 (0.35)	5.226 (0.47)
				3.839 (0.55)	4.125 (0.38)	4.412 (0.33)	4.611 (0.35)	4.762 (0.32)	4.805 (0.34)	4.824 (0.46)
			3.152 (0.60)	3.489 (0.40)	3.765 (0.38)	3.994 (0.35)	4.201 (0.34)	4.308 (0.38)	4.384 (0.35)	4.402 (0.52)
		2.601 (0.64)	2.827 (0.45)	3.120 (0.42)	3.374 (0.40)	3.577 (0.41)	3.735 (0.37)	3.861 (0.39)	3.933 (0.37)	3.954 (0.56)
	2.180 (0.76)	2.373 (0.47)	2.634 (0.45)	2.897 (0.44)	3.116 (0.42)	3.317 (0.44)	3.488 (0.39)	3.597 (0.37)	3.641 (0.41)	3.642 (0.57)
2.423 (0.70)	2.365 (0.50)	2.614 (0.49)	2.928 (0.42)	3.239 (0.43)	3.492 (0.39)	3.697 (0.36)	3.883 (0.36)	3.998 (0.39)	4.081 (0.36)	4.134 (0.53)

Fig. 4.8a. Pin-power distribution for CENTRM benchmark TCA-4. Value in parentheses is percent standard deviation.

										6.212 (0.86)
	1.54 (0.66)								6.114 (0.44)	6.159 (0.45)
								5.831 (0.44)	5.974 (0.31)	5.984 (0.46)
							5.529 (0.46)	5.708 (0.33)	5.770 (0.31)	5.819 (0.41)
						5.102 (0.47)	5.229 (0.35)	5.445 (0.32)	5.522 (0.33)	5.533 (0.42)
					4.470 (0.51)	4.777 (0.34)	4.968 (0.33)	5.140 (0.35)	5.202 (0.33)	5.243 (0.45)
				3.832 (0.54)	4.116 (0.40)	4.387 (0.37)	4.630 (0.35)	4.727 (0.32)	4.837 (0.33)	4.850 (0.46)
			3.129 (0.62)	3.495 (0.38)	3.735 (0.41)	4.030 (0.39)	4.197 (0.38)	4.309 (0.34)	4.374 (0.35)	4.458 (0.50)
		2.582 (0.69)	2.840 (0.45)	3.132 (0.46)	3.388 (0.42)	3.581 (0.39)	3.754 (0.40)	3.870 (0.38)	3.961 (0.38)	3.971 (0.51)
	2.185 (0.71)	2.350 (0.49)	2.643 (0.44)	2.904 (0.44)	3.128 (0.43)	3.330 (0.42)	3.500 (0.40)	3.601 (0.40)	3.672 (0.39)	3.710 (0.48)
2.436 (0.71)	2.386 (0.49)	2.626 (0.48)	2.916 (0.44)	3.228 (0.44)	3.505 (0.41)	3.706 (0.43)	3.883 (0.39)	3.981 (0.41)	4.062 (0.38)	4.100 (0.55)

Fig. 4.8b. Pin-power distribution for NITAWL benchmark TCA-4. Value in parentheses is percent standard deviation.

Table 4.35. Selected reaction rates for CENTRM case TCA-4

Pin	Region	$\langle \sigma_a \phi \rangle$ ($cm^{-3} - s^{-1}$)	$\langle \nu\sigma_f \phi \rangle$ ($cm^{-3} - s^{-1}$)	$\langle \sigma_f \phi \rangle$ ($cm^{-3} - s^{-1}$)	ϕ ($cm - s^{-1}$)	ϕ/ϕ_t
	Fuel	1.440E-05	2.393E-05	8.480E-06	5.581E-03	0.235
1	Clad	2.746E-07	0.0	0.0	1.739E-03	0.073
	Mod.	7.889E-07	0.0	0.0	1.642E-02	0.692
	Fuel	4.055E-05	6.181E-05	2.186E-05	2.281E-02	0.235
66	Clad	8.066E-07	0.0	0.0	7.166E-03	0.074
	Mod.	1.867E-06	0.0	0.0	6.712E-02	0.691

Table 4.36. Selected reaction rates for NITAWL case TCA-4

Pin	Region	$\langle \sigma_a \phi \rangle$ ($cm^{-3} - s^{-1}$)	$\langle \nu\sigma_f \phi \rangle$ ($cm^{-3} - s^{-1}$)	$\langle \sigma_f \phi \rangle$ ($cm^{-3} - s^{-1}$)	ϕ ($cm - s^{-1}$)	ϕ/ϕ_t
	Fuel	1.464E-05	2.446E-05	8.665E-06	5.642E-03	0.236
1	Clad	2.772E-07	0.0	0.0	1.754E-03	0.073
	Mod.	7.942E-07	0.0	0.0	1.652E-02	0.691
	Fuel	4.061E-05	6.263E-05	2.216E-05	2.295E-02	0.234
66	Clad	8.106E-07	0.0	0.0	7.227E-03	0.074
	Mod.	1.885E-06	0.0	0.0	6.790E-02	0.692

Table 4.37. TCA-4, Pin-1 four-group fluxes

Group	CENTRM Φ (cm^{-2} - s^{-1})	NITAWL Φ (cm^{-2} - s^{-1})
1	5.137E-05	5.198E-05
2	1.508E-05	1.488E-05
3	3.637E-06	3.684E-06
4	3.178E-05	3.244E-05

Table 4.38. TCA-4, Pin-1 four-group U-235 cross sections

Group	CENTRM cross sections (cm^{-1})			NITAWL cross sections (cm^{-1})		
	σ_a	$\langle\sigma_f$	σ_f	σ_a	$\langle\sigma_f$	σ_f
1	1.42972E-04	3.25729E-04	1.25284E-04	1.42717E-04	3.25108E-04	1.25072E-04
2	3.54777E-03	5.40060E-03	2.21636E-03	3.49262E-03	5.32638E-03	2.18590E-03
3	5.19612E-03	1.06384E-02	4.36591E-03	5.19563E-03	1.06220E-02	4.35917E-03
4	4.87823E-02	1.01563E-01	4.16806E-02	4.89171E-02	1.01845E-01	4.17962E-02

Table 4.39. TCA-4, Pin-1 four-group U-238 cross sections

Group	CENTRM cross sections (cm^{-1})			NITAWL cross sections (cm^{-1})		
	σ_a	$\langle\sigma_f$	σ_f	σ_a	$\langle\sigma_f$	σ_f
1	4.51308E-03	8.46385E-03	3.00241E-03	4.47482E-03	8.38222E-03	2.97205E-03
2	3.86113E-02	3.72395E-06	1.54282E-06	3.54513E-02	3.52350E-06	1.45977E-06
3	7.00737E-03	2.46436E-08	1.02103E-08	7.01355E-03	2.47048E-08	1.02357E-08
4	2.77151E-02	1.30278E-07	5.39767E-08	2.77735E-02	1.30557E-07	5.40922E-08

Table 4.40. TCA-4, Pin-1 four-group Pu-239 cross sections

Group	CENTRM cross sections (cm^{-1})			NITAWL cross sections (cm^{-1})		
	σ_a	$\langle\sigma_f$	σ_f	σ_a	$\langle\sigma_f$	σ_f
1	5.12178E-04	1.49692E-03	4.81232E-04	5.11274E-04	1.49406E-03	4.80446E-04
2	1.11540E-02	1.83841E-02	6.38377E-03	1.08239E-02	1.78689E-02	6.20489E-03
3	3.46250E-02	6.79736E-02	2.36035E-02	3.48586E-02	6.84167E-02	2.37574E-02
4	2.65578E-01	5.38310E-01	1.86183E-01	2.66229E-01	5.39667E-01	1.86654E-01

Table 4.41. TCA-4, Pin-66 four-group fluxes

Group	CENTRM Φ (cm^{-2} - s^{-1})	NITAWL Φ (cm^{-2} - s^{-1})
1	2.378E-04	2.383E-04
2	8.358E-05	8.422E-05
3	1.882E-05	1.898E-05
4	7.623E-05	7.746E-05

Table 4.42. TCA-4, Pin-66 four-group U-235 cross sections

Group	CENTRM cross sections (cm^{-1})			NITAWL cross sections (cm^{-1})		
	Σ_a	$\langle\Sigma_f$	Σ_f	Σ_a	$\langle\Sigma_f$	Σ_f
1	1.47181E-04	3.29323E-04	1.27404E-04	1.47030E-04	3.28757E-04	1.27281E-04
2	3.46397E-03	5.28525E-03	2.16902E-03	3.45056E-03	5.27803E-03	2.16605E-03
3	5.05350E-03	1.03193E-02	4.23494E-03	5.07799E-03	1.03695E-02	4.25556E-03
4	4.64067E-02	9.65304E-02	3.96152E-02	4.62458E-02	9.61957E-02	3.94779E-02

Table 4.43. TCA-4, Pin-66 four-group U-238 cross sections

Group	CENTRM cross sections (cm^{-1})			NITAWL cross sections (cm^{-1})		
	Σ_a	$\langle\Sigma_f$	Σ_f	Σ_a	$\langle\Sigma_f$	Σ_f
1	4.36716E-03	7.64672E-03	2.70927E-03	4.35812E-03	7.61288E-03	2.70342E-03
2	4.02182E-02	3.82265E-06	1.58372E-06	3.67393E-02	3.69650E-06	1.53144E-06
3	6.96068E-03	2.41878E-08	1.00214E-08	6.97476E-03	2.43271E-08	1.00792E-08
4	2.64749E-02	1.24324E-07	5.15096E-08	2.63939E-02	1.23940E-07	5.13506E-08

Table 4.44. TCA-4, Pin-66 four-group Pu-239 cross sections

Group	CENTRM cross sections (cm^{-1})			NITAWL cross sections (cm^{-1})		
	Σ_a	$\langle\Sigma_f$	Σ_f	Σ_a	$\langle\Sigma_f$	Σ_f
1	5.13616E-04	1.47840E-03	4.77839E-04	5.13256E-04	1.47677E-03	4.77633E-04
2	1.11268E-02	1.82952E-02	6.35292E-03	1.07160E-02	1.75431E-02	6.09175E-03
3	3.23976E-02	6.38268E-02	2.21636E-02	3.30910E-02	6.51217E-02	2.26133E-02
4	2.81830E-01	5.60508E-01	1.93933E-01	2.81951E-01	5.60363E-01	1.93887E-01

										5.973 (0.85)
	0.164 (0.72)								5.841 (0.44)	5.875 (0.49)
								5.617 (0.45)	5.723 (0.34)	5.821 (0.42)
							5.245 (0.44)	5.464 (0.33)	5.537 (0.33)	5.623 (0.44)
						4.824 (0.47)	5.071 (0.31)	5.205 (0.30)	5.288 (0.29)	5.352 (0.47)
					4.271 (0.53)	4.523 (0.33)	4.753 (0.30)	4.916 (0.31)	4.981 (0.34)	5.050 (0.44)
				3.643 (0.55)	3.966 (0.37)	4.187 (0.38)	4.389 (0.35)	4.507 (0.34)	4.630 (0.34)	4.648 (0.50)
			3.029 (0.59)	3.330 (0.42)	3.604 (0.41)	3.798 (0.40)	3.987 (0.38)	4.110 (0.36)	4.165 (0.36)	4.228 (0.48)
		2.450 (0.65)	2.713 (0.44)	2.973 (0.41)	3.230 (0.39)	3.385 (0.41)	3.574 (0.39)	3.709 (0.42)	3.777 (0.37)	3.781 (0.56)
	2.050 (0.75)	2.254 (0.48)	2.522 (0.47)	2.750 (0.45)	2.981 (0.46)	3.176 (0.38)	3.331 (0.38)	3.429 (0.35)	3.508 (0.41)	3.534 (0.55)
2.283 (0.66)	2.260 (0.50)	2.500 (0.47)	2.828 (0.43)	3.060 (0.41)	3.331 (0.40)	3.528 (0.37)	3.725 (0.37)	3.815 (0.39)	3.867 (0.37)	3.921 (0.50)

Fig. 4.9a. Pin-power distribution for CENTRM benchmark TCA-5. Value in parentheses is percent standard deviation.

										5.872 (0.90)
	0.161 (0.77)								5.824 (0.44)	5.930 (0.43)
								5.663 (0.47)	5.775 (0.33)	5.815 (0.46)
							5.278 (0.44)	5.523 (0.31)	5.575 (0.32)	5.572 (0.46)
						4.844 (0.50)	5.069 (0.31)	5.219 (0.32)	5.311 (0.31)	5.323 (0.47)
					4.326 (0.49)	4.538 (0.35)	4.742 (0.33)	4.945 (0.33)	5.011 (0.32)	5.054 (0.46)
				3.679 (0.54)	3.942 (0.34)	4.189 (0.36)	4.400 (0.36)	4.534 (0.35)	4.638 (0.33)	4.691 (0.53)
			3.002 (0.59)	3.342 (0.40)	3.606 (0.38)	3.840 (0.35)	4.021 (0.35)	4.138 (0.38)	4.209 (0.38)	4.213 (0.54)
		2.468 (0.64)	2.720 (0.49)	2.999 (0.42)	3.225 (0.45)	3.440 (0.39)	3.582 (0.41)	3.702 (0.40)	3.771 (0.38)	3.783 (0.53)
	2.075 (0.66)	2.259 (0.54)	2.518 (0.45)	2.768 (0.45)	3.015 (0.41)	3.168 (0.43)	3.345 (0.39)	3.455 (0.40)	3.474 (0.39)	3.504 (0.54)
2.297 (0.69)	2.263 (0.45)	2.480 (0.49)	2.792 (0.42)	3.046 (0.38)	3.316 (0.41)	3.535 (0.39)	3.708 (0.38)	3.801 (0.38)	3.876 (0.36)	3.904 (0.55)

Fig. 4.9b. Pin-power distribution for NITAWL benchmark TCA-5. Value in parentheses is percent standard deviation.

Table 4.45. Selected reaction rates for CENTRM case TCA-5

Pin	Region	$\langle \sigma_a \phi \rangle$ ($cm^{-3} - s^{-1}$)	$\langle \nu\sigma_f \phi \rangle$ ($cm^{-3} - s^{-1}$)	$\langle \sigma_f \phi \rangle$ ($cm^{-3} - s^{-1}$)	ϕ ($cm - s^{-1}$)	ϕ/ϕ_t
	Fuel	1.374E-05	2.280E-05	8.078E-06	5.603E-03	0.235
1	Clad	2.618E-07	0.0	0.0	1.747E-03	0.074
	Mod.	7.503E-07	0.0	0.0	1.646E-02	0.691
	Fuel	3.907E-05	5.970E-05	2.112E-05	2.311E-02	0.235
66	Clad	7.783E-07	0.0	0.0	7.263E-03	0.074
	Mod.	1.793E-06	0.0	0.0	6.806E-02	0.691

Table 4.46. Selected reaction rates for NITAWL case TCA-5

Pin	Region	$\langle \sigma_a \phi \rangle$ ($cm^{-3} - s^{-1}$)	$\langle \nu\sigma_f \phi \rangle$ ($cm^{-3} - s^{-1}$)	$\langle \sigma_f \phi \rangle$ ($cm^{-3} - s^{-1}$)	ϕ ($cm - s^{-1}$)	ϕ/ϕ_t
	Fuel	1.378E-05	2.293E-05	8.127E-06	5.603E-03	0.235
1	Clad	2.619E-07	0.0	0.0	1.745E-03	0.074
	Mod.	7.543E-07	0.0	0.0	1.646E-02	0.691
	Fuel	3.868E-05	5.889E-05	2.084E-05	2.304E-02	0.234
66	Clad	7.727E-07	0.0	0.0	7.281E-03	0.074
	Mod.	1.803E-06	0.0	0.0	6.824E-02	0.692

Table 4.47. TCA-5, Pin-1 four-group fluxes

Group	CENTRM Φ (cm^{-2} - s^{-1})	NITAWL Φ (cm^{-2} - s^{-1})
1	4.939E-05	4.938E-05
2	1.446E-05	1.412E-05
3	3.466E-06	3.579E-06
4	3.035E-05	3.059E-05

Table 4.48. TCA-5, Pin-1 four-group U-235 cross sections

Group	CENTRM cross sections (cm^{-1})			NITAWL cross sections (cm^{-1})		
	Σ_a	$\langle\Sigma_f$	Σ_f	Σ_a	$\langle\Sigma_f$	Σ_f
1	1.42994E-04	3.26070E-04	1.25328E-04	1.43122E-04	3.25555E-04	1.25325E-04
2	3.42309E-03	5.26214E-03	2.15954E-03	3.47849E-03	5.29943E-03	2.17484E-03
3	5.14146E-03	1.04884E-02	4.30436E-03	5.22434E-03	1.06706E-02	4.37913E-03
4	4.87407E-02	1.01475E-01	4.16445E-02	4.86829E-02	1.01355E-01	4.15953E-02

Table 4.49. TCA-5, Pin-1 four-group U-238 cross sections

Group	CENTRM cross sections (cm^{-1})			NITAWL cross sections (cm^{-1})		
	Σ_a	$\langle\Sigma_f$	Σ_f	Σ_a	$\langle\Sigma_f$	Σ_f
1	4.50583E-03	8.47688E-03	2.99982E-03	4.48281E-03	8.35527E-03	2.96632E-03
2	3.83667E-02	3.84273E-06	1.59203E-06	3.62671E-02	3.53982E-06	1.46653E-06
3	7.00150E-03	2.45134E-08	1.01563E-08	7.02110E-03	2.47448E-08	1.02522E-08
4	2.76871E-02	1.30144E-07	5.39213E-08	2.76564E-02	1.30000E-07	5.38614E-08

Table 4.50. TCA-5, Pin-1 four-group Pu-239 cross sections

Group	CENTRM cross sections (cm^{-1})			NITAWL cross sections (cm^{-1})		
	Σ_a	$\langle\Sigma_f$	Σ_f	Σ_a	$\langle\Sigma_f$	Σ_f
1	5.12069E-04	1.49754E-03	4.81215E-04	5.11841E-04	1.49393E-03	4.80664E-04
2	1.09615E-02	1.82420E-02	6.33444E-03	1.10261E-02	1.81861E-02	6.31503E-03
3	3.50990E-02	6.88148E-02	2.38956E-02	3.48620E-02	6.84733E-02	2.37771E-02
4	2.66585E-01	5.39901E-01	1.86737E-01	2.66263E-01	5.39232E-01	1.86508E-01

Table 4.51. TCA-5, Pin-66 four-group fluxes

Group	CENTRM Φ (cm^{-2} - s^{-1})	NITAWL Φ (cm^{-2} - s^{-1})
1	2.303E-04	2.296E-04
2	8.041E-05	8.059E-05
3	1.804E-05	1.799E-05
4	7.411E-05	7.336E-05

Table 4.52. TCA-5, Pin-66 four-group U-235 cross sections

Group	CENTRM cross sections (cm^{-1})			NITAWL cross sections (cm^{-1})		
	Σ_a	$\langle\Sigma_f$	Σ_f	Σ_a	$\langle\Sigma_f$	Σ_f
1	1.47516E-04	3.29683E-04	1.27617E-04	1.46906E-04	3.28595E-04	1.27226E-04
2	3.45804E-03	5.28540E-03	2.16908E-03	3.42799E-03	5.19278E-03	2.13107E-03
3	5.21778E-03	1.06625E-02	4.37578E-03	5.17950E-03	1.05856E-02	4.34425E-03
4	4.63091E-02	9.63284E-02	3.95323E-02	4.61333E-02	9.59635E-02	3.93825E-02

Table 4.53. TCA-5, Pin-66 four-group U-238 cross sections

Group	CENTRM cross sections (cm^{-1})			NITAWL cross sections (cm^{-1})		
	Σ_a	$\langle\Sigma_f$	Σ_f	Σ_a	$\langle\Sigma_f$	Σ_f
1	4.38259E-03	7.65041E-03	2.71517E-03	4.35318E-03	7.60571E-03	2.70175E-03
2	3.76966E-02	3.76282E-06	1.55892E-06	3.76657E-02	3.47384E-06	1.43920E-06
3	7.01397E-03	2.46319E-08	1.02054E-08	6.99839E-03	2.45177E-08	1.01581E-08
4	2.64310E-02	1.24116E-07	5.14236E-08	2.63412E-02	1.23688E-07	5.12462E-08

Table 4.54. TCA-5, Pin-66 four-group Pu-239 cross sections

Group	CENTRM cross sections (cm^{-1})			NITAWL cross sections (cm^{-1})		
	Σ_a	$\langle\Sigma_f$	Σ_f	Σ_a	$\langle\Sigma_f$	Σ_f
1	5.14155E-04	1.47850E-03	4.78094E-04	5.13349E-04	1.47737E-03	4.77888E-04
2	1.09920E-02	1.80785E-02	6.27768E-03	1.06624E-02	1.75079E-02	6.07953E-03
3	3.48251E-02	6.83614E-02	2.37382E-02	3.45711E-02	6.78516E-02	2.35613E-02
4	2.81194E-01	5.59228E-01	1.93491E-01	2.80259E-01	5.57291E-01	1.92823E-01

										5.446 (0.87)
	0.191 (1.58)								5.462 (0.45)	5.433 (0.42)
								5.225 (0.40)	5.327 (0.30)	5.357 (0.42)
							4.915 (0.44)	5.049 (0.30)	5.160 (0.34)	5.185 (0.43)
						4.477 (0.48)	4.691 (0.37)	4.860 (0.33)	4.954 (0.36)	4.957 (0.47)
					3.976 (0.52)	4.231 (0.37)	4.430 (0.37)	4.569 (0.33)	4.651 (0.31)	4.688 (0.46)
				3.440 (0.56)	3.685 (0.42)	3.916 (0.36)	4.084 (0.36)	4.239 (0.34)	4.317 (0.35)	4.338 (0.50)
			2.811 (0.62)	3.097 (0.39)	3.347 (0.37)	3.552 (0.34)	3.704 (0.36)	3.855 (0.39)	3.900 (0.33)	3.925 (0.48)
		2.272 (0.65)	2.533 (0.42)	2797 (0.37)	3.010 (0.43)	3.216 (0.43)	3.339 (0.40)	3.445 (0.33)	3.528 (0.38)	3.528 (0.59)
	1.928 (0.76)	2.090 (0.51)	2.327 (0.47)	2.570 (0.45)	2.789 (0.40)	2.962 (0.40)	3.081 (0.42)	3.182 (0.38)	3.274 (0.42)	3.260 (0.56)
2.123 (0.72)	2.094 (0.47)	2.324 (0.47)	2.602 (0.41)	2.847 (0.39)	3.072 (0.40)	3.294 (0.40)	3.461 (0.41)	3.543 (0.36)	3.638 (0.36)	3.680 (0.54)

Fig. 4.10a. Pin-power distribution for CENTRM benchmark TCA-6. Value in parentheses is percent standard deviation.

										5.535 (0.82)
	0.192 (1.50)								5.433 (0.45)	5.485 (0.41)
								5.208 (0.43)	5.336 (0.30)	5.380 (0.44)
							4.903 (0.45)	5.056 (0.32)	5.155 (0.31)	5.224 (0.42)
						4.478 (0.50)	4.745 (0.32)	4.840 (0.32)	4.949 (0.31)	5.009 (0.47)
					3.945 (0.51)	4.219 (0.35)	4.437 (0.34)	4.592 (0.34)	4.656 (0.35)	4.662 (0.46)
				3.402 (0.55)	3.677 (0.37)	3.935 (0.36)	4.103 (0.36)	4.259 (0.35)	4.279 (0.33)	4.347 (0.51)
			2.808 (0.56)	3.096 (0.43)	3.349 (0.38)	3.556 (0.37)	3.711 (0.36)	3.858 (0.35)	3.908 (0.35)	3.932 (0.47)
		2.286 (0.62)	2.545 (0.44)	2795 (0.38)	3.014 (0.42)	3.211 (0.41)	3.340 (0.38)	3.434 (0.35)	3.501 (0.39)	3.547 (0.56)
	1.930 (0.79)	2.114 (0.47)	2.328 (0.48)	2.571 (0.47)	2.784 (0.43)	2.977 (0.38)	3.106 (0.36)	3.198 (0.41)	3.269 (0.38)	3.308 (0.52)
2.129 (0.65)	2.105 (0.45)	2.328 (0.49)	2.622 (0.41)	2.861 (0.43)	3.096 (0.38)	3.292 (0.40)	3.450 (0.38)	3.563 (0.40)	3.618 (0.35)	3.656 (0.57)

Fig. 4.10b. Pin-power distribution for NITAWL benchmark TCA-6. Value in parentheses is percent standard deviation.

Table 4.55. Selected reaction rates for CENTRM case TCA-6

Pin	Region	$\langle \sigma_a \phi \rangle$ ($cm^{-3} - s^{-1}$)	$\langle \nu\sigma_f \phi \rangle$ ($cm^{-3} - s^{-1}$)	$\langle \sigma_f \phi \rangle$ ($cm^{-3} - s^{-1}$)	ϕ ($cm - s^{-1}$)	ϕ/ϕ_t
	Fuel	1.298E-05	2.136E-05	7.574E-06	5.637E-03	0.235
1	Clad	2.474E-07	0.0	0.0	1.759E-03	0.073
	Mod.	7.049E-07	0.0	0.0	1.659E-02	0.692
	Fuel	3.599E-05	5.470E-05	1.936E-05	2.295E-02	0.234
66	Clad	7.226E-07	0.0	0.0	7.268E-03	0.074
	Mod.	1.669E-06	0.0	0.0	6.776E-02	0.692

Table 4.56. Selected reaction rates for NITAWL case TCA-6

Pin	Region	$\langle \sigma_a \phi \rangle$ ($cm^{-3} - s^{-1}$)	$\langle \nu\sigma_f \phi \rangle$ ($cm^{-3} - s^{-1}$)	$\langle \sigma_f \phi \rangle$ ($cm^{-3} - s^{-1}$)	ϕ ($cm - s^{-1}$)	ϕ/ϕ_t
	Fuel	1.301E-05	2.152E-05	7.630E-06	5.677E-03	0.236
1	Clad	2.482E-07	0.0	0.0	1.771E-03	0.073
	Mod.	7.104E-07	0.0	0.0	1.663E-02	0.691
	Fuel	3.641E-05	5.549E-05	1.964E-05	2.328E-02	0.235
66	Clad	7.250E-07	0.0	0.0	7.322E-03	0.074
	Mod.	1.692E-06	0.0	0.0	6.857E-02	0.691

Table 4.57. TCA-6, Pin-1 four-group fluxes

Group	CENTRM Φ (cm^{-2} - s^{-1})	NITAWL Φ (cm^{-2} - s^{-1})
1	4.562E-05	4.614E-05
2	1.353E-05	1.361E-05
3	3.260E-06	3.167E-06
4	2.877E-05	2.891E-05

Table 4.58. TCA-6, Pin-1 four-group U-235 cross sections

Group	CENTRM cross sections (cm^{-1})			NITAWL cross sections (cm^{-1})		
	Σ_a	$\langle\Sigma_f$	Σ_f	Σ_a	$\langle\Sigma_f$	Σ_f
1	1.43180E-04	3.25454E-04	1.25334E-04	1.42890E-04	3.25301E-04	1.25170E-04
2	3.45574E-03	5.26068E-03	2.15894E-03	3.46874E-03	5.30446E-03	2.17691E-03
3	5.12187E-03	1.04432E-02	4.28580E-03	5.18636E-03	1.05942E-02	4.34774E-03
4	4.87091E-02	1.01408E-01	4.16173E-02	4.87392E-02	1.01468E-01	4.16413E-02

Table 4.59. TCA-6, Pin-1 four-group U-238 cross sections

Group	CENTRM cross sections (cm^{-1})			NITAWL cross sections (cm^{-1})		
	Σ_a	$\langle\Sigma_f$	Σ_f	Σ_a	$\langle\Sigma_f$	Σ_f
1	4.44759E-03	8.24022E-03	2.92337E-03	4.46693E-03	8.35598E-03	2.96179E-03
2	3.90256E-02	3.50820E-06	1.45343E-06	3.57765E-02	3.56985E-06	1.47897E-06
3	6.98181E-03	2.44734E-08	1.01398E-08	7.00395E-03	2.46168E-08	1.01992E-08
4	2.76742E-02	1.30082E-07	5.38954E-08	2.76818E-02	1.30118E-07	5.39104E-08

Table 4.60. TCA-6, Pin-1 four-group Pu-239 cross sections

Group	CENTRM cross sections (cm^{-1})			NITAWL cross sections (cm^{-1})		
	Σ_a	$\langle\Sigma_f$	Σ_f	Σ_a	$\langle\Sigma_f$	Σ_f
1	5.11662E-04	1.49257E-03	4.80489E-04	5.11324E-04	1.49329E-03	4.80338E-04
2	1.13135E-02	1.86601E-02	6.47963E-03	1.07085E-02	1.75213E-02	6.08419E-03
3	3.39736E-02	6.67666E-02	2.31844E-02	3.36473E-02	6.62052E-02	2.29895E-02
4	2.66162E-01	5.39117E-01	1.86465E-01	2.67553E-01	5.41501E-01	1.87294E-01

Table 4.61. TCA-6, Pin-66 four-group fluxes

Group	CENTRM Φ (cm^{-2} - s^{-1})	NITAWL Φ (cm^{-2} - s^{-1})
1	2.129E-04	2.141E-04
2	7.322E-05	7.593E-05
3	1.668E-05	1.698E-05
4	6.844E-05	6.955E-05

Table 4.62. TCA-6, Pin-66 four-group U-235 cross sections

Group	CENTRM cross sections (cm^{-1})			NITAWL cross sections (cm^{-1})		
	Σ_a	$\langle\Sigma_f$	Σ_f	Σ_a	$\langle\Sigma_f$	Σ_f
1	1.46734E-04	3.28401E-04	1.27150E-04	1.47522E-04	3.29450E-04	1.27598E-04
2	3.38204E-03	5.17330E-03	2.12307E-03	3.41355E-03	5.23610E-03	2.14885E-03
3	5.13990E-03	1.04899E-02	4.30497E-03	5.04984E-03	1.02714E-02	4.21529E-03
4	4.64337E-02	9.65915E-02	3.96403E-02	4.61970E-02	9.60939E-02	3.94361E-02

Table 4.63. TCA-6, Pin-66 four-group U-238 cross sections

Group	CENTRM cross sections (cm^{-1})			NITAWL cross sections (cm^{-1})		
	Σ_a	$\langle\Sigma_f$	Σ_f	Σ_a	$\langle\Sigma_f$	Σ_f
1	4.34898E-03	7.60907E-03	2.70457E-03	4.36295E-03	7.58351E-03	2.69381E-03
2	3.85262E-02	3.68752E-06	1.52772E-06	3.74174E-02	3.59244E-06	1.48833E-06
3	6.99508E-03	2.44889E-08	1.01462E-08	6.96908E-03	2.42193E-08	1.00345E-08
4	2.64864E-02	1.24380E-07	5.15332E-08	2.63675E-02	1.23812E-07	5.12979E-08

Table 4.64. TCA-6, Pin-66 four-group Pu-239 cross sections

Group	CENTRM cross sections (cm^{-1})			NITAWL cross sections (cm^{-1})		
	Σ_a	$\langle\Sigma_f$	Σ_f	Σ_a	$\langle\Sigma_f$	Σ_f
1	5.13250E-04	1.47784E-03	4.78051E-04	5.13989E-04	1.47716E-03	4.77940E-04
2	1.13093E-02	1.84779E-02	6.41636E-03	1.07147E-02	1.76559E-02	6.13092E-03
3	3.39521E-02	6.67206E-02	2.31683E-02	3.32187E-02	6.53557E-02	2.26946E-02
4	2.81522E-01	5.60045E-01	1.93774E-01	2.81843E-01	5.60105E-01	1.93799E-01

									7.308 (0.44)
	0.155 (0.61)							7.112 (0.39)	7.241 (0.35)
							6.694 (0.43)	6.907 (0.26)	7.038 (0.31)
						6.068 (0.46)	6.408 (0.30)	6.595 (0.30)	6.694 (0.30)
					5.368 (0.55)	5.743 (0.35)	6.028 (0.33)	6.153 (0.34)	6.308 (0.29)
				4.563 (0.47)	4.998 (0.34)	5.297 (0.35)	5.515 (0.33)	5.710 (0.30)	5.792 (0.32)
			3.708 (0.54)	4.107 (0.38)	4.467 (0.38)	4.726 (0.34)	4.996 (0.34)	5.135 (0.34)	5.182 (0.36)
		2.884 (0.72)	3.250 (0.41)	3.615 (0.38)	3.950 (0.39)	4.203 (0.34)	4.373 (0.37)	4.511 (0.36)	4.579 (0.39)
	2.218 (0.76)	2.524 (0.48)	2.866 (0.44)	3.179 (0.45)	3.463 (0.41)	3.694 (0.41)	3.852 (0.37)	3.966 (0.40)	4.027 (0.40)
2.112 (0.73)	2.218 (0.54)	2.550 (0.48)	2.879 (0.44)	3.211 (0.40)	3.481 (0.45)	3.706 (0.38)	3.893 (0.38)	4.026 (0.39)	4.085 (0.37)

Fig. 4.11a. Pin-power distribution for CENTRM benchmark TCA-7. Value in parentheses is percent standard deviation.

									7.408 (0.42)
	0.157 (0.64)							7.147 (0.41)	7.221 (0.26)
							6.690 (0.44)	6.948 (0.30)	7.021 (0.30)
						6.147 (0.44)	6.439 (0.33)	6.607 (0.32)	6.750 (0.30)
					5.413 (0.49)	5.784 (0.37)	6.036 (0.33)	6.174 (0.32)	6.317 (0.30)
				4.575 (0.52)	5.009 (0.37)	5.294 (0.35)	5.496 (0.34)	5.716 (0.32)	5.817 (0.31)
			3.668 (0.55)	4.106 (0.38)	4.503 (0.34)	4.750 (0.37)	4.980 (0.35)	5.1116 (0.36)	5.231 (0.33)
		2.847 (0.66)	3.251 (0.41)	3.587 (0.40)	3.919 (0.38)	4.192 (0.41)	4.381 (0.40)	4.515 (0.36)	4.586 (0.37)
	2.218 (0.66)	2.533 (0.50)	2.857 (0.45)	3.206 (0.44)	3.499 (0.42)	3.700 (0.35)	3.863 (0.35)	3.987 (0.43)	4.057 (0.39)
2.101 (0.67)	2.211 (0.53)	2.557 (0.45)	2.878 (0.46)	3.214 (0.43)	3.494 (0.40)	3.723 (0.40)	3.929 (0.39)	4.019 (0.36)	4.082 (0.39)

Fig. 4.11b. Pin-power distribution for NITAWL benchmark TCA-7. Value in parentheses is percent standard deviation.

Table 4.65. Selected reaction rates for CENTRM case TCA-7

Pin	Region	$\langle \sigma_a \phi \rangle$ ($cm^{-3} - s^{-1}$)	$\langle \nu\sigma_f \phi \rangle$ ($cm^{-3} - s^{-1}$)	$\langle \sigma_f \phi \rangle$ ($cm^{-3} - s^{-1}$)	ϕ ($cm - s^{-1}$)	ϕ/ϕ_t
	Fuel	1.250E-05	2.098E-05	7.436E-06	4.475E-03	0.181
1	Clad	2.338E-07	0.0	0.0	1.390E-03	0.056
	Mod.	7.159E-07	0.0	0.0	1.884E-02	0.763
	Fuel	4.638E-05	7.357E-05	2.604E-05	2.167E-02	0.182
55	Clad	8.926E-07	0.0	0.0	6.796E-03	0.057
	Mod.	2.331E-06	0.0	0.0	9.081E-02	0.761

Table 4.66. Selected reaction rates for NITAWL case TCA-7

Pin	Region	$\langle \sigma_a \phi \rangle$ ($cm^{-3} - s^{-1}$)	$\langle \nu\sigma_f \phi \rangle$ ($cm^{-3} - s^{-1}$)	$\langle \sigma_f \phi \rangle$ ($cm^{-3} - s^{-1}$)	ϕ ($cm - s^{-1}$)	ϕ/ϕ_t
	Fuel	1.239E-05	2.081E-05	7.375E-06	4.405E-03	0.181
1	Clad	2.328E-07	0.0	0.0	1.370E-03	0.056
	Mod.	7.088E-07	0.0	0.0	1.861E-02	0.763
	Fuel	4.646E-05	7.384E-05	2.619E-05	2.180E-02	0.182
55	Clad	8.849E-07	0.0	0.0	6.807E-03	0.057
	Mod.	2.324E-06	0.0	0.0	9.112E-02	0.761

Table 4.67. TCA-7, Pin-1 four-group fluxes

Group	CENTRM Φ (cm^{-2} - s^{-1})	NITAWL Φ (cm^{-2} - s^{-1})
1	4.076E-05	4.002E-05
2	1.156E-05	1.122E-05
3	2.916E-06	2.849E-06
4	2.805E-05	2.789E-05

Table 4.68. TCA-7, Pin-1 four-group U-235 cross sections

Group	CENTRM cross sections (cm^{-1})			NITAWL cross sections (cm^{-1})		
	$\bar{\sigma}_a$	$\bar{\nu\sigma}_f$	$\bar{\sigma}_f$	$\bar{\sigma}_a$	$\bar{\nu\sigma}_f$	$\bar{\sigma}_f$
1	1.42491E-04	3.25106E-04	1.25005E-04	1.41299E-04	3.24300E-04	1.24414E-04
2	3.44975E-03	5.22773E-03	2.14542E-03	3.47152E-03	5.26026E-03	2.15876E-03
3	5.21159E-03	1.06607E-02	4.37503E-03	5.27529E-03	1.08126E-02	4.43738E-03
4	4.89248E-02	1.01867E-01	4.18053E-02	4.88655E-02	1.01743E-01	4.17544E-02

Table 4.69. TCA-7, Pin-1 four-group U-238 cross sections

Group	CENTRM cross sections (cm^{-1})			NITAWL cross sections (cm^{-1})		
	$\bar{\sigma}_a$	$\bar{\nu\sigma}_f$	$\bar{\sigma}_f$	$\bar{\sigma}_a$	$\bar{\nu\sigma}_f$	$\bar{\sigma}_f$
1	4.51148E-03	8.48982E-03	3.01170E-03	4.53551E-03	8.70929E-03	3.08361E-03
2	3.80608E-02	3.86401E-06	1.60085E-06	3.81145E-02	3.57483E-06	1.48104E-06
3	7.01523E-03	2.46902E-08	1.02296E-08	7.02506E-03	2.48652E-08	1.03021E-08
4	2.77876E-02	1.30626E-07	5.41212E-08	2.77567E-02	1.30480E-07	5.40602E-08

Table 4.70. TCA-7, Pin-1 four-group Pu-239 cross sections

Group	CENTRM cross sections (cm^{-1})			NITAWL cross sections (cm^{-1})		
	$\bar{\sigma}_a$	$\bar{\nu\sigma}_f$	$\bar{\sigma}_f$	$\bar{\sigma}_a$	$\bar{\nu\sigma}_f$	$\bar{\sigma}_f$
1	5.11889E-04	1.49757E-03	4.81327E-04	5.11022E-04	1.50238E-03	4.81994E-04
2	1.09768E-02	1.79177E-02	6.22185E-03	1.09889E-02	1.81187E-02	6.29163E-03
3	3.46245E-02	6.80175E-02	2.36188E-02	3.47959E-02	6.83577E-02	2.37369E-02
4	2.64817E-01	5.37348E-01	1.85848E-01	2.63994E-01	5.35812E-01	1.85317E-01

Table 4.71. TCA-7, Pin-55 four-group fluxes

Group	CENTRM Φ (cm^{-2} - s^{-1})	NITAWL Φ (cm^{-2} - s^{-1})
1	2.186E-04	2.205E-04
2	7.342E-05	7.405E-05
3	1.743E-05	1.715E-05
4	9.388E-05	9.404E-05

Table 4.72. TCA-7, Pin-55 four-group U-235 cross sections

Group	CENTRM cross sections (cm^{-1})			NITAWL cross sections (cm^{-1})		
	σ_a	$\langle\sigma_f$	σ_f	σ_a	$\langle\sigma_f$	σ_f
1	1.46008E-04	3.28325E-04	1.26835E-04	1.45867E-04	3.28061E-04	1.26745E-04
2	3.45407E-03	5.28814E-03	2.17020E-03	3.44685E-03	5.26736E-03	2.16167E-03
3	5.22363E-03	1.06689E-02	4.37843E-03	5.15115E-03	1.05143E-02	4.31500E-03
4	4.73673E-02	9.85703E-02	4.04524E-02	4.74047E-02	9.86425E-02	4.04820E-02

Table 4.73. TCA-7, Pin-55 four-group U-238 cross sections

Group	CENTRM cross sections (cm^{-1})			NITAWL cross sections (cm^{-1})		
	σ_a	$\langle\sigma_f$	σ_f	σ_a	$\langle\sigma_f$	σ_f
1	4.42752E-03	7.91693E-03	2.81011E-03	4.41279E-03	7.88612E-03	2.79909E-03
2	3.99843E-02	3.82517E-06	1.58476E-06	3.88724E-02	3.70637E-06	1.53553E-06
3	7.01291E-03	2.46832E-08	1.02267E-08	6.99207E-03	2.45220E-08	1.01599E-08
4	2.69759E-02	1.26733E-07	5.25080E-08	2.69906E-02	1.26799E-07	5.25354E-08

Table 4.74. TCA-7, Pin-55 four-group Pu-239 cross sections

Group	CENTRM cross sections (cm^{-1})			NITAWL cross sections (cm^{-1})		
	σ_a	$\langle\sigma_f$	σ_f	σ_a	$\langle\sigma_f$	σ_f
1	5.13362E-04	1.48414E-03	4.78998E-04	5.13238E-04	1.48384E-03	4.78975E-04
2	1.13505E-02	1.86607E-02	6.47983E-03	1.09736E-02	1.80388E-02	6.26385E-03
3	3.48495E-02	6.84159E-02	2.37571E-02	3.38470E-02	6.65440E-02	2.31071E-02
4	2.74694E-01	5.50591E-01	1.90475E-01	2.75966E-01	5.52786E-01	1.91235E-01

									7.058 (0.42)
	0.163 (0.75)							6.778 (0.45)	6.930 (0.30)
							6.434 (0.40)	6.596 (0.28)	6.745 (0.31)
						5.871 (0.47)	6.133 (0.33)	6.327 (0.30)	6.451 (0.29)
					5.168 (0.48)	5.489 (0.32)	5.742 (0.35)	5.939 (0.31)	6.053 (0.31)
				4.377 (0.49)	4.767 (0.33)	5.039 (0.34)	5.336 (0.33)	5.465 (0.33)	5.519 (0.32)
			3.520 (0.56)	3.936 (0.40)	4.294 (0.38)	4.552 (0.35)	4.754 (0.36)	4.920 (0.32)	4.979 (0.34)
		2.777 (0.66)	3.119 (0.45)	3.500 (0.39)	3.787 (0.45)	4.040 (0.37)	4.186 (0.35)	4.325 (0.33)	4.397 (0.36)
	2.148 (0.70)	2.439 (0.51)	2.772 (0.46)	3.062 (0.39)	3.330 (0.39)	3.540 (0.40)	3.714 (0.42)	3.803 (0.37)	3.857 (0.39)
2.037 (0.75)	2.140 (0.50)	2.445 (0.49)	2.777 (0.46)	3.109 (0.42)	3.342 (0.42)	3.553 (0.38)	3.728 (0.41)	3.851 (0.40)	3.923 (0.39)

Fig. 4.12a. Pin-power distribution for CENTRM benchmark TCA-8. Value in parentheses is percent standard deviation.

									7.087 (0.46)
	0.162 (0.72)							6.790 (0.41)	6.919 (0.28)
							6.419 (0.42)	6.669 (0.27)	6.737 (0.32)
						5.900 (0.43)	6.151 (0.30)	6.328 (0.27)	6.378 (0.33)
					5.179 (0.50)	5.512 (0.31)	5.799 (0.30)	5.942 (0.31)	6.021 (0.31)
				4.388 (0.53)	4.751 (0.35)	5.082 (0.35)	5.308 (0.31)	5.501 (0.31)	5.566 (0.31)
			3.547 (0.55)	3.954 (0.39)	4.305 (0.40)	4.595 (0.33)	4.764 (0.36)	4.941 (0.34)	4.987 (0.34)
		2.717 (0.67)	3.141 (0.42)	3.469 (0.43)	3.797 (0.38)	4.026 (0.36)	4.223 (0.36)	4.326 (0.36)	4.387 (0.37)
	2.140 (0.71)	2.434 (0.47)	2.753 (0.43)	3.061 (0.44)	3.313 (0.40)	3.540 (0.40)	3.695 (0.40)	3.832 (0.42)	3.886 (0.38)
2.055 (0.75)	2.128 (0.49)	2.452 (0.45)	2.780 (0.44)	3.082 (0.44)	3.377 (0.39)	3.615 (0.40)	3.740 (0.39)	3.859 (0.40)	3.928 (0.38)

Fig. 4.12b. Pin-power distribution for NITAWL benchmark TCA-8. Value in parentheses is percent standard deviation.

Table 4.75. Selected reaction rates for CENTRM case TCA-8

Pin	Region	$\langle \sigma_a \phi \rangle$ ($cm^{-3} - s^{-1}$)	$\langle \nu\sigma_f \phi \rangle$ ($cm^{-3} - s^{-1}$)	$\langle \sigma_f \phi \rangle$ ($cm^{-3} - s^{-1}$)	ϕ ($cm - s^{-1}$)	ϕ/ϕ_t
	Fuel	1.219E-05	2.033E-05	7.204E-06	4.521E-03	0.182
1	Clad	2.267E-07	0.0	0.0	1.397E-03	0.056
	Mod.	6.904E-07	0.0	0.0	1.890E-02	0.762
	Fuel	4.454E-05	7.082E-05	2.507E-05	2.182E-02	0.182
55	Clad	8.569E-07	0.0	0.0	6.833E-03	0.057
	Mod.	2.247E-06	0.0	0.0	9.140E-02	0.761

Table 4.76. Selected reaction rates for NITAWL case TCA-8

Pin	Region	$\langle \sigma_a \phi \rangle$ ($cm^{-3} - s^{-1}$)	$\langle \nu\sigma_f \phi \rangle$ ($cm^{-3} - s^{-1}$)	$\langle \sigma_f \phi \rangle$ ($cm^{-3} - s^{-1}$)	ϕ ($cm - s^{-1}$)	ϕ/ϕ_t
	Fuel	1.228E-05	2.056E-05	7.288E-06	4.508E-03	0.182
1	Clad	2.273E-07	0.0	0.0	1.396E-03	0.056
	Mod.	6.917E-07	0.0	0.0	1.890E-02	0.762
	Fuel	4.442E-05	7.058E-05	2.499E-05	2.172E-02	0.182
55	Clad	8.512E-07	0.0	0.0	6.810E-03	0.057
	Mod.	2.244E-06	0.0	0.0	9.104E-02	0.761

Table 4.77. TCA-8, Pin-1 four-group fluxes

Group	CENTRM Φ (cm^{-2} - s^{-1})	NITAWL Φ (cm^{-2} - s^{-1})
1	3.944E-05	3.890E-05
2	1.103E-05	1.116E-05
3	2.823E-06	2.632E-06
4	2.727E-05	2.765E-05

Table 4.78. TCA-8, Pin-1 four-group U-235 cross sections

Group	CENTRM cross sections (cm^{-1})			NITAWL cross sections (cm^{-1})		
	$\bar{\sigma}_a$	$\bar{\sigma}_f$	$\bar{\nu}\bar{\sigma}_f$	$\bar{\sigma}_a$	$\bar{\sigma}_f$	$\bar{\nu}\bar{\sigma}_f$
1	1.42334E-04	3.25312E-04	1.24980E-04	1.42088E-04	3.25219E-04	1.24828E-04
2	3.53127E-03	5.35172E-03	2.19630E-03	3.46204E-03	5.26653E-03	2.16133E-03
3	5.12848E-03	1.04583E-02	4.29199E-03	5.21250E-03	1.06698E-02	4.37876E-03
4	4.88629E-02	1.01736E-01	4.17514E-02	4.88872E-02	1.01784E-01	4.17714E-02

Table 4.79. TCA-8, Pin-1 four-group U-238 cross sections

Group	CENTRM cross sections (cm^{-1})			NITAWL cross sections (cm^{-1})		
	$\bar{\sigma}_a$	$\bar{\sigma}_f$	$\bar{\nu}\bar{\sigma}_f$	$\bar{\sigma}_a$	$\bar{\sigma}_f$	$\bar{\nu}\bar{\sigma}_f$
1	4.53489E-03	8.60396E-03	3.05003E-03	4.52758E-03	8.62663E-03	3.05064E-03
2	4.11256E-02	3.90524E-06	1.61793E-06	3.90452E-02	3.64034E-06	1.50818E-06
3	6.97793E-03	2.43563E-08	1.00913E-08	7.01079E-03	2.46993E-08	1.02334E-08
4	2.77529E-02	1.30460E-07	5.40521E-08	2.77661E-02	1.30523E-07	5.40785E-08

Table 4.80. TCA-8, Pin-1 four-group Pu-239 cross sections

Group	CENTRM cross sections (cm^{-1})			NITAWL cross sections (cm^{-1})		
	$\bar{\sigma}_a$	$\bar{\sigma}_f$	$\bar{\nu}\bar{\sigma}_f$	$\bar{\sigma}_a$	$\bar{\sigma}_f$	$\bar{\nu}\bar{\sigma}_f$
1	5.11790E-04	1.49952E-03	4.81643E-04	5.11429E-04	1.50018E-03	4.81447E-04
2	1.15051E-02	1.87178E-02	6.49966E-03	1.06573E-02	1.75647E-02	6.09924E-03
3	3.42439E-02	6.71877E-02	2.33306E-02	3.42088E-02	6.72576E-02	2.33550E-02
4	2.65649E-01	5.38621E-01	1.86291E-01	2.65522E-01	5.38441E-01	1.86228E-01

Table 4.81. TCA-8, Pin-55 four-group fluxes

Group	CENTRM Φ (cm^{-2} - s^{-1})	NITAWL Φ (cm^{-2} - s^{-1})
1	2.110E-04	2.107E-04
2	7.037E-05	6.962E-05
3	1.673E-05	1.667E-05
4	9.070E-05	9.010E-05

Table 4.82. TCA-8, Pin-55 four-group U-235 cross sections

Group	CENTRM cross sections (cm^{-1})			NITAWL cross sections (cm^{-1})		
	Σ_a	$\langle\Sigma_f$	Σ_f	Σ_a	$\langle\Sigma_f$	Σ_f
1	1.45480E-04	3.27674E-04	1.26526E-04	1.45435E-04	3.27709E-04	1.26510E-04
2	3.39048E-03	5.20276E-03	2.13517E-03	3.47111E-03	5.30325E-03	2.17640E-03
3	5.13229E-03	1.04562E-02	4.29112E-03	5.19965E-03	1.06013E-02	4.35069E-03
4	4.74630E-02	9.87671E-02	4.05332E-02	4.77188E-02	9.92999E-02	4.07518E-02

Table 4.83. TCA-8, Pin-55 four-group U-238 cross sections

Group	CENTRM cross sections (cm^{-1})			NITAWL cross sections (cm^{-1})		
	Σ_a	$\langle\Sigma_f$	Σ_f	Σ_a	$\langle\Sigma_f$	Σ_f
1	4.41327E-03	7.93014E-03	2.81274E-03	4.42132E-03	7.95819E-03	2.82199E-03
2	3.87344E-02	3.80772E-06	1.57752E-06	3.76439E-02	3.63710E-06	1.50684E-06
3	6.98380E-03	2.43899E-08	1.01051E-08	7.00174E-03	2.45717E-08	1.01805E-08
4	2.70204E-02	1.26942E-07	5.25946E-08	2.71446E-02	1.27535E-07	5.28402E-08

Table 4.84. TCA-8, Pin-55 four-group Pu-239 cross sections

Group	CENTRM cross sections (cm^{-1})			NITAWL cross sections (cm^{-1})		
	Σ_a	$\langle\Sigma_f$	Σ_f	Σ_a	$\langle\Sigma_f$	Σ_f
1	5.12787E-04	1.48453E-03	4.78981E-04	5.12848E-04	1.48514E-03	4.79084E-04
2	1.11398E-02	1.83762E-02	6.38104E-03	1.10696E-02	1.81030E-02	6.28615E-03
3	3.39692E-02	6.67376E-02	2.31743E-02	3.43528E-02	6.74775E-02	2.34313E-02
4	2.75637E-01	5.52375E-01	1.91090E-01	2.76264E-01	5.53948E-01	1.91632E-01

									6.747 (0.46)
	0.172 (0.90)							6.520 (0.40)	6.616 (0.30)
							6.164 (0.40)	6.297 (0.32)	6.417 (0.30)
						5.649 (0.43)	5.915 (0.30)	6.064 (0.29)	6.158 (0.28)
					4.974 (0.43)	5.311 (0.34)	5.553 (0.30)	5.732 (0.31)	5.793 (0.30)
				4.210 (0.48)	4.568 (0.33)	4.907 (0.35)	5.111 (0.33)	5.265 (0.31)	5.318 (0.33)
			3.447 (0.56)	3.807 (0.37)	4.124 (0.34)	4.379 (0.38)	4.589 (0.34)	4.729 (0.33)	4.777 (0.33)
		2.642 (0.62)	2.995 (0.40)	3.353 (0.42)	3.657 (0.39)	3.869 (0.38)	4.027 (0.38)	4.147 (0.35)	4.236 (0.38)
	2.049 (0.75)	2.330 (0.49)	2.663 (0.46)	3.948 (0.44)	3.206 (0.42)	3.412 (0.41)	3.586 (0.37)	3.704 (0.39)	3.745 (0.38)
1.975 (0.75)	2.076 (0.52)	2.378 (0.48)	2.685 (0.44)	2.993 (0.43)	3.228 (0.41)	3.452 (0.36)	3.579 (0.39)	3.723 (0.38)	3.736 (0.38)

Fig. 4.13a. Pin-power distribution for CENTRM benchmark TCA-9. Value in parentheses is percent standard deviation.

									6.800 (0.46)
	0.171 (0.91)							6.580 (0.38)	6.670 (0.31)
							6.176 (0.41)	6.363 (0.29)	6.453 (0.30)
						5.635 (0.47)	5.898 (0.29)	6.091 (0.28)	6.195 (0.30)
					5.005 (0.45)	5.293 (0.32)	5.511 (0.31)	5.719 (0.32)	5.831 (0.31)
				4.282 (0.51)	4.566 (0.35)	4.892 (0.32)	5.110 (0.33)	5.264 (0.32)	5.384 (0.35)
			3.411 (0.61)	3.800 (0.41)	4.089 (0.37)	4.402 (0.33)	4.609 (0.32)	4.756 (0.36)	4.821 (0.34)
		2.650 (0.64)	3.001 (0.39)	3.317 (0.42)	3.641 (0.39)	3.876 (0.38)	4.059 (0.39)	4.143 (0.33)	4.226 (0.35)
	2.086 (0.76)	2.348 (0.51)	2.677 (0.50)	3.966 (0.40)	3.202 (0.42)	3.410 (0.40)	3.561 (0.40)	3.662 (0.37)	3.742 (0.39)
1.957 (0.65)	2.055 (0.51)	2.361 (0.51)	2.691 (0.44)	3.012 (0.43)	3.213 (0.43)	3.430 (0.40)	3.584 (0.37)	3.714 (0.37)	3.782 (0.39)

Fig. 4.13b. Pin-power distribution for NITAWL benchmark TCA-9. Value in parentheses is percent standard deviation.

Table 4.85. Selected reaction rates for CENTRM case TCA-9

Pin	Region	$\langle \sigma_a \phi \rangle$ (cm^{-3} - s^{-1})	$\langle \nu\sigma_f \phi \rangle$ (cm^{-3} - s^{-1})	$\langle \sigma_f \phi \rangle$ (cm^{-3} - s^{-1})	ϕ (cm - s^{-1})	ϕ/ϕ_t
	Fuel	1.197E-05	1.995E-05	7.072E-06	4.613E-03	0.183
1	Clad	2.247E-07	0.0	0.0	1.425E-03	0.056
	Mod.	6.729E-07	0.0	0.0	1.919E-02	0.761
	Fuel	4.255E-05	6.730E-05	2.383E-05	2.168E-02	0.181
55	Clad	8.192E-07	0.0	0.0	6.794E-03	0.057
	Mod.	2.155E-06	0.0	0.0	9.111E-02	0.762

Table 4.86. Selected reaction rates for NITAWL case TCA-9

Pin	Region	$\langle \sigma_a \phi \rangle$ (cm^{-3} - s^{-1})	$\langle \nu\sigma_f \phi \rangle$ (cm^{-3} - s^{-1})	$\langle \sigma_f \phi \rangle$ (cm^{-3} - s^{-1})	ϕ (cm - s^{-1})	ϕ/ϕ_t
	Fuel	1.173E-05	1.955E-05	6.931E-06	4.554E-03	0.182
1	Clad	2.206E-07	0.0	0.0	1.420E-03	0.056
	Mod.	6.680E-07	0.0	0.0	1.910E-02	0.762
	Fuel	4.279E-05	6.771E-05	2.398E-05	2.188E-02	0.182
55	Clad	8.213E-07	0.0	0.0	6.844E-03	0.057
	Mod.	2.172E-06	0.0	0.0	9.168E-02	0.761

Table 4.87. TCA-9, Pin-1 four-group fluxes

Group	CENTRM Φ (cm^{-2} - s^{-1})	NITAWL Φ (cm^{-2} - s^{-1})
1	3.851E-05	3.808E-05
2	1.088E-05	1.068E-05
3	2.665E-06	2.690E-06
4	2.684E-05	2.644E-05

Table 4.88. TCA-9, Pin-1 four-group U-235 cross sections

Group	CENTRM cross sections (cm^{-1})			NITAWL cross sections (cm^{-1})		
	Σ_a	$\langle\Sigma_f$	Σ_f	Σ_a	$\langle\Sigma_f$	Σ_f
1	1.42657E-04	3.25414E-04	1.25101E-04	1.41875E-04	3.24320E-04	1.24670E-04
2	3.42835E-03	5.22619E-03	2.14479E-03	3.51588E-03	5.33745E-03	2.19045E-03
3	5.02206E-03	1.01901E-02	4.18195E-03	5.22963E-03	1.07319E-02	4.40428E-03
4	4.91554E-02	1.02344E-01	4.20007E-02	4.86914E-02	1.01377E-01	4.16040E-02

Table 4.89. TCA-9, Pin-1 four-group U-238 cross sections

Group	CENTRM cross sections (cm^{-1})			NITAWL cross sections (cm^{-1})		
	Σ_a	$\langle\Sigma_f$	Σ_f	Σ_a	$\langle\Sigma_f$	Σ_f
1	4.50192E-03	8.46604E-03	2.99920E-03	4.50218E-03	8.53582E-03	3.03046E-03
2	4.14411E-02	3.76574E-06	1.56013E-06	3.83075E-02	3.58055E-06	1.48341E-06
3	6.94867E-03	2.40724E-08	9.97362E-09	7.02602E-03	2.48603E-08	1.03001E-08
4	2.78966E-02	1.31143E-07	5.43353E-08	2.76690E-02	1.30061E-07	5.38869E-08

Table 4.90 TCA-9, Pin-1 four-group Pu-239 cross sections

Group	CENTRM cross sections (cm^{-1})			NITAWL cross sections (cm^{-1})		
	Σ_a	$\langle\Sigma_f$	Σ_f	Σ_a	$\langle\Sigma_f$	Σ_f
1	5.11763E-04	1.49708E-03	4.81127E-04	5.10995E-04	1.49750E-03	4.81258E-04
2	1.10924E-02	1.84326E-02	6.40062E-03	1.10329E-02	1.80993E-02	6.28488E-03
3	3.20870E-02	6.32248E-02	2.19544E-02	3.47840E-02	6.83283E-02	2.37267E-02
4	2.66228E-01	5.40183E-01	1.86826E-01	2.64971E-01	5.37118E-01	1.85773E-01

Table 4.91. TCA-9, Pin-55 four-group fluxes

Group	CENTRM Φ (cm^{-2} - s^{-1})	NITAWL Φ (cm^{-2} - s^{-1})
1	2.010E-04	2.034E-04
2	6.739E-05	6.769E-05
3	1.576E-05	1.591E-05
4	8.667E-05	8.728E-05

Table 4.92. TCA-9, Pin-55 four-group U-235 cross sections

Group	CENTRM cross sections (cm^{-1})			NITAWL cross sections (cm^{-1})		
	Σ_a	$\langle\Sigma_f$	Σ_f	Σ_a	$\langle\Sigma_f$	Σ_f
1	1.45454E-04	3.27423E-04	1.26486E-04	1.45607E-04	3.27771E-04	1.26597E-04
2	3.41193E-03	5.23067E-03	2.14662E-03	3.48574E-03	5.30232E-03	2.17602E-03
3	5.17154E-03	1.05678E-02	4.33692E-03	5.13163E-03	1.04658E-02	4.29508E-03
4	4.74074E-02	9.86494E-02	4.04848E-02	4.74735E-02	9.87892E-02	4.05423E-02

Table 4.93. TCA-9, Pin-55 four-group U-238 cross sections

Group	CENTRM cross sections (cm^{-1})			NITAWL cross sections (cm^{-1})		
	Σ_a	$\langle\Sigma_f$	Σ_f	Σ_a	$\langle\Sigma_f$	Σ_f
1	4.40327E-03	7.89249E-03	2.80210E-03	4.40840E-03	7.90103E-03	2.80352E-03
2	3.82984E-02	3.87376E-06	1.60488E-06	3.80297E-02	3.68119E-06	1.52510E-06
3	6.99689E-03	2.45553E-08	1.01737E-08	6.98259E-03	2.44124E-08	1.01145E-08
4	2.69919E-02	1.26807E-07	5.25386E-08	2.70262E-02	1.26972E-07	5.26067E-08

Table 4.94. TCA-9, Pin-55 four-group Pu-239 cross sections

Group	CENTRM cross sections (cm^{-1})			NITAWL cross sections (cm^{-1})		
	Σ_a	$\langle\Sigma_f$	Σ_f	Σ_a	$\langle\Sigma_f$	Σ_f
1	5.12642E-04	1.48335E-03	4.78804E-04	5.12945E-04	1.48419E-03	4.78995E-04
2	1.10458E-02	1.82405E-02	6.33394E-03	1.08837E-02	1.78922E-02	6.21299E-03
3	3.38276E-02	6.65209E-02	2.30991E-02	3.35685E-02	6.60145E-02	2.29233E-02
4	2.75620E-01	5.52218E-01	1.91037E-01	2.75080E-01	5.51449E-01	1.90770E-01

										6.856 (0.85)
	0.141 (0.76)								6.768 (0.41)	6.823 (0.42)
								6.535 (0.43)	6.644 (0.30)	6.692 (0.44)
							6.073 (0.44)	6.278 (0.31)	6.452 (0.32)	6.462 (0.48)
						5.443 (0.46)	5.760 (0.35)	5.984 (0.30)	6.074 (0.35)	6.161 (0.44)
					4.729 (0.48)	5.080 (0.34)	5.339 (0.33)	5.561 (0.32)	5.648 (0.33)	5.659 (0.48)
				3.888 (0.57)	4.322 (0.37)	4.641 (0.36)	4.858 (0.32)	5.062 (0.33)	5.192 (0.34)	5.200 (0.49)
			3.115 (0.64)	3.500 (0.43)	3.840 (0.39)	4.093 (0.37)	4.339 (0.38)	4.483 (0.39)	4.605 (0.39)	4.604 (0.53)
		2.358 (0.72)	2.681 (0.47)	3.033 (0.43)	3.323 (0.38)	3.532 (0.43)	3.760 (0.40)	3.875 (0.42)	3.955 (0.37)	3.936 (0.55)
	1.684 (0.85)	1.983 (0.56)	2.291 (0.51)	2.553 (0.46)	2.823 (0.46)	3.029 (0.41)	3.208 (0.45)	3.286 (0.41)	3.384 (0.39)	3.418 (0.59)
1.428 (0.77)	1.569 (0.61)	1.859 (0.57)	2.158 (0.49)	2.398 (0.51)	2.643 (0.49)	2.831 (0.45)	2.995 (0.47)	3.099 (0.42)	3.141 (0.43)	3.185 (0.58)

Fig. 4.14a. Pin-power distribution for CENTRM benchmark TCA-10. Value in parentheses is percent standard deviation.

										6.908 (0.85)
	0.144 (0.76)								6.810 (0.41)	6.858 (0.43)
								6.535 (0.42)	6.640 (0.31)	6.685 (0.43)
							6.057 (0.47)	6.279 (0.33)	6.387 (0.31)	6.470 (0.43)
						5.486 (0.45)	5.776 (0.31)	6.008 (0.31)	6.085 (0.33)	6.152 (0.45)
					4.750 (0.51)	5.094 (0.33)	5.371 (0.31)	5.545 (0.30)	5.669 (0.34)	5.702 (0.44)
				3.961 (0.55)	4.306 (0.33)	4.671 (0.38)	4.906 (0.32)	5.079 (0.34)	5.159 (0.36)	5.240 (0.48)
			3.100 (0.59)	3.517 (0.38)	3.850 (0.40)	4.088 (0.40)	4.342 (0.36)	4.512 (0.35)	4.599 (0.34)	4.621 (0.50)
		2.323 (0.70)	2.712 (0.44)	3.010 (0.46)	3.318 (0.45)	3.576 (0.42)	3.745 (0.40)	3.898 (0.41)	3.962 (0.39)	4.025 (0.59)
	1.667 (0.84)	2.010 (0.56)	2.295 (0.51)	2.584 (0.45)	2.808 (0.48)	3.022 (0.46)	3.184 (0.45)	3.312 (0.43)	3.374 (0.41)	3.412 (0.57)
1.422 (0.85)	1.576 (0.65)	1.865 (0.58)	2.122 (0.51)	2.401 (0.50)	2.644 (0.46)	2.824 (0.47)	2.996 (0.45)	3.102 (0.39)	3.155 (0.44)	3.217 (0.56)

Fig. 4.14b. Pin-power distribution for NITAWL benchmark TCA-10. Value in parentheses is percent standard deviation.

Table 4.95. Selected reaction rates for CENTRM case TCA-10

Pin	Region	$\langle \sigma_a \phi \rangle$ (cm^{-3} - s^{-1})	$\langle \nu\sigma_f \phi \rangle$ (cm^{-3} - s^{-1})	$\langle \sigma_f \phi \rangle$ (cm^{-3} - s^{-1})	ϕ (cm - s^{-1})	ϕ/ϕ_t
	Fuel	8.487E-06	1.430E-05	5.068E-06	2.952E-03	0.146
1	Clad	1.587E-07	0.0	0.0	9.168E-04	0.046
	Mod.	4.949E-07	0.0	0.0	1.630E-02	0.808
	Fuel	4.238E-05	6.861E-05	2.429E-05	1.833E-02	0.147
66	Clad	8.072E-07	0.0	0.0	5.748E-03	0.046
	Mod.	2.263E-06	0.0	0.0	1.007E-01	0.807

Table 4.96. Selected reaction rates for NITAWL case TCA-10

Pin	Region	$\langle \sigma_a \phi \rangle$ (cm^{-3} - s^{-1})	$\langle \nu\sigma_f \phi \rangle$ (cm^{-3} - s^{-1})	$\langle \sigma_f \phi \rangle$ (cm^{-3} - s^{-1})	ϕ (cm - s^{-1})	ϕ/ϕ_t
	Fuel	8.415E-06	1.413E-05	5.006E-06	2.931E-03	0.146
1	Clad	1.562E-07	0.0	0.0	9.141E-04	0.046
	Mod.	4.895E-07	0.0	0.0	1.618E-02	0.808
	Fuel	4.266E-05	6.930E-05	2.454E-05	1.832E-02	0.147
66	Clad	8.014E-07	0.0	0.0	5.729E-03	0.045
	Mod.	2.297E-06	0.0	0.0	1.009E-01	0.808

Table 4.97. TCA-10, Pin-1 four-group fluxes

Group	CENTRM Φ (cm^{-2} - s^{-1})	NITAWL Φ (cm^{-2} - s^{-1})
1	2.547E-05	2.512E-05
2	7.003E-06	7.231E-06
3	1.709E-06	1.737E-06
4	1.922E-05	1.894E-05

Table 4.98. TCA-10, Pin-1 four-group U-235 cross sections

Group	CENTRM cross sections (cm^{-1})			NITAWL cross sections (cm^{-1})		
	Σ_a	$\langle\Sigma_f$	Σ_f	Σ_a	$\langle\Sigma_f$	Σ_f
1	1.40788E-04	3.23363E-04	1.24110E-04	1.41106E-04	3.24338E-04	1.24311E-04
2	3.64170E-03	5.55391E-03	2.27928E-03	3.51527E-03	5.32391E-03	2.18488E-03
3	5.30350E-03	1.08803E-02	4.46517E-03	5.18458E-03	1.06225E-02	4.35935E-03
4	4.91298E-02	1.02298E-01	4.19822E-02	4.92076E-02	1.02458E-01	4.20476E-02

Table 4.99. TCA-10, Pin-1 four-group U-238 cross sections

Group	CENTRM cross sections (cm^{-1})			NITAWL cross sections (cm^{-1})		
	Σ_a	$\langle\Sigma_f$	Σ_f	Σ_a	$\langle\Sigma_f$	Σ_f
1	4.53168E-03	8.72356E-03	3.09660E-03	4.53467E-03	8.75482E-03	3.09219E-03
2	4.29217E-02	3.81724E-06	1.58147E-06	4.01630E-02	3.94182E-06	1.63309E-06
3	7.03335E-03	2.49018E-08	1.03173E-08	7.00443E-03	2.45869E-08	1.01868E-08
4	2.78924E-02	1.31130E-07	5.43293E-08	2.79251E-02	1.31284E-07	5.43933E-08

Table 4.100. TCA-10, Pin-1 four-group Pu-239 cross sections

Group	CENTRM cross sections (cm^{-1})			NITAWL cross sections (cm^{-1})		
	Σ_a	$\langle\Sigma_f$	Σ_f	Σ_a	$\langle\Sigma_f$	Σ_f
1	5.10742E-04	1.50232E-03	4.82148E-04	5.10768E-04	1.50322E-03	4.81907E-04
2	1.13157E-02	1.86831E-02	6.48763E-03	1.14534E-02	1.87359E-02	6.50593E-03
3	3.56099E-02	6.98250E-02	2.42465E-02	3.42803E-02	6.73431E-02	2.33847E-02
4	2.63607E-01	5.35739E-01	1.85285E-01	2.64216E-01	5.36885E-01	1.85682E-01

Table 4.101. TCA-10, Pin-66 four-group fluxes

Group	CENTRM Φ (cm^{-2} - s^{-1})	NITAWL Φ (cm^{-2} - s^{-1})
1	1.721E-04	1.716E-04
2	5.659E-05	5.611E-05
3	1.360E-05	1.336E-05
4	8.928E-05	9.041E-05

Table 4.102. TCA-10, Pin-66 four-group U-235 cross sections

Group	CENTRM cross sections (cm^{-1})			NITAWL cross sections (cm^{-1})		
	Σ_a	$\langle\Sigma_f$	Σ_f	Σ_a	$\langle\Sigma_f$	Σ_f
1	1.44765E-04	3.27146E-04	1.26179E-04	1.44207E-04	3.26568E-04	1.25881E-04
2	3.42458E-03	5.21627E-03	2.14071E-03	3.45678E-03	5.26794E-03	2.16191E-03
3	5.10952E-03	1.04097E-02	4.27204E-03	5.28578E-03	1.08415E-02	4.44925E-03
4	4.80156E-02	9.99418E-02	4.10152E-02	4.77411E-02	9.93647E-02	4.07783E-02

Table 4.103. TCA-10, Pin-66 four-group U-238 cross sections

Group	CENTRM cross sections (cm^{-1})			NITAWL cross sections (cm^{-1})		
	Σ_a	$\langle\Sigma_f$	Σ_f	Σ_a	$\langle\Sigma_f$	Σ_f
1	4.43964E-03	8.07600E-03	2.86439E-03	4.43787E-03	8.12821E-03	2.88138E-03
2	3.89892E-02	3.80924E-06	1.57815E-06	3.85192E-02	3.58239E-06	1.48417E-06
3	6.97667E-03	2.43379E-08	1.00837E-08	7.03071E-03	2.48865E-08	1.03109E-08
4	2.73091E-02	1.28331E-07	5.31703E-08	2.71792E-02	1.27709E-07	5.29124E-08

Table 4.104. TCA-10, Pin-66 four-group Pu-239 cross sections

Group	CENTRM cross sections (cm^{-1})			NITAWL cross sections (cm^{-1})		
	Σ_a	$\langle\Sigma_f$	Σ_f	Σ_a	$\langle\Sigma_f$	Σ_f
1	5.12740E-04	1.48833E-03	4.79719E-04	5.12294E-04	1.48952E-03	4.79891E-04
2	1.11449E-02	1.83349E-02	6.36671E-03	1.12214E-02	1.84762E-02	6.41579E-03
3	3.30546E-02	6.50683E-02	2.25947E-02	3.57615E-02	7.00931E-02	2.43396E-02
4	2.70972E-01	5.45716E-01	1.88771E-01	2.70533E-01	5.44404E-01	1.88319E-01

										6.654 (0.79)
	0.147 (0.81)								6.562 (0.44)	6.611 (0.46)
								6.263 (0.44)	6.409 (0.32)	6.449 (0.43)
							5.818 (0.46)	6.026 (0.31)	6.170 (0.31)	6.207 (0.44)
						5.216 (0.46)	5.552 (0.35)	5.746 (0.30)	5.878 (0.30)	5.943 (0.39)
					4.527 (0.58)	4.898 (0.35)	5.157 (0.31)	5.351 (0.31)	5.483 (0.32)	5.471 (0.45)
				3.745 (0.51)	4.139 (0.38)	4.467 (0.35)	4.724 (0.35)	4.888 (0.33)	5.001 (0.33)	4.991 (0.49)
			3.030 (0.65)	3.377 (0.41)	3.691 (0.40)	3.991 (0.38)	4.178 (0.39)	4.331 (0.34)	4.457 (0.36)	4.431 (0.50)
		2.212 (0.70)	2.576 (0.52)	2.912 (0.43)	3.174 (0.42)	3.439 (0.38)	3.611 (0.39)	3.748 (0.36)	3.825 (0.40)	3.884 (0.50)
	1.604 (0.82)	1.905 (0.50)	2.200 (0.49)	2.472 (0.45)	2.710 (0.48)	2.905 (0.41)	3.084 (0.47)	3.215 (0.41)	3.268 (0.43)	3.263 (0.55)
1.350 (0.84)	1.492 (0.56)	1.764 (0.57)	2.050 (0.50)	2.302 (0.49)	2.553 (0.45)	2.722 (0.44)	2.886 (0.45)	2.980 (0.46)	3.036 (0.44)	3.092 (0.56)

Fig. 4.15a. Pin-power distribution for CENTRM benchmark TCA-11. Value in parentheses is percent standard deviation.

										6.756 (0.82)
	0.148 (0.84)								6.609 (0.41)	6.637 (0.39)
								6.358 (0.42)	6.453 (0.31)	6.510 (0.44)
							5.866 (0.43)	6.087 (0.31)	6.184 (0.31)	6.208 (0.44)
						5.248 (0.45)	5.518 (0.31)	5.748 (0.29)	5.874 (0.31)	5.922 (0.43)
					4.565 (0.51)	4.901 (0.35)	5.149 (0.31)	5.364 (0.31)	5.480 (0.32)	5.535 (0.47)
				3.782 (0.57)	4.171 (0.39)	4.444 (0.38)	4.672 (0.37)	4.911 (0.33)	4.984 (0.30)	5.039 (0.47)
			2.969 (0.61)	3.380 (0.38)	3.683 (0.38)	3.961 (0.37)	4.175 (0.40)	4.337 (0.35)	4.431 (0.36)	4.489 (0.53)
		2.266 (0.73)	2.599 (0.49)	2.912 (0.47)	3.209 (0.40)	3.419 (0.44)	3.625 (0.39)	3.746 (0.38)	3.823 (0.39)	3.855 (0.60)
	1.628 (0.86)	1.918 (0.54)	2.205 (0.51)	2.470 (0.48)	2.727 (0.45)	2.946 (0.52)	3.062 (0.42)	3.184 (0.42)	3.282 (0.42)	3.293 (0.59)
1.376 (0.81)	1.498 (0.61)	1.770 (0.54)	2.049 (0.51)	2.320 (0.50)	2.536 (0.45)	2.723 (0.45)	2.861 (0.49)	2.983 (0.44)	3.037 (0.42)	3.032 (0.61)

Fig. 4.15b. Pin-power distribution for NITAWL benchmark TCA-11. Value in parentheses is percent standard deviation.

Table 4.105. Selected reaction rates for CENTRM case TCA-11

Pin	Region	$\langle \sigma_a \phi \rangle$ ($cm^{-3} - s^{-1}$)	$\langle \nu\sigma_f \phi \rangle$ ($cm^{-3} - s^{-1}$)	$\langle \sigma_f \phi \rangle$ ($cm^{-3} - s^{-1}$)	ϕ ($cm - s^{-1}$)	ϕ/ϕ_t
	Fuel	7.995E-06	1.342E-05	4.759E-06	2.922E-03	0.146
1	Clad	1.494E-07	0.0	0.0	8.994E-04	0.046
	Mod.	4.727E-07	0.0	0.0	1.613E-02	0.808
	Fuel	4.112E-05	6.652E-05	2.356E-05	1.831E-02	0.147
66	Clad	7.801E-07	0.0	0.0	5.719E-03	0.045
	Mod.	2.193E-06	0.0	0.0	1.009E-01	0.808

Table 4.106. Selected reaction rates for NITAWL case TCA-11

Pin	Region	$\langle \sigma_a \phi \rangle$ ($cm^{-3} - s^{-1}$)	$\langle \nu\sigma_f \phi \rangle$ ($cm^{-3} - s^{-1}$)	$\langle \sigma_f \phi \rangle$ ($cm^{-3} - s^{-1}$)	ϕ ($cm - s^{-1}$)	ϕ/ϕ_t
	Fuel	8.237E-06	1.382E-05	4.898E-06	2.946E-03	0.146
1	Clad	1.536E-07	0.0	0.0	9.201E-04	0.046
	Mod.	4.780E-07	0.0	0.0	1.632E-02	0.808
	Fuel	4.210E-05	6.785E-05	2.403E-05	1.881E-02	0.149
66	Clad	7.944E-07	0.0	0.0	5.881E-03	0.045
	Mod.	2.226E-06	0.0	0.0	1.019E-01	0.805

Table 4.107. TCA-11, Pin-1 four-group fluxes

Group	CENTRM Φ (cm^{-2} - s^{-1})	NITAWL Φ (cm^{-2} - s^{-1})
1	2.428E-05	2.418E-05
2	6.754E-06	6.771E-06
3	1.616E-06	1.716E-06
4	1.818E-05	1.859E-05

Table 4.108. TCA-11, Pin-1 four-group U-235 cross sections

Group	CENTRM cross sections (cm^{-1})			NITAWL cross sections (cm^{-1})		
	Σ_a	$\langle\Sigma_f$	Σ_f	Σ_a	$\langle\Sigma_f$	Σ_f
1	1.41872E-04	3.24906E-04	1.24701E-04	1.41020E-04	3.23700E-04	1.24222E-04
2	3.59017E-03	5.46494E-03	2.24276E-03	3.58779E-03	5.48985E-03	2.25299E-03
3	5.18994E-03	1.06233E-02	4.35970E-03	5.10914E-03	1.04368E-02	4.28316E-03
4	4.91039E-02	1.02248E-01	4.19618E-02	4.92082E-02	1.02458E-01	4.20477E-02

Table 4.109. TCA-11, Pin-1 four-group U-238 cross sections

Group	CENTRM cross sections (cm^{-1})			NITAWL cross sections (cm^{-1})		
	Σ_a	$\langle\Sigma_f$	Σ_f	Σ_a	$\langle\Sigma_f$	Σ_f
1	4.53707E-03	8.65445E-03	3.06352E-03	4.50757E-03	8.64413E-03	3.06142E-03
2	3.77442E-02	3.89227E-06	1.61256E-06	4.14119E-02	3.44468E-06	1.42711E-06
3	6.97847E-03	2.44523E-08	1.01310E-08	6.97541E-03	2.44034E-08	1.01108E-08
4	2.78818E-02	1.31080E-07	5.43088E-08	2.79222E-02	1.31269E-07	5.43873E-08

Table 4.110. TCA-11, Pin-1 four-group Pu-239 cross sections

Group	CENTRM cross sections (cm^{-1})			NITAWL cross sections (cm^{-1})		
	Σ_a	$\langle\Sigma_f$	Σ_f	Σ_a	$\langle\Sigma_f$	Σ_f
1	5.11446E-04	1.50099E-03	4.81647E-04	5.10571E-04	1.50108E-03	4.81762E-04
2	1.15859E-02	1.88543E-02	6.54708E-03	1.15115E-02	1.90902E-02	6.62899E-03
3	3.43188E-02	6.73416E-02	2.33841E-02	3.42125E-02	6.71562E-02	2.33196E-02
4	2.62911E-01	5.34534E-01	1.84867E-01	2.65492E-01	5.39053E-01	1.86434E-01

Table 4.111. TCA-11, Pin-66 four-group fluxes

Group	CENTRM Φ (cm^{-2} - s^{-1})	NITAWL Φ (cm^{-2} - s^{-1})
1	1.657E-04	1.701E-04
2	5.293E-05	5.558E-05
3	1.316E-05	1.301E-05
4	8.674E-05	8.849E-05

Table 4.112. TCA-11, Pin-66 four-group U-235 cross sections

Group	CENTRM cross sections (cm^{-1})			NITAWL cross sections (cm^{-1})		
	Σ_a	$\langle\Sigma_f$	Σ_f	Σ_a	$\langle\Sigma_f$	Σ_f
1	1.44711E-04	3.27220E-04	1.26172E-04	1.44755E-04	3.27436E-04	1.26225E-04
2	3.46220E-03	5.28876E-03	2.17045E-03	3.45516E-03	5.25847E-03	2.15802E-03
3	5.16589E-03	1.05595E-02	4.33352E-03	5.18064E-03	1.05839E-02	4.34357E-03
4	4.81825E-02	1.00288E-01	4.11571E-02	4.80322E-02	9.99713E-02	4.10273E-02

Table 4.113. TCA-11, Pin-66 four-group U-238 cross sections

Group	CENTRM cross sections (cm^{-1})			NITAWL cross sections (cm^{-1})		
	Σ_a	$\langle\Sigma_f$	Σ_f	Σ_a	$\langle\Sigma_f$	Σ_f
1	4.47467E-03	8.17996E-03	2.90346E-03	4.47739E-03	8.19447E-03	2.90690E-03
2	3.91615E-02	3.93752E-06	1.63130E-06	4.02064E-02	3.76053E-06	1.55797E-06
3	6.99303E-03	2.44910E-08	1.01470E-08	6.99198E-03	2.45410E-08	1.01678E-08
4	2.73917E-02	1.28724E-07	5.33326E-08	2.73197E-02	1.28377E-07	5.31893E-08

Table 4.114. TCA-11, Pin-66 four-group Pu-239 cross sections

Group	CENTRM cross sections (cm^{-1})			NITAWL cross sections (cm^{-1})		
	Σ_a	$\langle\Sigma_f$	Σ_f	Σ_a	$\langle\Sigma_f$	Σ_f
1	5.12696E-04	1.48906E-03	4.79759E-04	5.13031E-04	1.49057E-03	4.80148E-04
2	1.14152E-02	1.88409E-02	6.54241E-03	1.11940E-02	1.81913E-02	6.31686E-03
3	3.48957E-02	6.84264E-02	2.37608E-02	3.45817E-02	6.78782E-02	2.35705E-02
4	2.71706E-01	5.47283E-01	1.89309E-01	2.72174E-01	5.47792E-01	1.89488E-01

5. CALCULATIONAL BENCHMARKS

5.1 DESCRIPTION

The calculational benchmarks examined in this report are divided into two distinct geometric sets of cases. The first set of cases consists of an infinitely long pin in an infinite triangular-pitched lattice. The second set of cases consists of a buckled pin in an infinite triangular-pitched lattice. The radii of the fuel, clad, and moderator are all the same for all variants and states. Also, the buckling height is the same in all buckled problems. All variants and states are calculated in both geometric configurations. The state parameters are given in Table 5.1. [4]

The calculational benchmarks in each geometric set are divided into variants, with five states in each of the variants. The variants differ only by the isotopic composition of the fuel. Within each variant, the fuel composition is the same for each state, with the exception of the presence or absence of ^{135}Xe and ^{149}Sm. The differences in the states are due to the presence or absence of ^{135}Xe and ^{149}Sm in the fuel, the fuel temperature, and the type of moderator.

There are four basic types of fuel: fresh uranium fuel, fresh MOX fuel, spent uranium fuel and fresh MOX fuel containing Pu recycled from a reactor. The spent uranium fuel is used in two variants: variant V3 uses spent uranium fuel with only the actinides, whereas variant V4 uses spent uranium fuel with actinides and fission products. There are also four variations of the fresh MOX fuel: fresh MOX fuel, MOX fuel with only ^{239}Pu, MOX fuel with only ^{240}Pu, and MOX fuel with only ^{241}Pu. The basic fuel material isotopic composition for each variant is given in Table 5.2.

There are four nonfuel material compositions in the set of calculational benchmarks: 1 clad composition, which is common to all problems, and 3 moderator material compositions. The variations in the moderator compositions are due to the presence or absence of ^{10}B and ^{11}B, the clad and moderator temperature, and the moderator density. The material isotopic compositions for the clad and each moderator are given in Table 5.3.

Table 5.1. State parameters for the calculational benchmark variants

State	Fuel zone temp (K)	Nonfuel zone temp (K)	^{135}Xe, ^{149}Sm in fuel	^{10}B, ^{11}B in moderator	Moderator material
S1	1027	579	Yes	Yes	MOD1
S3	1027	579	Yes	No	MOD2
S4	1027	579	No	Yes	MOD1
S5	579	579	No	Yes	MOD1
S6	300	300	No	Yes	MOD3

Table 5.2. Basic fuel isotopic composition for each computational benchmark variant

Variant	Comment	Isotope	Atom density (10^{-24} cm^{-3})	Isotope	Atom density (10^{-24} cm^{-3})
V1	Fresh uranium fuel	^{235}U	8.7370×10^{-4}	^{16}O	3.9235×10^{-2}
		^{238}U	1.8744×10^{-2}		
V2	Fresh MOX fuel	^{235}U	3.8393×10^{-5}	^{239}Pu	6.5875×10^{-4}
		^{238}U	1.8917×10^{-2}	^{240}Pu	4.2323×10^{-5}
		^{16}O	4.1707×10^{-2}	^{41}Pu	7.0246×10^{-4}
V3	Spent uranium fuel with no fission products (actinides only)	^{235}U	3.7843×10^{-4}	^{242}Pu	4.7576×10^{-6}
		^{236}U	8.6365×10^{-5}	^{241}Am	4.9491×10^{-7}
		^{238}U	1.8327×10^{-2}	^{242m}Am	7.9194×10^{-9}
		^{237}Np	2.4823×10^{-5}	^{243}Am	6.6925×10^{-7}
		^{238}Pu	6.7254×10^{-6}	^{242}Cm	1.2582×10^{-7}
		^{239}Np	1.8332×10^{-6}	^{243}Cm	2.0629×10^{-9}
		^{239}Pu	1.3111×10^{-4}	^{244}Cm	1.2387×10^{-7}
		^{240}Pu	3.6233×10^{-5}	^{16}O	3.9235×10^{-2}
		^{241}Pu	2.1701×10^{-5}		
V4	Spent uranium fuel (actinides + fission products) (V3 + listed isotopes)	^{103}Rh	1.8890×10^{-4}	^{145}Nd	1.9975×10^{-6}
		^{131}Xe	1.4255×10^{-5}	^{153}Eu	2.4801×10^{-7}
		^{143}Nd	2.6692×10^{-2}	^{109}Ag	2.2037×10^{-9}
		^{147}Pm	6.1574×10^{-5}	^{155}Eu	9.6857×10^{-7}
		^{133}Cs	3.5974×10^{-6}	^{95}Mo	3.3720×10^{-7}
		^{99}Tc	3.3320×10^{-6}	^{154}Eu	5.1189×10^{-9}
		^{152}Sm	2.6842×10^{-4}	^{101}Ru	3.1134×10^{-7}
		^{151}Sm	3.0757×10^{-5}		
V7	Fresh MOX fuel with ^{239}Pu as only Pu	^{235}U	3.8393×10^{-5}	^{239}Pu	6.5875×10^{-4}
		^{238}U	1.8917×10^{-2}	^{16}O	4.1707×10^{-2}
V8	Fresh MOX fuel with ^{240}Pu as only Pu	^{235}U	6.9714×10^{-4}	^{240}Pu	4.2323×10^{-5}
		^{238}U	1.8917×10^{-2}	^{16}O	4.1707×10^{-2}
V9	Fresh MOX fuel with ^{241}Pu as only Pu	^{235}U	3.8393×10^{-5}	^{41}Pu	6.6577×10^{-4}
		^{238}U	1.8917×10^{-2}	^{16}O	4.1707×10^{-2}
V10	Fresh MOX fuel with recycled reactor Pu	^{235}U	5.0000×10^{-5}	^{240}Pu	4.9000×10^{-4}
		^{238}U	2.2100×10^{-2}	^{241}Pu	1.9000×10^{-4}
		^{16}O	4.6300×10^{-2}	^{242}Pu	1.0500×10^{-4}
		^{238}Pu	3.0000×10^{-5}	^{241}Am	2.5000×10^{-5}
		^{239}Pu	1.1600×10^{-3}		

Table 5.3. Nonfuel material isotopic composition

Material	Comment	Isotope	Atom density (10^{-24} cm^{-3})	Isotope	Atom density (10^{-24} cm^{-3})
Clad	Cladding	Zr	4.2300×10^{-2}		
MOD1	Hot moderator	H	4.7830×10^{-2}	^{10}B	4.7344×10^{-6}
	with boric acid	^{16}O	2.3910×10^{-2}	^{11}B	1.9177×10^{-5}
MOD2	Hot moderator	H	4.7830×10^{-2}		
	without boric acid	^{16}O	2.3910×10^{-2}		
MOD3	Cold moderator	H	6.6940×10^{-2}	^{10}B	6.6262×10^{-6}
	with boric acid	^{16}O	3.3470×10^{-2}	^{11}B	2.6839×10^{-5}

5.2 ANALYSIS

All computational benchmarks were processed using SCALE 5.0. The cases labeled NITAWL utilize the following sequence: CSAS, BONAMI, NITAWL, XSDRNPM. The cases labeled CENTRM utilize the following sequence: CSAS, BONAMI, NITAWL, CENTRM, PMC, WORKER, XSDRNPM. In the NITAWL cases the resolved resonance region is self-shielded using NITAWL. In the CENTRM cases the resolved resonance region is self-shielded using CENTRM and PMC, which removes the limitations of the Nordheim Integral Treatment. Table 5.4 contains the results for the infinite arrays, and Table 5.5 contains the results for the buckled arrays.

For each variant and state, the differences between the NITAWL and CENTRM multiplication factors (k_4 and buckled k_4) and the energy of the average lethargy causing fission (EALCF) are almost identical for the infinite and buckled geometries as shown in Tables 5.4 and 5.5. The differences in the multiplication between the CENTRM and NITAWL cases range from -0.09% to -0.55%. Trends are apparent based on both fuel material and temperature. The smallest difference occurs for variant V4, state S6, which is spent uranium fuel with actinides and fission products at room temperature. The largest difference occurs for variant V9, state S1, which is fresh MOX fuel with all the Pu as ^{241}Pu at reactor temperatures.

The selection and number of nuclides in the fuel has little effect on the difference between NITAWL and CENTRM, at most ~0.25%, which occurs when the amount of ^{241}Pu is at its maximum. The effects of resonance overlap do not seem to be significant. The lowest difference at any given temperature occurs for spent uranium fuel with actinides and fission products. The amount of absorbers in the fuel (^{135}Xe and ^{149}Sm) and in the moderator (^{10}B) also does not affect the differences.

Fuel and moderator temperature have the most obvious, albeit still small, effect on the difference between NITAWL and CENTRM results. For a given variant, the largest difference always occurs with the fuel at 1027 K and the moderator at 579 K. Decreasing the fuel temperature to 579 K always decreases the difference, as much as 0.1% . Further decreasing the fuel and moderator temperature to 300 K always further decreases the difference, as much as another 0.1%. Both NITAWL and

CENTRM interpolate data between temperatures.

The EALCF is also calculated for each variant and state. The differences in the average-energy between the NITAWL and CENTRM cases range from a low of -0.41% to a high of 1.66%. Trends are apparent based only on temperature. The smallest differences with each variant occur in state S6, and the largest differences occurs for states 1, 2, and 3. As the pin temperature drops, the differences between the CSAS and CENTRM results lessen.

5.3 CONCLUSIONS

For this set of cases using either NITAWL or CENTRM as the resonance region processor produces consistent results. The k_{eff} values are slightly lower, ~0.3%, for all CENTRM cases. The nuclides selected do not appear to have an effect on the difference, but the temperature of the system does have a slight effect: the point library has temperature data well above that available in the multigroup library. The approximations used to process the resolved resonance data in NITAWL do not significantly affect the results, as shown by the good agreement with the CENTRM results.

Table 5.4a. k_4 and EALCF values and differences for the variant cases

VARIANTS V1 - V4	NITAWL k_4	CENTRM k_4	k_4 % DIFF	NITAWL EALCF (eV)	CENTRM EALCF (eV)	EALCF % DIFF
V1S1	1.2593	1.2541	-0.41	0.7766	0.7806	0.52
V1S3	1.3144	1.3090	-0.41	0.6984	0.7019	0.5
V1S4	1.3069	1.3015	-0.41	0.7052	0.7087	0.5
V1S5	1.3249	1.3205	-0.33	0.6846	0.6877	0.45
V1S6	1.3669	1.3634	-0.26	0.2808	0.2819	0.39
V2S1	1.2074	1.2017	-0.47	1.5678	1.5873	1.24
V2S3	1.2360	1.2300	-0.49	1.4690	1.4871	1.23
V2S4	1.2270	1.2212	-0.47	1.4907	1.5090	1.23
V2S5	1.2474	1.2428	-0.37	1.4305	1.4460	1.08
V2S6	1.3256	1.3210	-0.35	0.5514	0.5568	0.98
V3S1	1.0821	1.0767	-0.5	0.9976	1.0064	0.88
V3S3	1.1267	1.1210	-0.51	0.8982	0.9058	0.85
V3S4	1.1218	1.1162	-0.5	0.9027	0.9103	0.84
V3S5	1.1412	1.1357	-0.48	0.8694	0.877	0.87
V3S6	1.1902	1.1862	-0.34	0.3271	0.3289	0.55
V4S1	1.0158	1.0140	-0.18	1.1496	1.1532	0.31
V4S3	1.0558	1.0536	-0.21	1.0346	1.0385	0.38
V4S4	1.0510	1.0490	-0.19	1.0411	1.0442	0.3
V4S5	1.0688	1.0669	-0.18	1.0081	1.0055	-0.26
V4S6	1.1197	1.1187	-0.09	0.3678	0.368	0.05

Table 5.4b. k_4 and EALCF values and differences for the variant cases (cont.)

VARIANTS V7 - V10	CSAS k_4	CENTRM k_4	k_4 % DIFF	CSAS EALCF (eV)	CENTRM EALCF (eV)	EALCF % DIFF
V7S1	1.3047	1.2984	-0.48	1.2704	1.2851	1.16
V7S3	1.3372	1.3307	-0.49	1.1922	1.2058	1.14
V7S4	1.3270	1.3206	-0.48	1.2090	1.2228	1.14
V7S5	1.3459	1.3404	-0.41	1.1687	1.1816	1.1
V7S6	1.4112	1.4067	-0.32	0.4793	0.4835	0.88
V8S1	1.0904	1.0859	-0.41	0.8038	0.8083	0.56
V8S3	1.1442	1.1395	-0.41	0.7108	0.7146	0.53
V8S4	1.1399	1.1351	-0.42	0.7147	0.7186	0.55
V8S5	1.1596	1.1557	-0.34	0.6881	0.6912	0.45
V8S6	1.2115	1.2084	-0.26	0.2694	0.2704	0.37
V9S1	1.5290	1.5207	-0.54	1.4193	1.4140	-0.37
V9S3	1.5644	1.5561	-0.53	1.3346	1.3293	-0.4
V9S4	1.5515	1.5432	-0.53	1.3585	1.3529	-0.41
V9S5	1.5736	1.5668	-0.43	1.3191	1.3181	-0.08
V9S6	1.6195	1.6140	-0.34	0.5601	0.5602	0.02
V10S1	1.0952	1.0902	-0.46	9.5809	9.7345	1.6
V10S3	1.1078	1.1027	-0.46	9.118	9.2636	1.6
V10S4	1.1010	1.0958	-0.47	9.3374	9.4863	1.59
V10S5	1.1196	1.1160	-0.32	8.7717	8.8831	1.27
V10S6	1.1937	1.1917	-0.17	2.614	2.6373	0.89

Table 5.5a. Buckled k_4 and EALCF values and differences for the variant cases

VARIANTS V1 - V4	CSAS buckled k_4	CENTRM buckled k_4	k_4 % DIFF	CSAS EALCF (eV)	CENTRM EALCF (eV)	EALCF % DIFF
V1S1	1.0802	1.0757	-0.42	0.8408	0.8455	0.56
V1S3	1.1266	1.1218	-0.43	0.755	0.7592	0.56
V1S4	1.1201	1.1154	-0.42	0.7628	0.7670	0.55
V1S5	1.1353	1.1314	-0.34	0.7402	0.7438	0.49
V1S6	1.2286	1.2253	-0.27	0.2932	0.2944	0.41
V2S1	1.0396	1.0346	-0.48	1.6927	1.7146	1.29
V2S3	1.0638	1.0586	-0.49	1.5847	1.605	1.28
V2S4	1.0562	1.0511	-0.48	1.6086	1.6293	1.29
V2S5	1.1050	1.1007	-0.39	1.5477	1.5659	1.18
V2S6	1.2167	1.2125	-0.35	0.5755	0.5814	1.03
V3S1	0.9547	0.9499	-0.5	1.0872	1.0973	0.93
V3S3	0.9932	0.9882	-0.5	0.9775	0.9863	0.9
V3S4	0.9889	0.9839	-0.51	0.9827	0.9917	0.92
V3S5	1.0059	1.0011	-0.48	0.9457	0.9542	0.9
V3S6	1.0887	1.0850	-0.34	0.3425	0.3445	0.58
V4S1	0.8975	0.8958	-0.19	1.2555	1.2600	0.36
V4S3	0.9322	0.9301	-0.23	1.1285	1.1334	0.43
V4S4	0.9279	0.9261	-0.19	1.1361	1.1400	0.34
V4S5	0.9435	0.9418	-0.18	1.0923	1.0963	0.37
V4S6	1.0253	1.0242	-0.11	0.3847	0.3858	0.29

Table 5.5b. Buckled k_4 and EALCF values and differences for the variant cases (cont.)

VARIANTS V7 - V10	CSAS buckled k_4	CENTRM buckled k_4	k_4 % DIFF	CSAS EALCF (eV)	CENTRM EALCF (eV)	EALCF % DIFF
V7S1	1.1560	1.1504	-0.48	1.3698	1.3865	1.22
V7S3	1.1844	1.1786	-0.49	1.2846	1.300	1.2
V7S4	1.1755	1.1697	-0.49	1.3031	1.3187	1.2
V7S5	1.1920	1.1870	-0.42	1.2589	1.2734	1.15
V7S6	1.2955	1.2913	-0.32	0.4991	0.5037	0.92
V8S1	0.9628	0.9588	-0.42	0.8777	0.8831	0.62
V8S3	1.0093	1.0050	-0.43	0.7748	0.7794	0.59
V8S4	1.0055	1.0012	-0.43	0.7794	0.7841	0.6
V8S5	1.0227	1.0192	-0.34	0.7496	0.7534	0.51
V8S6	1.1095	1.1066	-0.26	0.2819	0.2829	0.35
V9S1	1.3591	1.3515	-0.56	1.5135	1.5087	-0.32
V9S3	1.3901	1.3825	-0.55	1.4225	1.4177	-0.34
V9S4	1.3788	1.3712	-0.55	1.4481	1.4431	-0.35
V9S5	1.3982	1.3920	-0.44	1.4055	1.4052	-0.02
V9S6	1.4906	1.4855	-0.34	0.5802	0.5803	0.02
V10S1	0.9876	0.9831	-0.46	10.483	10.657	1.66
V10S3	0.9988	0.9941	-0.47	9.9769	10.142	1.65
V10S4	0.9927	0.9881	-0.46	10.216	10.385	1.65
V10S5	1.0094	1.0061	-0.33	9.5901	9.7165	1.32
V10S6	1.1087	1.1069	-0.16	2.7455	2.7705	0.91

REFERENCES

1. *SCALE: A Modular Code System for Performing Standardized Analyses for Licensing Evaluations*, NUREG/CR-0200, Rev. 4 (ORNL/NUREG/CSD-2/R4), Vols. I, II, and III, April 1995. Available from Radiation Safety Information Computational Center at Oak Ridge National Laboratory as CCC-545.

2. M. Williams and M. Asgari, "Computation of Continuous-Energy Neutron Spectra with Discrete Ordinates Transport Theory," *Nucl. Sci. Eng.* **121**, 173**B**201 (1995).

3. *International Handbook of Evaluated Criticality Safety Benchmark Experiments*, HEU-MET-FAST-035 Benchmark, The Uranium/Iron Benchmark Assembly: A 235U(93%)/Iron Cylinder Reflected by Stainless Steel, NEA/NSC/DOC(95)03 (September 1998).

4. *Neutronics Benchmarks for the Utilization of Mixed-oxide Fuel: Joint U.S./Russian Progress Report for Fiscal Year 1997, Volume 3 - Calculations Performed in the Russian Federation*, ORNL/TM-13603/V3, June 1998

INTERNAL DISTRIBUTION

1. B. B. Bevard
2. S. M. Bowman
3. B. L. Broadhead
4-8. W. C. Carter (5)
9. E. D. Collins
10. B. S. Cowell
11. M. D. DeHart
12. M. E. Dunn
13. K. R. Elam
14. R. J Ellis
15. M. B. Emmett
16. I. C. Gauld
17. J. C. Gehin
18. N. M. Greene
19. S. R. Greene
20. O. W. Hermann
21-25. D. F. Hollenbach (5)
26. C. M. Hopper
27. O. W. Hermann
28. D. T. Ingersoll
29. H. T. Kerr
30. M. A. Kuliasha
31. L. C. Leal
32. S. B. Ludwig
33. G. E. Michaels
34. D. L. Moses
35. B. D. Murphy
36. L. M. Petrie
37-41. C. V. Parks (5)
42. L. M. Petrie
43-47. R. T. Primm (5)
48. B. T. Rearden
49. C. H. Shappert
50. T. E. Valentine
51. J. C. Wagner
52. R. M. Westfall
53. R. Q. Wright
54. Central Research Library
Document Reference Section
55-56. ORNL Laboratory Records (2)
for submission to OSTI
57. ORNL Laboratory Records - RC

EXTERNAL DISTRIBUTION

58. M. L. Adams, Department of Nuclear Engineering, Texas A&M University, Zachry 129, College Station, TX 77843
59. R. E. Anderson, Los Alamos National Laboratory, P.O. Box 1663, NIS-6, MS J562, Los Alamos, NM 87545
60. W. L. Andrews, Defense Nuclear Facilities Safety Board, 625 Indiana Ave., Washington, DC 20004
61. M. G. Bailey, U.S. Nuclear Regulatory Commission, MS O6-G22, Washington, DC 20555
62. J. B. Briggs, INEEL, P.O. Box 1625, MS-3855, Idaho Falls, ID 83402
63. T. Burns, Defense Nuclear Facilities Safety Board, 625 Indiana Ave., Washington, DC 20004
64. D. E. Carlson, U.S. Nuclear Regulatory Commission, MS O6-F18, Washington, DC 20555

65. I. Carron, Department of Nuclear Engineering, Texas A&M University, 129 Zachry, College Station, TX 77843-3133
66. D. R. Damon, U.S. Nuclear Regulatory Commission, MS T8-H7, Washington, DC 20555
67. J. R. Davis, U.S. Nuclear Regulatory Commission, MS T8-A33, Washington, DC 20555
68. R. L. Dintaman, U.S. Department of Energy, DP-13, 19901 Germantown Rd., Germantown, MD 20874-1290
69. H. L. Dodds, University of Tennessee, Nuclear Engineering Dept., 214 Pasqua Engineering Bldg., Knoxville, TN 37922
70. T. W. Doering, Framatome Cogema Fuels, 1261 Town Center Drive, Las Vegas, NV 89124
71. J. D. Evans, U.S. Department of Energy, S-3.1/VISTA, 1000 Independence Ave., S.W., Washington, DC 22085
72. H. D. Felsher, U.S. Nuclear Regulatory Commission, MS T8-H7, Washington, DC 20555
73. P. Felsher, Rocky Flats Environment Technology Site, Bldg. T886B, P.O. Box 464, Golden, CO 80402-0464
74. J. R. Felty, Science Applications Int'l Corp., 2418 N. Dickerson St., Arlington, VA 22207
75. I. E. Fergus, U.S. Department of Energy, EH-22, 20300 Century Blvd., Germantown, MD 20874
76. E. K. Fujita, Argonne National Laboratory, 9700 South Cass Avenue, RA/208, Argonne, IL 60439-4842
77. A. S. Garcia, U.S. Department of Energy, Idaho Operations Office, 850 Energy Dr., MS 1154, Idaho Falls, ID 83401-1563
78. S. C. Keeton, Lawrence Livermore National Laboratory, P.O. Box 808 (L-128), Livermore, CA 94550
79. R. C. Little, Los Alamos National Laboratory, MS F663, P.O. Box 1663, Los Alamos, NM 87545
80. J. McKamy, U.S. Department of Energy, EH-34, 19901 Germantown Road, Germantown, MD 20874-1290
81. R. D. McKnight, Argonne National Laboratory, 9700 S. Cass Ave., Argonne, IL 60439-4842
82. T. P. McLaughlin, Los Alamos National Laboratory, P.O. Box 1663, Los Alamos, NM 87545
83. D. E.I. Mennerdal, E M Systems, Starvãgen 12, Täby, SWEDEN S-18357
84. D. C. Morey, U.S. Nuclear Regulatory Commission, MS T8-A33, Washington, DC 20555
85. J. A. Morman, Argonne National Laboratory, 9700 S. Cass Ave., Bldg. 208, C237B, Argonne, IL 60439-4842
86. R. D. Mosteller, Los Alamos National Laboratory, MS J562, Los Alamos, NM 87545
87. K. A. Niemer, Duke Engineering & Services, 400 S. Tryon St., WC26B, P.O. Box 1004, Charlotte, NC 28201-1004
88. H. Okuno, Japan Atomic Energy Research Institute, 2-4 Shirakara-shirane, Tokai-mura, Ibaraki-ken, JAPAN 319-1195

89. R. E. Pevey, University of Tennessee, Nuclear Engineering Dept., 214 Pasqua Engineering Bldg., Knoxville, TN 37922
90. M. Rahimi, U.S. Nuclear Regulatory Commission, M/S T7F3, Washington, DC 20555
91. P. T. Rhoads, Office of Fissile Materials Disposition, U.S. Department of Energy, MD-4, 1000 Independence Avenue SW, Washington, DC 20585
92. B. Rothleder, U.S. Department of Energy, EH-31, 19901 Germantown Rd., Germantown, MD 20874-1290
93. M. K. Sheaffer, Lawrence Livermore National Laboratory, P.O. Box 808, L-634, Livermore, CA 94550
94. T. Taylor, Lockheed Martin Idaho Tech. Co., P.O. Box 1625, MS 3458, Idaho Falls, ID 83415-3458
95. C. Tripp, U.S. Nuclear Regulatory Commission, MS T8-A33, Washington, DC 20555
96. J. A. Thornton, Duke Engineering & Services, 400 S. Tryon St., WC26B, P.O. Box 1004, Charlotte, NC 28201-1004
97. H. Toffer, Fluor Daniel Northwest, Inc., P.O. Box 1050, MSIN B4-44, 1100 Jadwin Ave., Richland, WA 99352-1050
98. E. F. Trumble, Westinghouse Safety Management Solutions, P.O. Box 5388, 1993 South Centennial Dr., Aiken, SC 29803
99. M. Wangler, Office of Site Operations, EM-70/CLV-1059, U.S. Department of Energy, 19901 Germantown Road, Germantown, MD 20874-1290
100. L. Wetzel, BWX Technologies, Inc., Naval Nuclear Fuel, P.O. Box 785, Lynchburg, VA 24505
101. B. H. White IV, U.S. Nuclear Regulatory Commission, MS O6-F18, Washington, DC 20555
102. Mark Williams, Louisiana State University, Baton Rouge, LA 70803-5820
103. R. E. Wilson, Safe Sites of Colorado, P.O. Box 464, Golden, CO 80402-0464
104 C. J. Withee, U.S. Nuclear Regulatory Commission, MS O6-G22, Washington, DC 20555